CANADIAN THESES ON MICROFICHE

THÈSES CANADIENNES SUR MICROFICHE

National Library of Canada
Collections Development Branch

Canadian Theses on
Microfiche Service

Ottawa, Canada
K1A 0N4

Bibliothèque nationale du Canada
Direction du développement des collections

Service des thèses canadiennes
sur microfiche

NOTICE

The quality of this microfiche is heavily dependent upon the quality of the original thesis submitted for microfilming. Every effort has been made to ensure the highest quality of reproduction possible.

If pages are missing, contact the university which granted the degree.

Some pages may have indistinct print especially if the original pages were typed with a poor typewriter ribbon or if the university sent us an inferior photocopy.

Previously copyrighted materials (journal articles, published tests, etc.) are not filmed.

Reproduction in full or in part of this film is governed by the Canadian Copyright Act, R.S.C. 1970, c. C-30. Please read the authorization forms which accompany this thesis.

AVIS

La qualité de cette microfiche dépend grandement de la qualité de la thèse soumise au microfilmage. Nous avons tout fait pour assurer une qualité supérieure de reproduction.

S'il manque des pages, veuillez communiquer avec l'université qui a conféré le grade.

La qualité d'impression de certaines pages peut laisser à désirer, surtout si les pages originales ont été dactylographiées à l'aide d'un ruban usé ou si l'université nous a fait parvenir une photocopie de qualité inférieure.

Les documents qui font déjà l'objet d'un droit d'auteur (articles de revue, examens publiés, etc.) ne sont pas microfilmés.

La reproduction, même partielle, de ce microfilm est soumise à la Loi canadienne sur le droit d'auteur, SRC 1970, c. C-30. Veuillez prendre connaissance des formules d'autorisation qui accompagnent cette thèse.

THIS DISSERTATION
HAS BEEN MICROFILMED
EXACTLY AS RECEIVED

LA THÈSE A ÉTÉ
MICROFILMÉE TELLE QUE
NOUS L'AVONS REÇUE

Canada

NL 339 (r. 86/09)

National Library of Canada
Bibliothèque nationale du Canada

Ottawa, Canada
K1A 0N4

⑫

TC –

ISBN 0-315-21208-X

CANADIAN THESES ON MICROFICHE SERVICE – SERVICE DES THÈSES CANADIENNES SUR MICROFICHE

PERMISION TO MICROFILM – AUTORISATION DE MICROFILMER

- Please print or type – Écrire en lettres moulées ou dactylographier

AUTHOR – AUTEUR

Full Name of Author – Nom complet de l'auteur: MASOUMZADEH • SHAHIN

Date of Birth – Date de naissance: 15-03-57

Canadian Citizen – Citoyen canadien: ☐ Yes / Oui ☑ No / Non

Country of Birth – Lieu de naissance: IRAN

Permanent Address – Résidence fixe:
#306, 10210, 118 ST
Edmonton, Alta
T5K 1Y5

THESIS – THÈSE

Title of Thesis – Titre de la thèse: ACCELERATING CREEP OF THE slopes OF LUSCAR OPEN-PIT COAL MINE

Degree for which thesis was presented / Grade pour lequel cette thèse fut présentée: M.Sc.

Year this degree conferred / Année d'obtention de ce grade: 1985,

University – Université: University of Alberta

Name of Supervisor – Nom du directeur de thèse: D.M. CRUDEN

AUTHORIZATION – AUTORISATION

Permission is hereby granted to the NATIONAL LIBRARY OF CANADA to **microfilm** this thesis and to **lend** or **sell copies of the film.**

The author reserves other publication rights, and neither the thesis nor extensive extracts from it may be printed or otherwise reproduced without the author's written permission.

L'autorisation est, par la présente, accordée à la BIBLIOTHÈQUE NATIONALE DU CANADA de **microfilmer** cette thèse et de **prêter** ou de **vendre des exemplaires du film.**

L'auteur se réserve les autres droits de publication; ni la thèse ni de longs extraits de celle-ci ne doivent être imprimés ou autrement reproduits sans l'autorisation écrite de l'auteur.

ATTACH FORM TO THESIS – VEUILLEZ JOINDRE CE FORMULAIRE À LA THÈSE

Signature:

Date: 18, April 85

NL-91 (r. 84/03)

Canada

THE UNIVERSITY OF ALBERTA

ACCELERATING CREEP OF THE SLOPES OF LUSCAR OPEN-PIT COAL MINE

by

© SHAHIN MASOUMZADEH

A THESIS
SUBMITTED TO THE FACULTY OF GRADUATE STUDIES AND RESEARCH
IN PARTIAL FULFILMENT OF THE REQUIREMENTS FOR THE DEGREE
OF MASTER OF SCIENCE

DEPARTMENT OF CIVIL ENGINEERING

EDMONTON, ALBERTA
SPRING, 1985

THE UNIVERSITY OF ALBERTA

RELEASE FORM

NAME OF AUTHOR SHAHIN MASOUMZADEH

TITLE OF THESIS **ACCELERATING CREEP OF THE SLOPES OF LUSCAR OPEN-PIT COAL MINE**

DEGREE FOR WHICH THESIS WAS PRESENTED MASTER OF SCIENCE

YEAR THIS DEGREE GRANTED SPRING, 1985

Permission is hereby granted to THE UNIVERSITY OF ALBERTA LIBRARY to reproduce single copies of this thesis and to lend or sell such copies for private, scholarly or scientific research purposes only.

The author reserves other publication rights, and neither the thesis nor extensive extracts from it may be printed or otherwise reproduced without the author's written permission.

(SIGNED)

PERMANENT ADDRESS:

Apt. 306 , 10210 118 St.
Edmonton , Alberta.
T5K 1Y5 Canada.

DATED April 1985

THE UNIVERSITY OF ALBERTA

FACULTY OF GRADUATE STUDIES AND RESEARCH

The undersigned certify that they have read, and recommend to the Faculty of Graduate Studies and Research, for acceptance, a thesis entitled **ACCELERATING CREEP OF THE SLOPES OF LUSCAR OPEN-PIT COAL MINE** submitted by SHAHIN MASOUMZADEH in partial fulfilment of the requirements for the degree of MASTER OF SCIENCE in CIVIL ENGINEERING.

D.M. Cruden ....

Supervisor

N.R. Morgenstern ....

H.A.K. Charlesworth ......HAKC

Date April 1985

Abstract

Movement of rock slopes in open pit coal mines can accelerate to high velocities hazardous to men and equipment. A critical slide velocity may be chosen for evacuation of pit personnel and equipment under moving slopes. The magnitude of this velocity depends on the local conditions of a mine.

A displacement monitoring program at Luscar mine of Cardinal River Coals Ltd. , showed that accelerating creep was taking place. Geological reports show that moderate to steeply dipping sandstone strata , jointed by four sets , and , overlying siltstone and shale strata , contributed to create accelerating creep processes.

Movement hypotheses are presented to interpret the displacements of the rock masses. Two major directions of movement are identified ; nearly parallel to the strike of the bedding and down the dip direction of the bedding. The latter movement is quantitatively much more important than the former. A common plane of movement dips 28° to the west.

A critical slide velocity of 0.5 mm/min was chosen. Four mathematical models are evaluated to predict the time of the critical slide velocity. For this evaluation , four computer simulated models were developed. The study of confidence limits for the slopes and intercepts of fitted lines allows group analyses of displacement data. Durbin Watson statistics and tests of slope significance are used to conduct linear regression analyses for all and parts of the displacement data.

The time of the most rapid sliding could not be usefully predicted by Saito's or Zavodni and Broadbent's methods. On the other hand two new methods , using power and exponential laws are practical , when three accelerating creep stages are identified. A threshold velocity of 0.1 mm/min , observed just before the initiation of the third accelerating creep stage , could be predicted 6 days in advance. Analyses of the data in the third accelerating creep stage showed that velocity accelerated to its critical value approximately 8.5 hours before the most rapid sliding. An operational procedure is recommended for the prediction of the time of the critical slide velocity as an indication of impending failure.

Acknowledgement

I would like to thank Dr. D.M. Cruden for his supervision, advice and patience throughout the preparation of this thesis. Thanks are also extended to Dr. N.R. Morgenstern for his guidence and encouragement during the last four years, and Dr. H.A.K. Charlesworth for his valuable comments on geology.

I would like to thank the following persons ; A.M.R. MacRae and R.S. Johnson for providing data and information, K.E. Hebil for explaining the geology and C.P. Acott for helping in the field. Thanks are further extended to Cardinal River Coals Ltd. and Luscar Ltd. for their cooperation by allowing access to Luscar mine and field data.

The financial support awarded by the Canadian Natural Science and Engineering Research Council through Dr. D.M. Cruden and graduate teaching assistantship by the Civil Engineering Department are appreciated.

Table of Contents

Chapter Page

1. INTRODUCTION 1

1.1 Overall View Of All Chapters 1

1.2 Objectives Of This Thesis 1

1.3 Mine History And Operations 2

1.4 51-B-2 Pit North Wall Slide 4

2. GEOLOGY AND THE SLIDE 6

2.1 General 6

2.2 Mine Geology 6

2.3 Geotechnical Investigation of the North Wall of 51-B-2 Pit 7

2.3.1 Introduction 7

2.3.2 North Wall Geology 7

2.3.2.1 East Portion of the Wall 9

2.3.2.2 West Portion Of The Wall 9

2.3.3 Jointing 13

2.3.3.1 Joint Set Interpretation 15

2.3.4 Faulting 15

2.3.5 Joint Sets Versus Movement Interpretation 18

2.3.6 Lithology 19

2.3.7 Hydrological Observations 19

2.3.8 Wall Slide-Geology Working Hypotheses 20

2.4 Back Analysis 22

2.4.1 Conclusions 23

3. MONITORING PROGRAM AND REMEDIAL MEASURES 25

3.1 Introduction 25

3.2 Slope Movements Measurements 26
3.2.0.1 Radial Survey Method 27
3.3 Existing Data 30
3.3.1 Prism Movements 31
3.3.1.1 Summary Of Events 31
3.3.2 Movement Hypotheses 33
3.3.2.1 First Hypothesis 33
3.3.2.2 Second Hypothesis 45
3.3.2.3 Third Hypothesis 45
3.3.3 Working Movement Hypothesis 46
3.3.4 Piezometric Levels 51
3.4 Remedial Measures 52
3.5 Factor Of Safety Determination 53
4. LITERATURE REVIEW 57
4.1 Introduction 57
4.2 Conventional Creep Curves 57
4.3 Saito-Type Relations 60
4.4 Exponential Form 63
4.5 Power of Time Form 63
4.6 Simultaneous Creep Stages 64
4.7 Case Studies Results 65
4.8 Zavodni and Broadbent s Fit 66
5. EVALUATION OF t_f (TIME OF FAILURE) PREDICTION METHODS 70
5.1 Introduction 70
5.2 Failure Definition 70
5.3 General Procedure 73

5.4 T_0 Known Case 74

5.5 T_0 Unknown Case 76

5.6 Analysis Of The Data 79

5.6.1 Computer Programs 79

5.6.2 Criteria For Goodness of Fit 81

5.6.3 Selection Of Data 87

5.6.4 Units 88

5.6.5 Spring Ahead And Fall Back Daylight Times 89

5.6.6 16 Prisms Displacement Analysis 89

5.6.7 26-B Prism Displacement Analysis 91

5.6.7.1 Slope Distance Analysis 91

5.6.7.2 Horizontal Displacement Analysis 100

5.6.7.3 Displacement Vector Resultant Analysis 109

5.6.8 Discussion 130

5.6.8.1 Power Law 130

5.6.8.2 Zavodni And Broadbent s Fit 132

5.6.9 Practical Applications 133

5.6.10 Consideration Of The Decelerating Creep .138

6. CONCLUSIONS AND RECOMMENDATIONS 141

6.1 Conclusions 141

6.1.1 Power and Exponential Laws 141

6.1.2 Saito Relation 142

6.1.3 Zavodni and Broadbent s fit 143

6.1.4 Movement Hypothesis 143

6.1.5 Other Conclusions 144

6.1.6 Limitation of application 145

6.2 Recommendations 145

BIBLIOGRAPHY 148

APPENDIX - COMPUTER PROGRAM DOCUMENTATION 154

List of Tables

Table Page

2.1 Attitude of joints and bedding in 51-B-2 pit north wall 14

2.2 Back analysis results 24

3.1 Slope prisms displacement monitoring results 34

3.2 26-B prism displacement monitoring results 35

3.3 Stabilizing toe berm effect in factor of safety 54

5.1 Line parameters for creep relations 77

5.2 A comparison of laws 80

5.3 Results of cumulative horizontal displacement analysis 92

5.4 Results of cumulative horizontal displacement analysis cont. 93

5.5 Results of cumulative horizontal displacement analysis cont. 94

5.6 Results of cumulative horizontal displacement analysis cont. 95

5.7 Slope distance analysis results 101

5.8 t effect in slope distance analysis results 102

5.9 t effect in slope distance analysis results cont. 103

5.10 t effect in slope distance analysis results cont. 104

5.11 Results of cumulative horizontal displacement analysis 106

5.12 X effect in power law statistics 107

5.13 Results of cumulative horizontal displacement analysis - divided data 110

Table Page

5.14 Results of analysis of the resultants of the displacement vectors 112

5.15 Results of analysis of the resultants of the displacement vectors - part 1 data 113

5.16 Results of analysis of the resultants of the displacement vectors - part 2 data 114

5.17 An examination of the Saito relation 115

5.18 Results of analysis of the resultants of the displacement vectors for decelerating creep of the 40-B prism 139

List of Figures

Figure Page

1.1 Location of Luscar mine 3

2.1 Stratigraphy of Cardinal River Area 8

2.2 The east portion of the north wall. Notice benching into sandstone below coal seam towards west. Section B-B lies beyond the left margin of thr picture , now covered by post slide berm. Photograph taken by S. Masoumzadeh on 11 August , 1983. 10

2.3 The north wall in the 51-B-2 pit. See Figure 1.1 for the pit location. 11

2.4 The north end of the east wall. Photograph taken by S. Masoumzadeh on 11 August , 1983. 12

2.5 51-B-2 pit north wall plot of great circles of joint planes and all potential wedge intersections 16

2.6 Major joints and faults in the north wall. Photograph taken by S. Masoumzadeh on 11 August , 1983. 17

3.1 Discontinuities and orientation of the resultants of the displacement vectors at 9:00 A.M November 10th 1979 36

3.2 Application of Hockings rule 37

3.3 The resultants of the displacement vectors and centers of rotation on the common plane of movement at 9:00 A.M November 10th 1979 38

3.4 The resultants of the displacement vectors and traces of discontinuities on the common plane of movement at 9:00 A.M November 10th 1979 39

3.5 Discontinuities and orientation of the resultants of the displacement vectors at 5:00 P.M November 10th 1979 40

Figure Page

3.6 The resultants of the displacement vectors and centers of rotation on the common plane of movement at 5:00 P.M November 10th 1979 41

3.7 The resultants of the displacement vectors and traces of discontinuities on the common plane of movement at 5:00 P.M November 10th 1979 42

3.8 Cross section (B-B) in Figure 2.4 proposed by S.Masoumzadeh 43

3.9 Simplified plan of the moving blocks at 5:00 P.M November 10th 1979 44

3.10 Stability analysis for north wall and stabilizing toe berm in 51-B-2 pit 55

4.1 Typical creep curves 59

4.2 Typical shape of movement/time plot preceding failure 59

4.3 Typical displacement rate versus time record of a large scale rock failure proceeding to collapse. Liberty pit failure No.1 67

5.1 Times definitions 71

5.2 Displacement vector and its components 71

5.3 Principal types of graphs used for analysis of creep curves 75

5.4 Saito fit flow diagram for the time of failure prediction 82

5.5 Saito fit flow diagram for the time of failure prediction cont. 83

5.6 Power law flow diagram 84

5.7 Power law(velocity/acceleration) flow diagram 85

5.8 Exponential law flow diagram 86

Figure Page

5.9 90 percent confidence limit for the Saito relation parameters 96

5.10 90 percent confidence limit for the Saito relation parameters 97

5.11 90 percent confidence limit for the Saito relation parameters 98

5.12 90 percent confidence limit for the Saito relation parameters 99

5.13 Saito fit to cumulative horizontal displacements (velocity in mm/min , time in min) 108

5.14 Power law fit to the resultants of the displacement vectors (velocity:mm/min , time:min) 116

5.15 Power law fit to the resultants of the displacement vectors (velocity/acceleration:min , time:min) 117

5.16 Saito fit to the resultants of the displacement vectors (velocity:mm/min , time:min) 118

5.17 Exponential law fit to the resultants of the displacement vectors (velocity:mm/min , time:min) 119

5.18 Power law fit to the resultants of the displacement vectors - part 1 data(velocity:mm/min , time:min) 120

5.19 Power law fit to the resultants of the displacement vectors - part 2 data(velocity:mm/min , time:min) 121

5.20 Power law fit to the resultants of the displacement vectors - part 1 data(velocity/acceleration:min , time:min) 122

5.21 Power law fit to the resultants of the displacement vectors - part 2 data(velocity/acceleration:min , time:min) 123

Figure Page

5.22 Saito fit to the resultants of the displacement vectors - part 1 data(velocity:mm/min , time:min) 124

5.23 Saito fit to the resultants of the displacement vectors - part 2 data(velocity:mm/min , time:min) 125

5.24 Exponential law fit to the resultants of the displacement vectors - part 1 data (velocity:mm/min , time:min) 126

5.25 Exponential law fit to the resultants of the displacement vectors - part 2 data (velocity:mm/min , time:min) 127

5.26 Saito fit to the resultants of the displacement vectors when t =700,000 minutes (velocity:mm/min , time:min) 128

5.27 Saito fit statistics - time of failure effect 129

5.28 Computation of velocity and acceleration 131

5.29 Comparison of laws beyond 165 minutes prior to failure 135

5.30 Power law fit to the resultants of the displacement vectors for decelerating creep of the 40-B prism (velocity:mm/min , time:min) 140

LIST OF SYMBOLS

t : Relative time

T : Absolute time

X : Time constant

t_f : Time of the most rapid sliding

$(t_f - t)$ = Time prior to the most rapid slide

ϵ : displacement

$\dot{\epsilon} = d\epsilon/dt$ = Velocity

$\ddot{\epsilon} = d^2\epsilon/dt^2$ = Acceleration

n : Constant

Chapter 1

INTRODUCTION

1.1 Overall View Of All Chapters

This chapter presents a general view and background information about a large slide on the North wall of 51-B-2 pit at Luscar mine of Cardinal River Coals Ltd. Chapters 2 and 3 summarize reports and papers written on the slide. Three movement hypotheses are studied in chapter 3. It was intended not to repeat information , present the material on a time sequential basis and avoid irrelevant information. Litrature on the accelerating creep of materials and in particular of rocks , is studied in chapter 4. The application of various laws for determining the time of sliding , for the slide in the 51-B-2 pit , is discussed in chapter 5. Two new methods for predicting the time of slide together with consideration of the decelerating creep are also presented in chapter 5. Finally chapter 6 derives conclusions from the present work and outlines recommendations for further research.

1.2 Objectives Of This Thesis

1. To create computer simulated models for linear regression analyses of displacement and time data.
2. To propose at least one practical method for the prediction of velocity in particular close to the time of failure.

3. To identify blocks of rock mass.
4. To present a working movement hypothesis

1.3 Mine History And Operations

Luscar Ltd. and its predecessor and subsidiary companies have been mining coal in Western Canada for 70 years. Luscar Ltd. was formed in 1967 through the amalgamation of Luscar Coals Ltd. and Mountain Park Collieries Ltd. Today , the company has five operating mines , and is one of the major and most diversified of the Western Canadian coal producers.

The Luscar Mine was reopened in 1970 as a joint venture (50 - 50) of Luscar Ltd. and the Consolidation Coal Company of Canada Ltd. to produce metallurgical coking coal for export. Operated by Cardinal River Coals Ltd. , the mine (NTS map 83F/3) is situated on the site of the original Luscar Mine , approximately 320 Km west of Edmonton (Figure 1-1). Annual production is approximately 2.7 million tonnes of clean coal. The development of an underground hydraulic mine is underway.

The mine is a truck-and-shovel operation employing 11.5 and 23 cubic metre electric shovels for overburden removal and trucks of 91 and 154 tonne capacity for rock and coal haul. Front end loaders of 7.6 and 11.5 cubic metre capacity are utilized for coal removal.

Munn (1983) explained the mine operations. Mining is carried out along the four baselines which generally follow

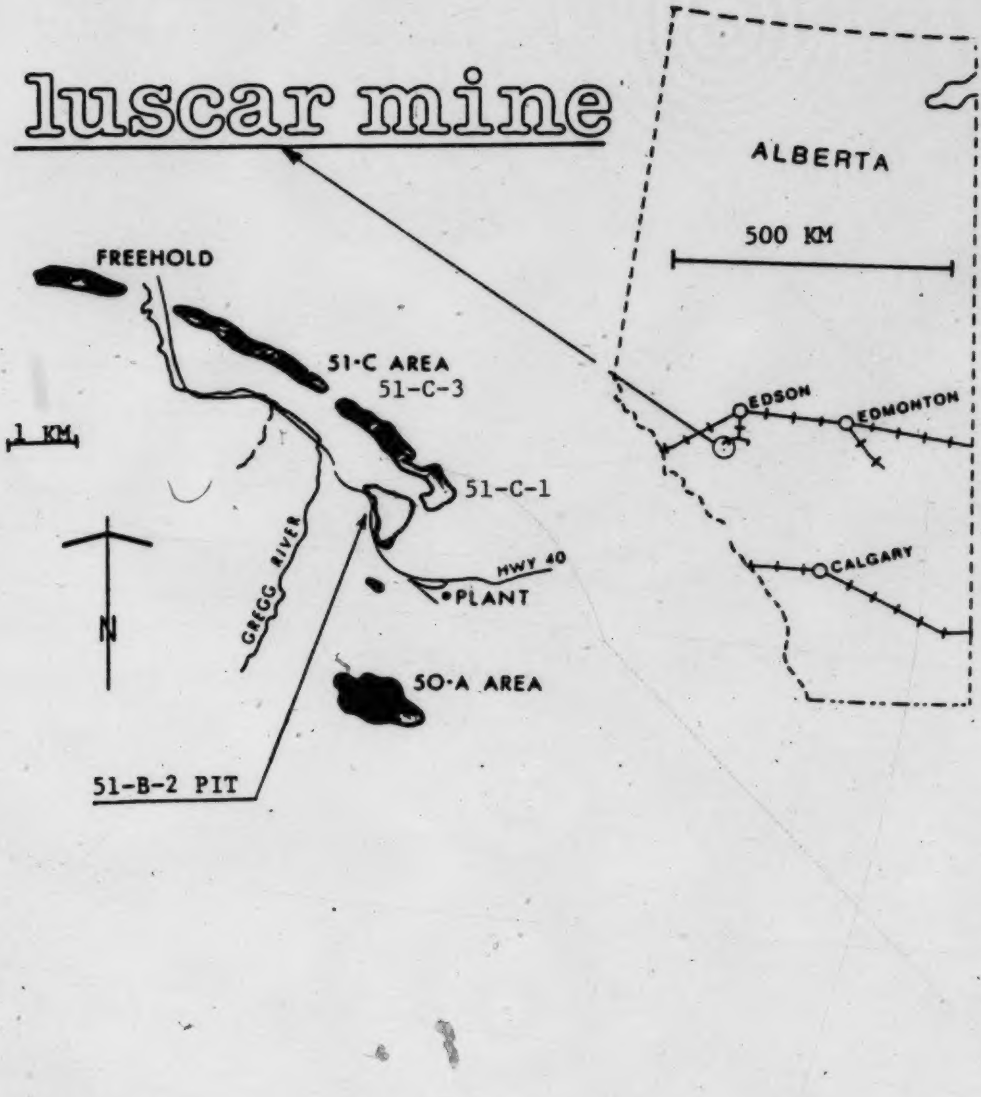
luscar mine
ALBERTA
500 KM
EDSON
EDMONTON
CALGARY
FREEHOLD
51-C AREA
51-C-3
51-C-1
1 KM.
N
GREGG RIVER
HWY 40
PLANT
50-A AREA
51-B-2 PIT

Figure 1.1 Location of Luscar mine

the outcrops of the synclines and anticlines. A series of pits is designed along each of the baselines. These pits vary in size from 3.5 million to 34 million bank cubic metres and in stripping ratios from 3.1:1 to 8.8:1 bank cubic metres per clean short ton.

There are usually three or four active pits. This number of pits is required to produce a constant coal release with a fixed mining fleet. Pits are designed to be as small as practical as this improves the rate of coal release. Large pits are subdivided into phases. Smaller pits also offer an advantage to wall stability by reducing the length of unsupported wall , and reducing the time that the wall is exposed.

Along any one baseline the pits are generally continuous. The sequence of mining is such as to develop the first pit in the series using an external rock dump. The rock from subsequent pits is then backfilled into the preceeding pit. Backfilling is efficient because it reduces the haul distance and also serves to stabilize the walls.

1.4 51-B-2 Pit North Wall Slide

Munn (1983) defined failure as excessive wall movement which may cause rock to fall into the active mine. He further stated that the term failure cannot be defined as a cataclysmic event but as just another mining problem.

Figure 1-1 shows the study area. Johnson (1982) described the slide. In November of 1979 a planar slide on the North wall of 51-B-2 pit took place. The zone was 245 metres in length and 106 metres high containing an estimated volume of 1.07 million cubic metres. The initial movement of 0.03 metres was first noticed on May 24 , 1979 from the results of the weekly monitoring program in that pit. The weekly monitoring frequency was maintained for the next five months with the movement continuing at the rate of 0.03 metres per week. On October 29 , there was a jump of 0.06 metres per day. Then on the morning of November 10 , 1979 , there was a jump of 0.34 metres horizontally and 0.15 metres vertically from the previous day's data. At this point in time continuous monitoring of slope distance , on a half hourly basis , was performed. This continued until mid afternoon when the difference between successive EDM readings had reached 2 Cm. By five O'clock that same day , the movement had somewhat stabilized to a rate of 0.06 metres per day. The total movement for the eight hour period was 2.65 metres horizontally and 1.52 metres vertically. It must be mentioned that by October 29 , the cracking in the wall slope had defined the size of the slide , and the area of influence on the pit floor was cordoned off to equipment and personnel. The mining continued in the rest of the pit and was only shut down for the one day of November 10 , 1979.

Chapter 2

GEOLOGY AND THE SLIDE

2.1 General

This chapter summarizes several reports and papers. The stratigraphy of the coal property at Cardinal River Coals Ltd. is described. A more detailed geotechnical investigation of the north wall of 51-B-2 pit is given. The causes of slides at this location are evaluated. Finally the strength parameters for the slide are estimated by the use of a back analysis.

2.2 Mine Geology

Wyllie and Munn (1979) and Munn (1983) described the mine geology.

The coal occurrs in the Luscar Group which is of Lower Cretaceous age. Two major faults, the Nikanassin Thrust to the southwest and the Folding Mountain Thrust to the northeast, formed the boundaries of the Luscar Formation in the area. These rocks are folded into synclines and anticlines whose fold axes trend approximately 300. Faulting and jointing has accompanied the folding (Hill , 1980 Figure 16). Luscar Formation consists of interbedded shales, sandstones and coal. The one mineable coal seam , the Jewel Seam , varies in thickness from 10 to 12 metres along the limbs of the folds to 60 metres at the crests and troughs.

A stratigraphic column for the Cardinal River area is illustrated in Figure 2.1 which has been compiled from Hill (1980) and McLean (1982).

2.3 Geotechnical Investigation of the North Wall of 51-B-2 Pit

2.3.1 Introduction

Section 2.3 outlines the results obtained from the geotechnical investigation which was reported by Milligan and Hebil (1980). This included a field mapping program which was undertaken on November 20 and 21 , 1979 to determine the geology at the slide location in the pit. Results of the stability analysis which was carried out in terms of a back analysis are presented in section 2.4.

2.3.2 North Wall Geology

The geology of the north wall was dominated by an interbedded series of sandstone and siltstone beds which dipped into the pit at an average angle of 38 degrees and a range of 35 to 40 degrees. Strong variations in the bedding attitude were caused by local structural features. Milligan and Hebil (1980) divided the wall into two portions which were bounded by the eastern extremity of the wall failure at approximately 104,600E.

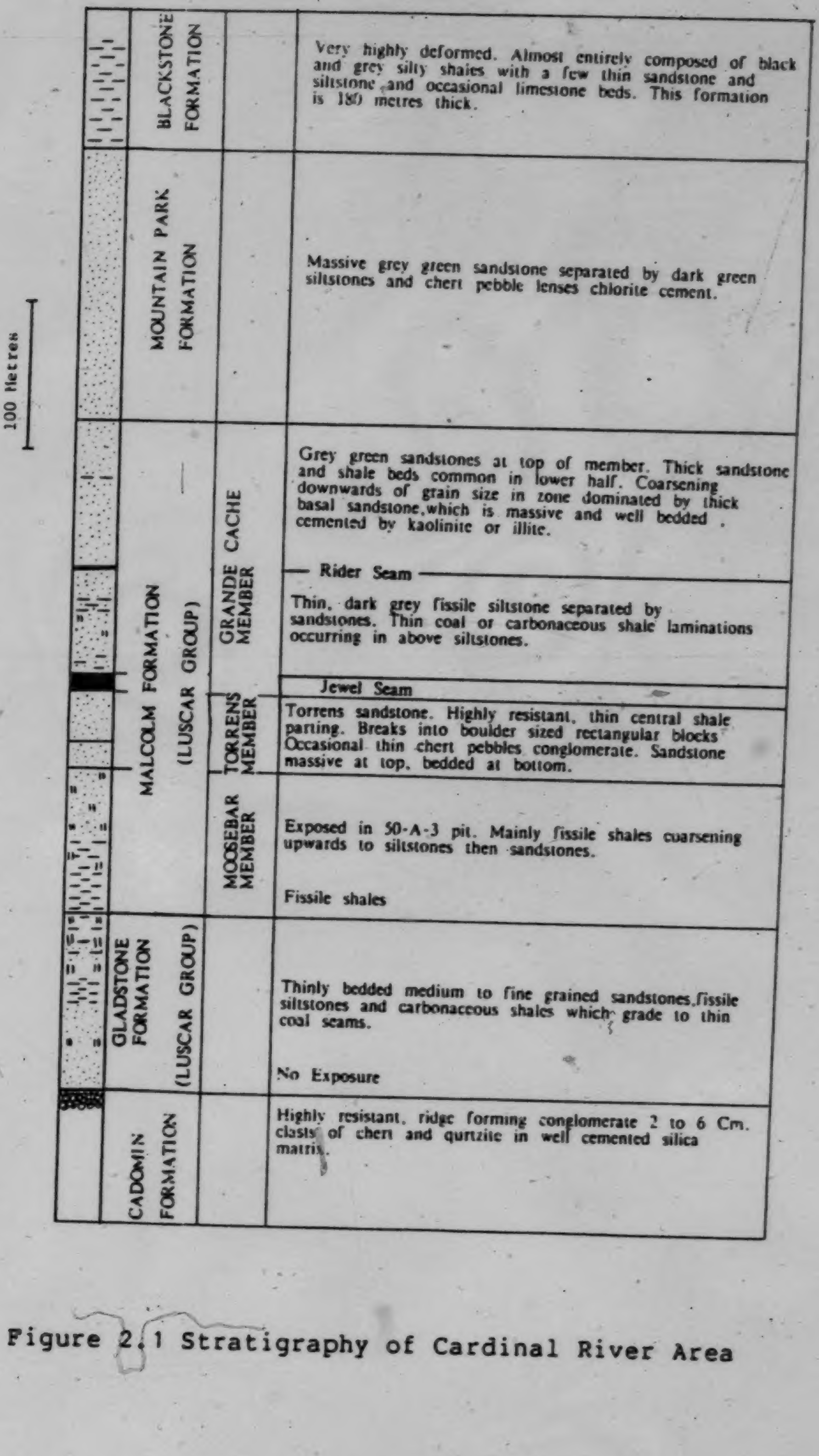

BLACKSTONE FORMATION		Very highly deformed. Almost entirely composed of black and grey silty shales with a few thin sandstone and siltstone and occasional limestone beds. This formation is 180 metres thick.
MOUNTAIN PARK FORMATION		Massive grey green sandstone separated by dark green siltstones and chert pebble lenses chlorite cement.
MALCOLM FORMATION (LUSCAR GROUP)	GRANDE CACHE MEMBER	Grey green sandstones at top of member. Thick sandstone and shale beds common in lower half. Coarsening downwards of grain size in zone dominated by thick basal sandstone,which is massive and well bedded , cemented by kaolinite or illite. Rider Seam Thin, dark grey fissile siltstone separated by sandstones. Thin coal or carbonaceous shale laminations occurring in above siltstones. Jewel Seam
	TORRENS MEMBER	Torrens sandstone. Highly resistant, thin central shale parting. Breaks into boulder sized rectangular blocks Occasional thin chert pebbles conglomerate. Sandstone massive at top, bedded at bottom.
	MOOSEBAR MEMBER	Exposed in 50-A-3 pit. Mainly fissile shales cuarsening upwards to siltstones then sandstones. Fissile shales
GLADSTONE FORMATION (LUSCAR GROUP)		Thinly bedded medium to fine grained sandstones,fissile siltstones and carbonaceous shales which grade to thin coal seams. No Exposure
CADOMIN FORMATION		Highly resistant, ridge forming conglomerate 2 to 6 Cm. clasts of chert and qurtzite in well cemented silica matrix.

Figure 2.1 Stratigraphy of Cardinal River Area

2.3.2.1 East Portion of the Wall

Figure 2.2 shows the east portion of the north wall. I have drawn Figure 2.3 from several reports and maps (Luscar Ltd. , 1980 , Milligan and Hebil , 1980 , Hebil , 1980). This figure illustrates the changes in bedding attitude along the north wall. The bedding in the eastern half of the pit wall was more uniform and planar than the western half where the slide occurred. An east-west striking thrust fault was identified by Rogan (1978). It dipped steeply to the south and was recognized to be associated with the tight chevron folding of the strata in this area as observed in the north end of the east wall (Figure 2.4). This fault did not occur anywhere in the north wall and was not involved in the north wall slide.

2.3.2.2 West Portion Of The Wall

The west part of the north wall contained the November , 1979 slide. In this area , the bedding was planar and dipped at an overall average angle of 38 degrees. As Figure 2.3 illustrates , a range of bedding values were found. Bedding values between 23 and 34 degrees appeared to be quite common in this portion of the pit wall.

The gentle undulations of the bedding mentioned above were found to steepen rapidly over a distance of 5 to 10 metres. This change in the bedding dip appeared to be related to a flexure which was restricted to the

Figure 2.2 The east portion of the north wall. Notice benching into sandstone below coal seam towards west. Section B-B lies beyond the left margin of the picture , now covered by post slide berm. Photograph taken by S. Masoumzadeh on 11 August , 1983.

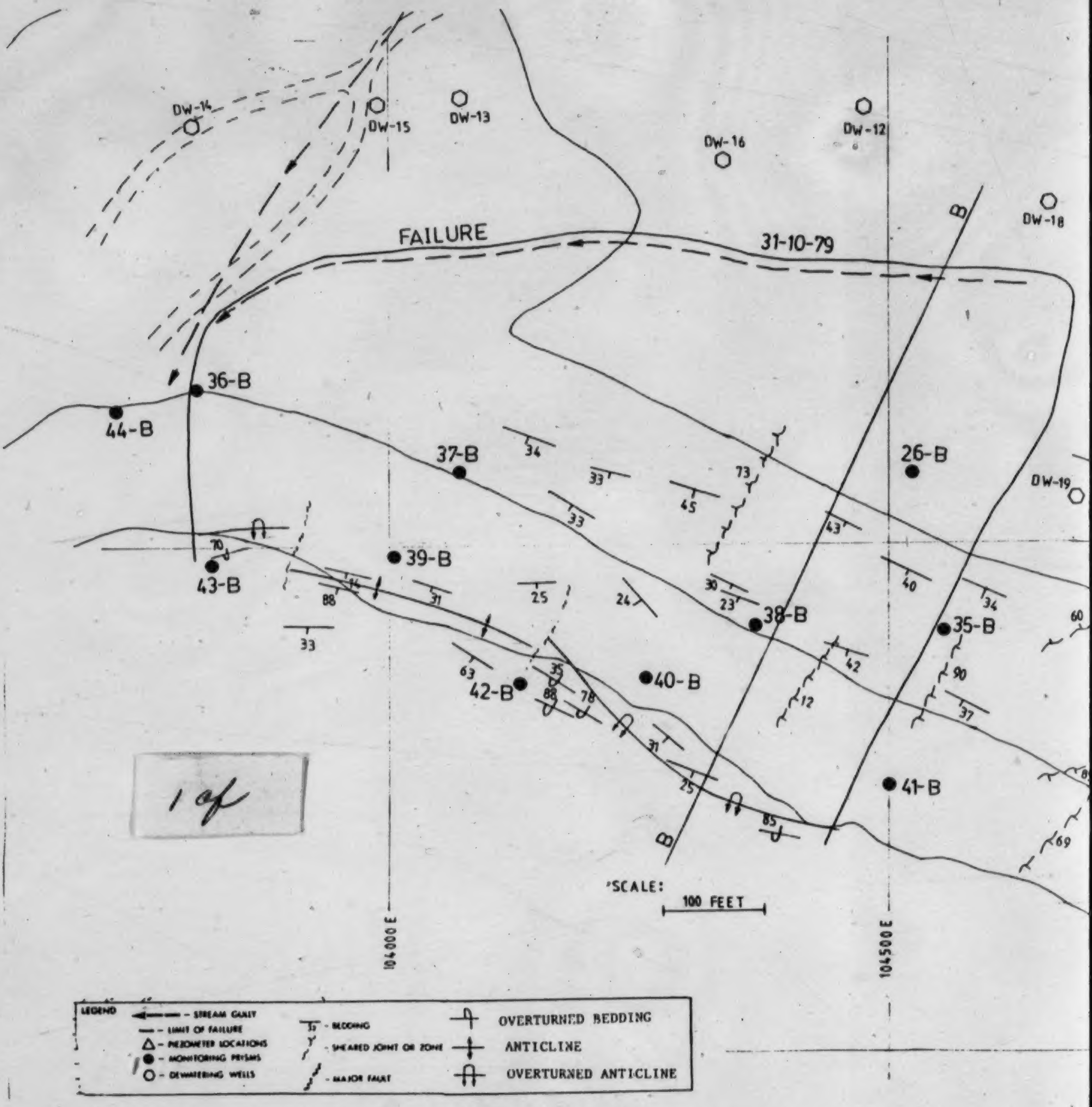
FAILURE
31-10-79
DW-14
DW-15
DW-13
DW-16
DW-12
DW-18
DW-19
B
B
36-B
44-B
37-B
26-B
39-B
43-B
38-B
35-B
40-B
42-B
41-B
SCALE:
100 FEET
104000 E
104500 E
LEGEND
STREAM GULLY
LIMIT OF FAILURE
PIEZOMETER LOCATIONS
MONITORING PRISMS
DEWATERING WELLS
BEDDING
SHEARED JOINT OR ZONE
MAJOR FAULT
OVERTURNED BEDDING
ANTICLINE
OVERTURNED ANTICLINE

1 of

Figure 2.3 The north wall in the 51-B-2 pit. See Figure 1.1 for the pit location.

2 of 2

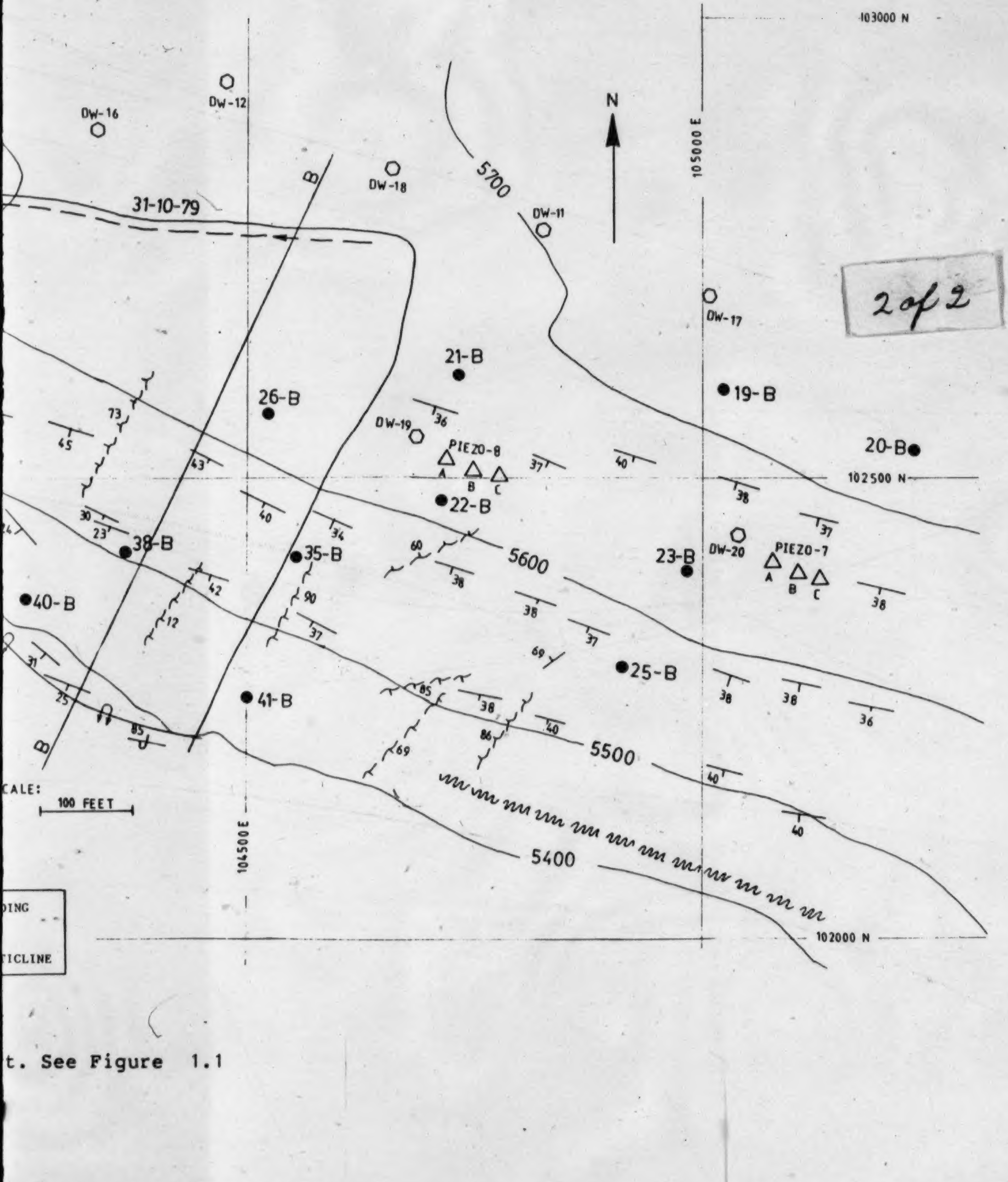
103000 N
105000 E
N
DW-16
DW-12
DW-18
DW-11
DW-17
5700
31-10-79
B
21-B
26-B
19-B
20-B
DW-19
PIEZO-8
A
B
C
22-B
102500 N
38-B
35-B
40-B
23-B
DW-20
PIEZO-7
A
B
C
5600
25-B
41-B
5500
5400
102000 N
104500 E
B
CALE:
100 FEET
DING
TICLINE
73
45
43
30
23
40
34
36
37
40
38
37
60
38
42
12
90
37
38
37
69
38
38
36
31
25
85
85
38
40
69
86
40
40

t. See Figure 1.1

Figure 2.4 The north end of the east wall. Photograph taken by S. Masoumzadeh on 11 August , 1983.

bottom of the wall. This fold whose limbs rapidly steepen in dip , locally resulted in overturned bedding which dipped to the north. These abrupt changes in bedding attitude were not observed further east than line 104,500 (Figure 2.3).

This structure was also observed in the western end of the pit at 103,500 east and 102,500 north , where there was no movements. This observation rejects the possibility that the slide caused this change in the dip of the bedding at the toe of the failed slope.

The part of the north wall , east of the slide , showed no indication of steeply dipping beds. This might have resulted from the divergence in the strike of the fault and fold planes with respect to the wall azimuth.

2.3.3 Jointing

A contoured sterographic plot of 260 poles to bedding , joint and shear surfaces constructed from data obtained by Luscar in September , 1979 and EBA in May, 1979 , provided the planar features listed in Table 2.1 (Milligan and Hebil , 1980).

The joint distribution pattern indicated that there was a direct relationship between the joint sets and the bedding. The intersection of the great circles of the joint planes illustrated in Figure 2.5 was nearly coincident with the pole concentration of the bedding planes. This indicated that the plunge of the line of intersection of these joint

Table 2.1 Attitude of joints and bedding in 51-B-2 pit north wall

STRUCTURE	DIP/DIP DIRECTION
BEDDING	38/204
J1	79/303
J2	54/011
J3	70/074
J4	58/053

sets was perpendicular , within ±5° variations , to the bedding planes and plunged into the wall at an azimuth of 023 degrees with a dip of 55 degrees. Figure 2.6 shows major joints and faults in the north wall.

2.3.3.1 Joint Set Interpretation

The joint sets summarized in Figure 2.5 were interpreted as follows ; Joint set J1 and the J3-J4 set were considered to be conjugate strike / slip shears which resulted from the major stress acting perpendicular to the strike of the bedding. The joint set J2 was sub-parallel in strike to the bedding and dipped at right angles to it. This set was likely to have resulted from the folding and buckling of the bedding and was therefore interpreted to be a joint set which had undergone extension. Milligan and Hebil (1980) stated that this interpretation was in agreement with what was normally found in this part of the Rocky Mountain area.

2.3.4 Faulting

The main fault mechanism observed in the 51-B-2 pit area was that of normal faulting as part of process of folding. No other fault attitudes were identified. However , moderate to intensly sheared joint surfaces parallel to the J1 joint set and , to a smaller degree , the J3-J4 joint sets , were observed. No apparent displacements were observed on these joint sets . It was likely that some movement occurred within highly broken rocks but it was

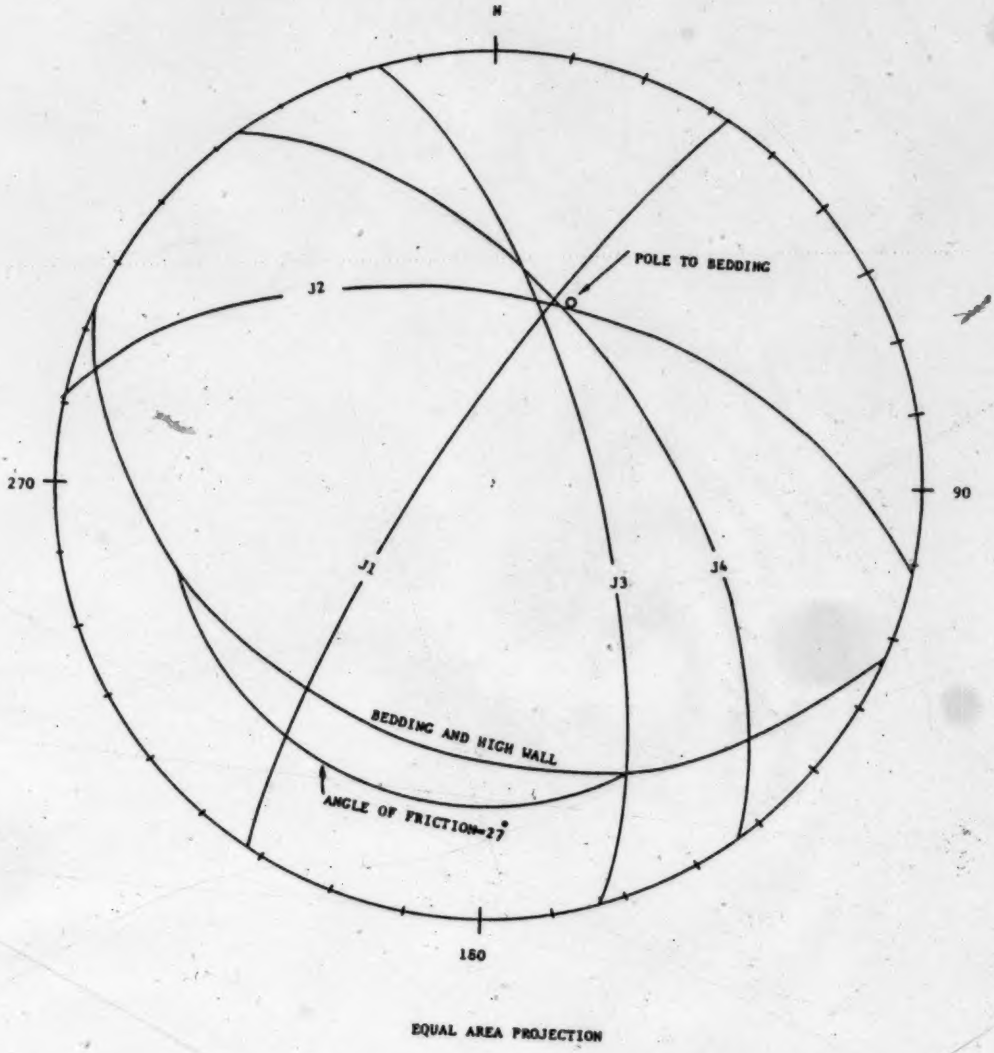
N
POLE TO BEDDING
J2
270
90
J1
J3
J4
BEDDING AND HIGH WALL
ANGLE OF FRICTION=27°
180
EQUAL AREA PROJECTION

Figure 2.5 51-B-2 pit north wall plot of great circles of joint planes and all potential wedge intersections

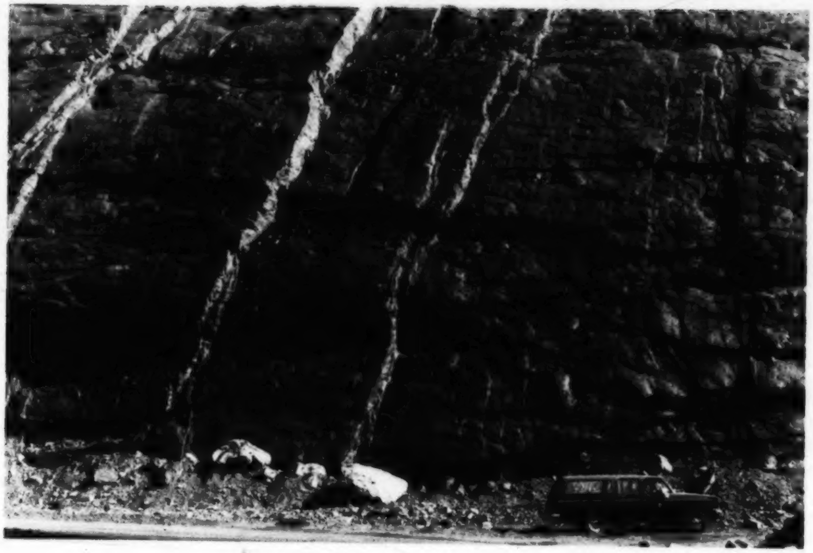

Figure 2.6 Major joints and faults in the north wall. Photograph taken by S. Masoumzadeh on 11 August , 1983.

probably of a local , limited extent in the pit area.

2.3.5 Joint Sets Versus Movement Interpretation

Milligan and Hebil (1980) observed tension cracks opened parallel to the attitude of joint set J1. This joint set , combined with the bedding plane and joint set , J2 , resulted in the major tension cracks which defined the east and west extent of the pit wall slide. The eastern portion of the main tension crack which cuts through the wall occurred in an area where the J1 joint frequency was higher than normal. The joint plane spacing here was commonly 5 to 10 centimetres whereas in most other parts of the wall , spacing on joint J1 was 30 to 90 centimetres (Milligan and Hebil , 1980). In this area , the J1 joint surfaces were found to be sheared and , over a distance of 50 metres , the J1 joint surfaces were iron-stained.

The J3 and J4 joint sets were generally more weakly sheared. Spacing between these joint surfaces was 30 to 60 centimetres. This pattern was found across the entire north wall.

Joint J2 was generally not observed to be sheared or altered. However , in the area of the pit where the bedding was steeply dipping or overturned , the failure surface has been found to develop along this joint set. In these areas , joint J2 was sub-horizontal which facilitated the development of the failure surface along this joint set (Milligan and Hebil , 1980).

2.3.6 Lithology

Due to the lack of coreholes and limited exposure , a cross-section of the lithology through the north wall to the movement surface could not be documented. Rocks observed on the surface of the north wall however , were found to be predominantly sandstone. This rock was not massive and was found to be locally interbedded with thin siltstone and coal seams. Bedding plane partings were usually striated and indicated a northerly movement of the upper beds.

In the north western end of the wall , thick beds of mudstone clast conglomerate predominated. This area coincided with the north western extremity of the main tension crack. These observations showed that for at least the exposed portions of the north wall , sandstone was interbedded with weaker coal and rock units. This was expected since these rocks occurred immediately below the Jewel coal seam. Although not confirmed by observations , there was a good possibility that other weak beds occurred further back in the wall and were likely to have contributed to wall instability. This was indicated by an east trending linear depression in the original topographic contours which coincided with the azimuth and position of the main tension crack.

2.3.7 Hydrological Observations

No seepages of ground water was observed on the north wall during the field mapping portion of the geotechnical investigation. This agreed with the piezometer data discussed in Section 3.3.4. Generally , groundwater elevations in the north wall area were found to be low.

Examination of pre-pit development topographic maps show that there were small gullies which were probably associated with intermittent streams in the immediate area of the wall failure. Figure 2.3 illustrates the position of these gullies with respect to the wall failure. These gullies coincided with the north and west portion of the main tension crack. During spring thaw and after heavy rains , it was expected that these gullies would have active streams draining the surrounding area and that some of the water would drain into the tension cracks adding to the problem of instability if these cracks were filled with water and did not freely drain.

2.3.8 Wall Slide-Geology Working Hypotheses

The following interpretations were made by Milligan and Hebil (1980) regarding the geology of the 51-B-2 north wall and the wall failure ;

1. The wall slide did not occur through intact rock but along previously formed bedding and joint planes.
2. Tension cracks preferentially developed along J1 as well as J2 and the J3-J4 joint sets.
3. The eastern extremity of the main tension crack cut across the north wall within a 60 metres wide zone where the J1 joints were moderately to strongly sheared.

4. The western extremity of the main tension crack cut across the wall in an area where (a) the wall changed azimuth and (b) weaker mudstone clast conglomerate beds were abundant.
5. The main tension crack along the back of the wall was found to be sub-parallel to the strike of the bedding and coincided with a local topographic depression. This depression was likely to be a manifestation of either a weak bedding layer or a thrust fault zone , along which the wall had slid. Local surface water drainage occurred along this depression.
6. Frequently , thin coal and siltstone laminations were found interbedded with sandstone beds. Most bedding plane partings were slickensided. The bedding dipped into the pit at angles as low as 23 degrees. This indicated that , at least on a local scale , the bedding would "daylight" in the pit.
7. A zone of steeply dipping and overturned bedding was found at the toe of the slide and was continuous into the western extremity of the pit where no failure of the wall occurred. This zone was likely to be related to the tight chevron folding observed in the eastern wall of the pit. This abrupt variation in bedding was not found in the stable eastern half of the pit wall.
8. In areas where the bedding dipped steeply , the joint set J2 , which was perpendicular to the dip of the bedding , would lie in a sub-horizontal attitude. This joint and

bedding geometry was restricted to the toe of the wall. In this area , the J2 joint set was found to be sheared and movement related to the slide occurred along these planes , resulting in overhang and toppling as the upper mobile portion of the wall moved towards the pit over the lower portion of the wall.

2.4 Back Analysis

Assuming the geometry of the pre-failure conditions of the north wall , a stability analysis was undertaken by Milligan and Hebil (1980) to determine the strength parameters in the rocks to result in a factor of safety of unity , i.e. , for slide to occur. As noted in Section 2.3.8 , it was felt that the wall movement was geologically controlled and involved sliding along a weak zone parallel to bedding. To accommodate this model , the configuration shown in Figure 3.10 (without the stabilizing berm) was used to assess the movement. The slide surface included a steep surface at the back of the wall and an approximately horizontal surface at the toe. The former surface followed the weak zone parallel to the bedding and the latter the effect of overturned bedding at the toe. The assumed water pressure acting on the back of the failure surface were also shown.

From the analysis the factors of safety summarized in Table 2.2 were obtained. The stability analysis used was the Janbu Composite Failure Analysis and all analyses were performed on the computer (Milligan and Hebil , 1980).

Assuming the water pressure distribution to be approximately accurate , the analysis indicated the strength parameters required for a factor of safety of unity. These values were consistent with typical strength values found elsewhere for the conditions assumed in the north wall.

2.4.1 Conclusions

Milligan and Hebil (1980) concluded that the instability in the north wall of 51-B-2 had resulted from adverse geological conditions , namely , a weak zone sub-parallel to the wall intersecting overturned beds at the toe of the wall. They also stated that Pore-pressures , as indicated from the piezometric levels in the standpipe nests , contributed to the failure.

Table 2.2 Back analysis results

STRENGTH PARAMETERS				FACTOR OF SAFETY
ACROSS BEDDING		WEAK ZONE		
COHESION	ANGLE OF FRICTION	COHESION	ANGLE OF FRICTION	
0	37	0	27	1.043
0	35	0	27	1.025
0	37	0	25	0.971

Chapter 3

MONITORING PROGRAM AND REMEDIAL MEASURES

3.1 Introduction

Munn (1983) explained the philosophy behind the monitoring program and the subsequent remedial measures.

The wall control program at Cardinal River Coals Ltd. was based on the premise that the walls were going to move. Monitoring was to confirm when. The program consisted of monitoring slope movements and piezometric levels as well as structural mapping and visual inspections (See Chapter 2). In case of excessive movement , the frequency and intensity of the monitoring was increased and , suitable remedial action was undertaken such as cutting down the crest , building up the toe , depressurization of the wall , artificial support , or a combination of the above. If remedial action was not possible , monitoring permitted operations to continue up to near the time of failure.

At the design stage , the emphasis was on identifying the potential movement mechanisms and the consequences of slide. Once the potential movement mechanisms were identified , a monitoring system could usually be employed to give sufficient response time , and providing the consequence of slide was not severe or remedial action could be taken to arrest the movements , then it was practical to mine pit slopes which have a higher probability of slide.

The primary method of displacement monitoring at Cardinal River Coals Ltd. employed electronic distance measuring (EDM) using AGA-122 Semi-Total Station and 3" Retro-Ray prisms. Background readings were taken weekly. If unusual movement was detected , additional monitoring points were established , and the monitoring frequency was increased to daily or hourly.

Piezometers supplemented the distance monitoring by providing information on ground water levels. Most failures were associated with an increase in groundwater levels.

Remedial action in case of impending slides consisted of doing as many of the following as possible ; cut down the crest , build up the toe , and depressurizing the wall. In some situations artificial support of the wall was employed where the other options were not possible. The application of monitoring and remedial actions permitted Cardinal River Coals to mine under walls which might otherwise be considered unsafe.

3.2 Slope Movements Measurements

Wyllie and Munn (1979) outlined methods of measuring slope movements.

Instrument stations are established opposite the slide , and their positions are determined from a reference station on stable ground some distance from the pit. It is essential that the position of the instrument stations be checked against the reference , because the slope beneath the instrument stations may also be moving. Monitoring points are established on the slide and by regularly determining their positions the movement of the whole slide can be obtained. These points should also be established behind , and to either side of , the expected extent of failure , so that the limits of instability as well as any increase in its size can be determined.

Johnson (1982) described the following surveying technique which may be employed.

3.2.0.1 Radial Survey Method

The standard method employed by industry today is the Radial Survey Method using a theodolite-EDM system , where the EDM prisms are permanently fixed to the highwall and the measurements taken from a single base station situated on stable ground opposite the highwall. By measuring the slope distance and the horizontal and vertical angles , the three dimensional position of each prism is obtained , from which vectors of movement between successive readings can be calculated. A standard deviation of 1.5 centimetres can be expected following recommended reading procedures of at least one set of angular observations and averaging four slope distance measurements per prism.

The simplest method of surveying involves measuring the distance between the instrument station and prisms on the slope. For this method to be accurate it is essential that measurements be made parallel to the expected direction of movement ; otherwise only a component of the movement will be measured. Information on the approximate vertical movement can be obtained by measuring the vertical angle to each station as well as the slope distance. This will give an indication of the mode of failure , since a toppling slide will tend to move horizontally , while in a circular slide the prisms will tend to move parallel to the movement surface.

Much additional information on the mechanism of slope movement can be obtained by finding the coordinates and elevation of each station , from which vectors of movement between successive readings can be calculated. If there is only one instrument station , angles can be turned from the reference station to each prism , and the distance measured with EDM equipment. If there are two instrument stations , the position of each prism can be determined either by triangulation , or by trilateration using EDM equipment. Best results are obtained if the three points form an equilateral triangle , and this should be taken into account when setting out the baseline between the instrument stations.

Another alternative , which does not require the measurement of any angles , is to determine the distance of the prisms from three stations forming a tetrahedron (Hedley 1969).

EDM measurements are rapid and accurate , and surveying is useful in that it gives the three-dimensional position of each prism. Surveying does have the disadvantage though that the measurements and the calculations are time-consuming and results are not immediately available. Another disadvantage of the surveying technique is that it is not possible to make readings during heavy rainstorms or snowstorms , or when clouds obscure the targets , and thus a back up system of extensometers may be useful during extended periods of poor weather. Access to the slope to inspect prisms is also desirable. Triangulation , under ideal conditions , using a 1-second theodolite with all angles doubled , and an EDM measuring to ±1 millimetres over sight distances of 300 metres , can give errors in coordinate positions of as little as 3.05 millimetres (Yu and Hedley 1973). However , it is likely that mine surveyors doing routine measurements in all weather conditions using equipment in less than perfect adjustment will obtain average error of ±10 centimetres to ±15 centimetres. For this reason , coordinate determinations should only be carried out when the expected movement distance between readings is greater than the magnitude of error.

Displacement quantities will be analyzed in four forms ; slope distance , the distance between the base station and moving prism , and the resultants of the displacement vectors and cumulative horizontal and vertical displacements.

The conventional EDM monitoring system has limitations for slabbing type failures because :

1. it measures movement perpendicular to the wall , not parallel to it
2. it cannot discriminate between overall wall relaxation and differential movement along bedding planes.
3. turn around time on measuring is too slow
4. monitoring is not continuous but is done , at best , at hourly intervals.

In the case of slabbing type failures , the conventional EDM system is to be supplemented with borehole extensometers and micro-seismic measurement (Munn , 1983). The micro seismic system is relatively unproven in surface mining but has been used successfully in underground mining (Munn , 1983). In this system geophones implanted in the rock detect the noises of rock cracking. Increase in the level of cracking noises is an indication of impending failure.

3.3 Existing Data

MacRae (1982) stated that the slope deformation measurements were conducted using an electronic distance meter to measure slope distances , and a theodolite to measure horizontal and vertical angles to permanently placed retroreflector targets. Slope displacement data , supplemented by piezometric data where available , were utilized to evaluate the slides and to plan remedial measures. Milligan and Hebil (1980) reported the following sections about the prism movements and piezometric levels.

3.3.1 Prism Movements

Prisms which were initially placed in the slide area of the wall gave a continuous record of wall movements. The locations of these prisms are shown in Figure 2.3.

Slope distance measurements from the monitoring station to the prisms were taken at least once a day after the slide occurred. Also , three dimensional monitoring of the prisms were undertaken. Records of the prism movements are not presented here but are on file at Cardinal River Coals Ltd. Tables 3.1 and 3.2 show samples of the records. In general , the prism monitoring data indicated the following :

1. the greatest movements occurred at the west end of the failure zone.
2. during December 1979 , the prisms within the failure zone were indicating a rate of movement of between 2 to 4 millimetres per hour.

Monitoring of these prisms and others in the immediate areas was continuous. Additional prisms were placed at the east end of the pit to assess the possibility of movements in this area.

3.3.1.1 Summary Of Events

The following events happened in 1979 and were reported by MacRae (1982):

Day	Event
0-71	(5 March to 15 May) , Routine slope deformation measurements showed no indication of slope movement.
71-80	(15 to 24 May) , Target 26-B moved by 30 millimetres over a nine day interval. This was interpreted as probable wall movement.
80-126	(24 May to 9 July) , Target 26-B cumulative displacement increased gradually to 100 millimetres. Mine wall instability was assumed.
126-162	(9 July to 15 August) , No additional slope movement was detected.
162-175	(15 to 28 August) , Target 26-B cumulative displacement increased to 15 millimetres. Piezometer data showed rapid interconnection of previously separated aquifers.
175-239	(28 August to 30 October) , Target 26-B gradually accelerated as the slide velocity increased (Figure 3-6). On Day 238 , the cumulative displacement of Target 26-B was 60 centimetres , and the velocity average over the previous week was 1.5 millimetres per hour.
239-250	(30 October to 10 November) , Deformation measurements were conducted on a 24 hour basis , taking readings every half an hour.
250	(10 November) , The critical slide velocity 30 millimetres per hour was reached approximately 8 hours before total failure , and pit personnel and

equipment were evacuated. Total slope failure occurred at 12:45 P.M approximately 4 hours after evacuation was completed. Pit production was resumed soon after total failure.

3.3.2 Movement Hypotheses

Figure 3.1 suggests three hypotheses for movement. The first hypothesis assumes three blocks of rock mass , the second , two rotational and toppling blocks , and the third , two translating wedge and toppling blocks. First all hypotheses are described. Then , through a discussion of the hypotheses , a working movement hypothesis is presented.

First displacement measurements were taken in 1979 ; on 6 March for the 19-B , 21-B , 22-B , 23-B , 25-B and 26-B prisms , and , on 15 October for the 35-B prism , and , on 31 October for the 36-B , 38-B , 39-B , 40-B and 41-B prisms.

3.3.2.1 First Hypothesis

There are three blocks in this hypothesis. The first block , represented by the 19-B , 21-B , 23-B and 25-B prisms , is located at the east margin of the slide. It toppled away from J3 and J4 joint sets. The second block , identified by the 22-B , 26-B and 35-B prisms , is located next to the first block. It showed two independent modes of movement. The first movement resulted from toppling away from J3 and J4 , and the second , resulted from sliding down the dip direction of

C.R.C. SLOPE MONITOR SYSTEM

Data for: KR-7 Backsight: PC-30 Location: 51-8-2 Date: 10/Nov/79 Time: 9:00 A.M.

	----Today's Location (ft)----			--------Incremental Slope Movement--------						-Cumulative Slope Movement--			
Prism	Northing	Easting	Elev.	Last Date	Time	Horiz (ft)	Dir	Vert (ft)	Vector Rate (mm/hr)	Date Est	Horiz (ft)	Dir	Vert (ft)
19B	102591.91	105020.97	5731.56	09/Nov/79	4:30	0.04	263	0.04	01	06/Mar/79	0.36	260	-0.11
20B	102524.34	105229.22	5742.22	09/Nov/79	4:30	0.04	196	-0.05	01	06/Mar/79	0.23	260	-0.05
21B	102610.08	104732.14	5680.49	09/Nov/79	4:30	0.03	166	0.09	01	06/Mar/79	0.61	255	-0.15
22B	102474.79	104715.09	5634.14	09/Nov/79	4:30	0.02	213	0.02	00	06/Mar/79	0.98	244	-0.52
23B	102396.58	104986.21	5638.45	09/Nov/79	4:30	0.06	47	0.06	01	06/Mar/79	0.29	259	-0.06
25B	102295.74	104914.91	5568.37	09/Nov/79	4:30	0.09	216	0.02	01	06/Mar/79	0.42	252	-0.09
26B	102563.86	104518.94	5632.37	09/Nov/79	4:30	0.97	230	-0.48	20	06/Mar/79	4.54	235	-2.34
27B	101704.41	105968.84	5702.51	09/Nov/79	4:30	0.01	66	0.04	01	06/Mar/79	0.10	307	0.09
28B	101200.36	105704.38	5699.13	09/Nov/79	4:30	0.04	185	0.03	01	06/Mar/79	0.04	0	0.05
29B	100999.80	105657.82	5697.58	09/Nov/79	4:30	0.01	297	0.01	00	06/Mar/79	0.07	292	0.04
30B	100587.02	105378.46	5698.15	09/Nov/79	4:30	0.01	165	0.03	01	06/Mar/79	0.05	295	0.03
31B	100410.75	105219.61	5699.37	09/Nov/79	4:30	0.02	251	0.02	00	06/Mar/79	0.04	324	0.05
32B	100204.55	105105.59	5704.18	09/Nov/79	4:30	0.02	203	0.00	00	06/Mar/79	0.05	340	0.01
33B	99349.39	104603.62	5697.15	09/Nov/79	4:30	0.16	304	-0.02	02	06/Mar/79	0.17	321	0.03
34B	99694.47	104773.46	5634.94	09/Nov/79	4:30	0.03	194	0.00	01	06/Mar/79	0.07	[illegible]	0.03
35B	102414.91	104556.40	5566.46	09/Nov/79	4:30	0.28	226	-0.08	05	15/Oct/79	1.17	223	-0.50
36B	102657.74	103808.42	5505.92	09/Nov/79	4:30	0.08	207	0.10	02	31/Oct/79	0.54	196	0.16
37B	102570.76	104069.09	5504.46	09/Nov/79	4:30	1.71	207	-0.64	33	31/Oct/79	4.94	211	-2.04
39B	102485.58	104009.49	5433.36	09/Nov/79	4:30	1.59	201	-0.89	33	31/Oct/79	4.58	204	-2.71
40B	102369.30	104259.06	5435.99	09/Nov/79	4:30	1.30	199	-0.41	25	31/Oct/79	3.57	204	-1.15
41B	102263.39	104504.53	5436.99	09/Nov/79	4:30	0.79	190	-0.06	14	31/Oct/79	2.09	196	-0.22
44B	102635.90	103736.10	5503.37	09/Nov/79	4:30	0.04	80	-0.02	01	03/Nov/79	0.02	288	-0.23

Table 3.1 Slope prisms displacement monitoring results

Table 3.2 26-B prism displacement monitoring results

PRISM REPORT

Prism: 26B Established: 06/Mar/79 Base Station: KR-7

Obs. Date	Time	Northing	Easting	Elev	(ft) Horiz	Dir	(ft) Vert
06/Mar/79	12:00	102566.47	104522.66	5634.71	0.00	0	0.00
23/Mar/79	12:00	102566.48	104522.61	5634.69	0.06	288	-0.02
28/Mar/79	12:00	102566.47	104522.59	5634.72	0.07	270	0.01
24/Apr/79	12:00	102566.45	104522.56	5634.76	0.11	261	0.06
02/May/79	12:00	102566.41	104522.68	5634.78	0.06	165	0.08
08/May/79	12:00	102566.42	104522.62	5634.76	0.06	222	0.05
15/May/79	12:00	102566.39	104522.60	5634.69	0.10	221	-0.02
24/May/79	12:00	102566.38	104522.50	5634.64	0.18	242	-0.07
29/May/79	11:00	102566.34	104522.52	5634.66	0.19	299	-0.05
05/Jun/79	10:00	102566.36	104522.51	5634.65	0.19	234	-0.06
11/Jun/79	10:45	102566.38	104522.42	5634.62	0.26	251	-0.09
18/Jun/79	13:00	102566.39	104522.43	5634.63	0.25	252	-0.07
28/Jun/79	8:29	102566.44	104522.29	5634.72	0.37	267	0.02
03/Jul/79	10:30	102566.40	104522.40	5634.65	0.27	257	-0.06
09/Jul/79	10:00	102566.39	104522.36	5634.67	0.31	256	-0.04
17/Jul/79	13:10	102566.40	104522.41	5634.66	0.27	256	-0.05
23/Jul/79	9:15	102566.44	104522.40	5634.67	0.26	265	-0.04
30/Jul/79	9:50	102566.44	104522.36	5634.73	0.30	265	0.02
07/Aug/79	10:15	102566.39	104522.45	5634.67	0.23	252	-0.04
13/Aug/79	10:15	102566.42	104522.36	5634.67	0.31	261	-0.04
20/Aug/79	12:30	102566.36	104522.25	5634.56	0.43	255	-0.15
27/Aug/79	10:00	102566.30	104522.25	5634.50	0.45	249	-0.21
04/Sep/79	10:30	102566.21	104522.11	5634.50	0.60	245	-0.21
10/Sep/79	10:30	102566.21	104522.08	5634.44	0,64	246	-0.27
04/Oct/79	13:00	102566.14	104521.98	5634.39	0.75	244	-0.32
09/Oct/79	12:30	102566.08	104521.95	5634.39	0.81	241	-0.31
15/Oct/79	1:30	102566.08	104521.86	5634.36	0.89	245	-0.35
22/Oct/79	13:00	102566.03	104521.78	5634.24	0.98	244	-0.47
29/Oct/79	2:00	102565.65	104521.19	5633.85	1.68	241	-0.86
31/Oct/79	14:01	102565.52	104521.06	5633.90	1.86	239	-0.81
01/Nov/79	1:45	102565.47	104520.93	5633.71	1.99	240	-0.10
01/Nov/79	11:15	102565.64	104520.63	5633.72	2.20	248	-0.99
02/Nov/79	8:45	102565.45	104520.75	5633.62	2.17	242	-1.09
02/Nov/79	14:00	102565.42	104520.83	5633.67	2.11	240	-1.04
03/Nov/79	9:30	102565.26	104520.70	5633.60	2.31	239	-1.11
03/Nov/79	14:01	102565.32	104520.75	5633.57	2.23	239	-1.13
04/Nov/79	10:15	102565.22	104520.58	5633.55	2.42	239	-1.16
04/Nov/79	14:00	102565.24	104520.60	5633.49	2.40	239	-1.22
05/Nov/79	12:30	102565.13	104520.57	5633.47	2.48	237	-1.24

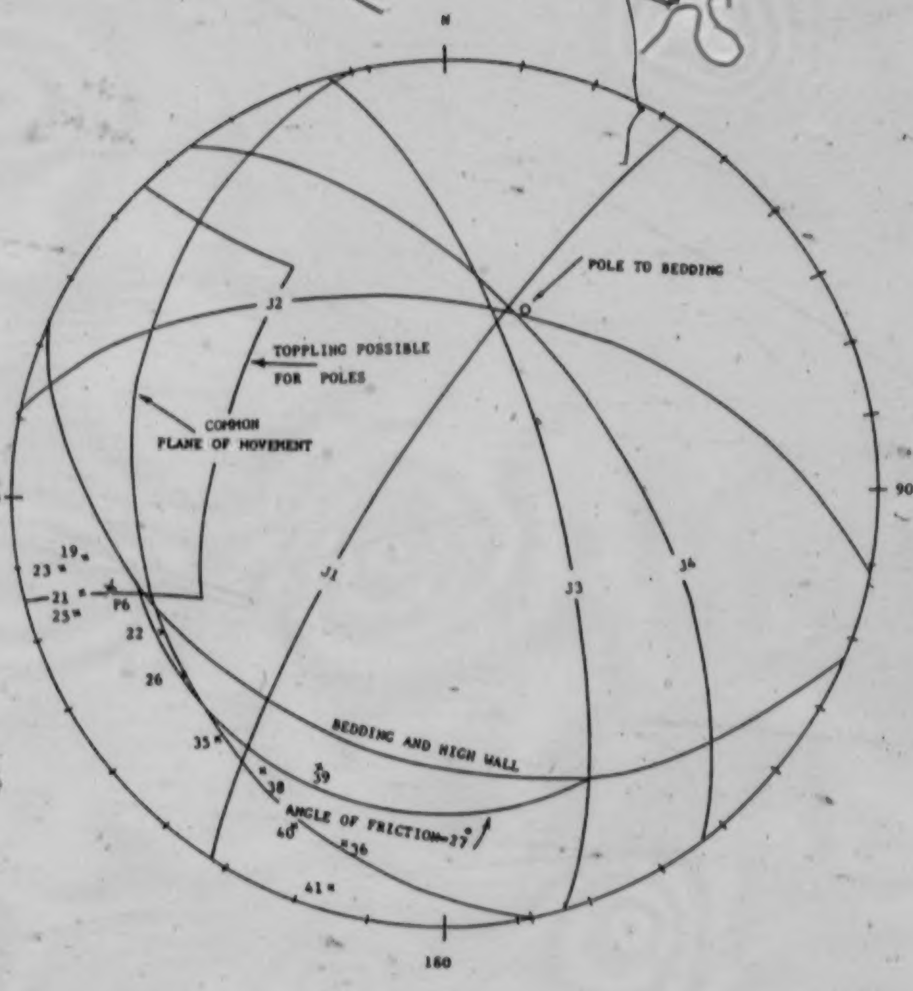
N
POLE TO BEDDING
J2
TOPPLING POSSIBLE
FOR POLES
COMMON
PLANE OF MOVEMENT
270
90
19
23
21
25
P6
22
26
J1
J3
J4
35
38
39
BEDDING AND HIGH WALL
ANGLE OF FRICTION-27°
40
36
41
180

EQUAL AREA PROJECTION

Figure 3.1 Discontinuities and orientation of the resultants of the displacement vectors at 9:00 A.M November 10th 1979

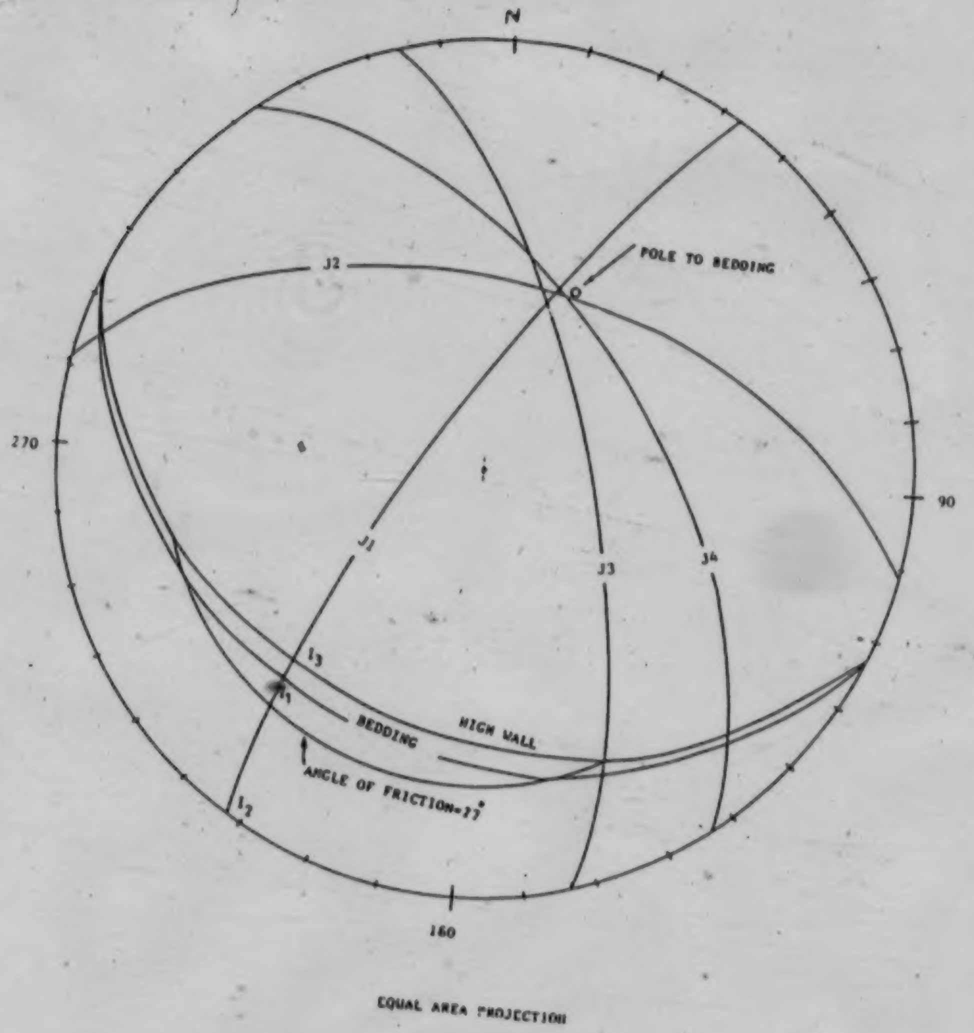
N
POLE TO BEDDING
J2
270
90
J1
J3
J4
I3
I1
BEDDING
HIGH WALL
ANGLE OF FRICTION=27°
I2
160
EQUAL AREA PROJECTION

Figure 3.2 Application of Hocking's rule

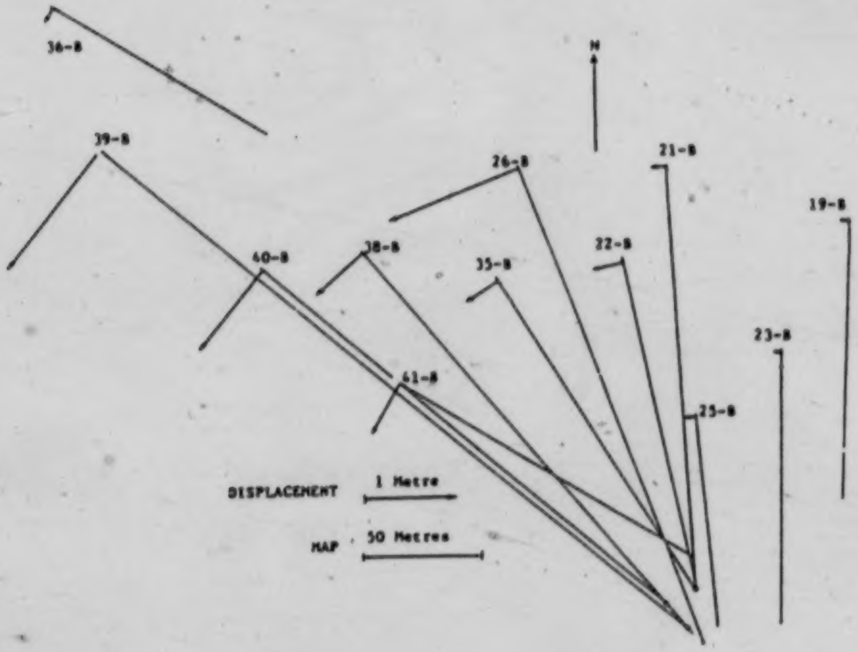
36-B
N
39-B
26-B
21-B
19-B
22-B
40-B
38-B
35-B
23-B
41-B
25-B
DISPLACEMENT
1 Metre
MAP
50 Metres

Figure 3.3 The resultants of the displacement vectors and centers of rotation on the common plane of movement at 9:00 A.M November 10th 1979

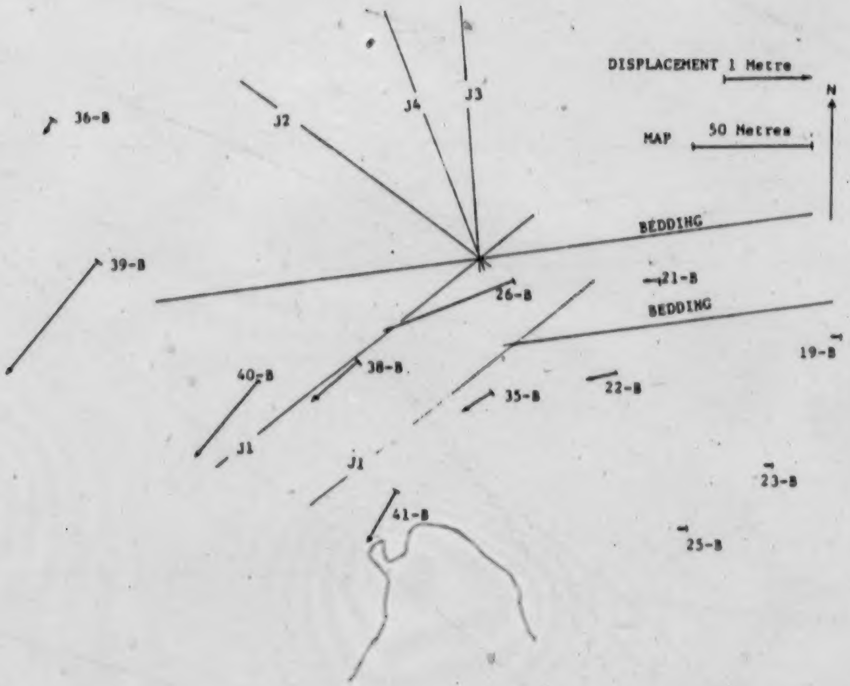
DISPLACEMENT 1 Metre
N
MAP 50 Metres
J2
J4
J3
36-B
BEDDING
39-B
21-B
26-B
BEDDING
19-B
40-B
38-B
22-B
35-B
J1
J1
23-B
41-B
25-B

Figure 3.4 The resultants of the displacement vectors and traces of discontinuities on the common plane of movement at 9:00 A.M November 10th 1979

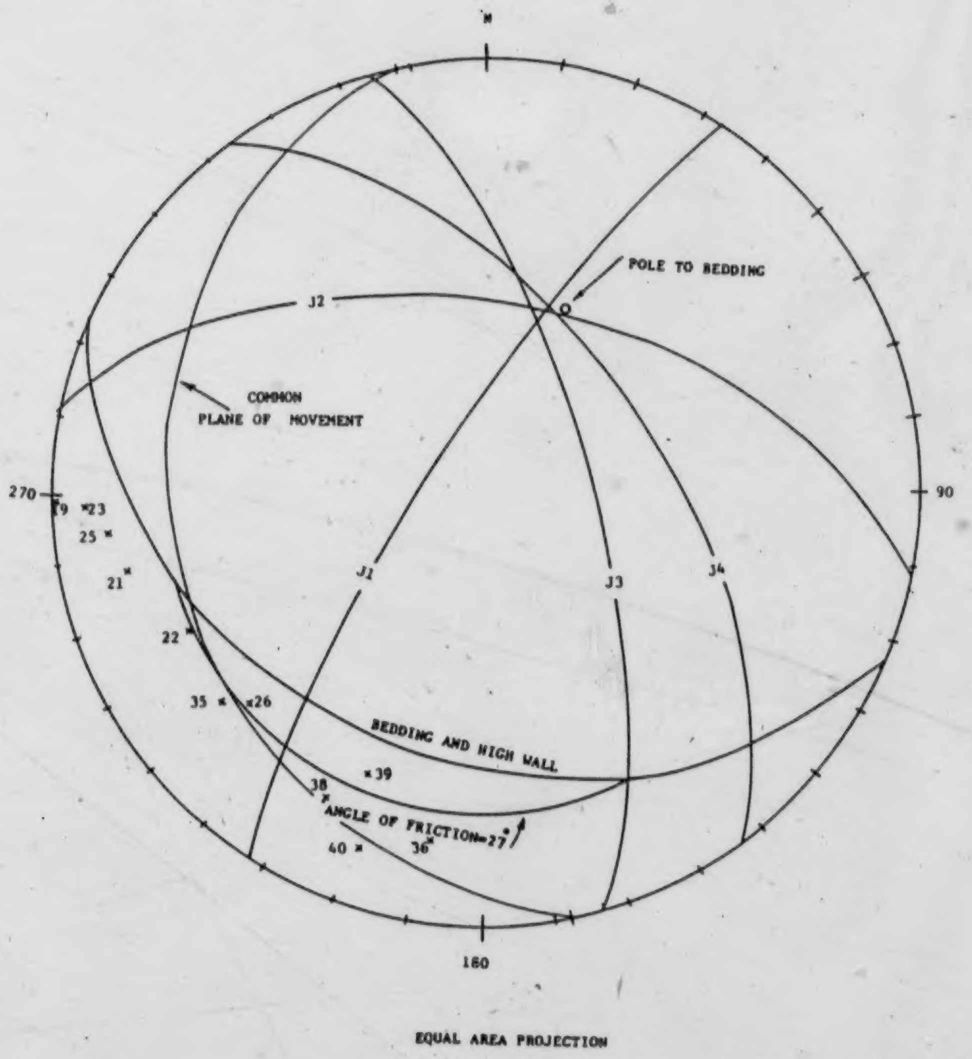
N
POLE TO BEDDING
J2
COMMON
PLANE OF MOVEMENT
270
90
19
23
25
21
J1
J3
J4
22
35
26
BEDDING AND HIGH WALL
39
38
ANGLE OF FRICTION=27°
40
36
180
EQUAL AREA PROJECTION

Figure 3.5 Discontinuities and orientation of the resultants of the displacement vectors at 5:00 P.M November 10th 1979

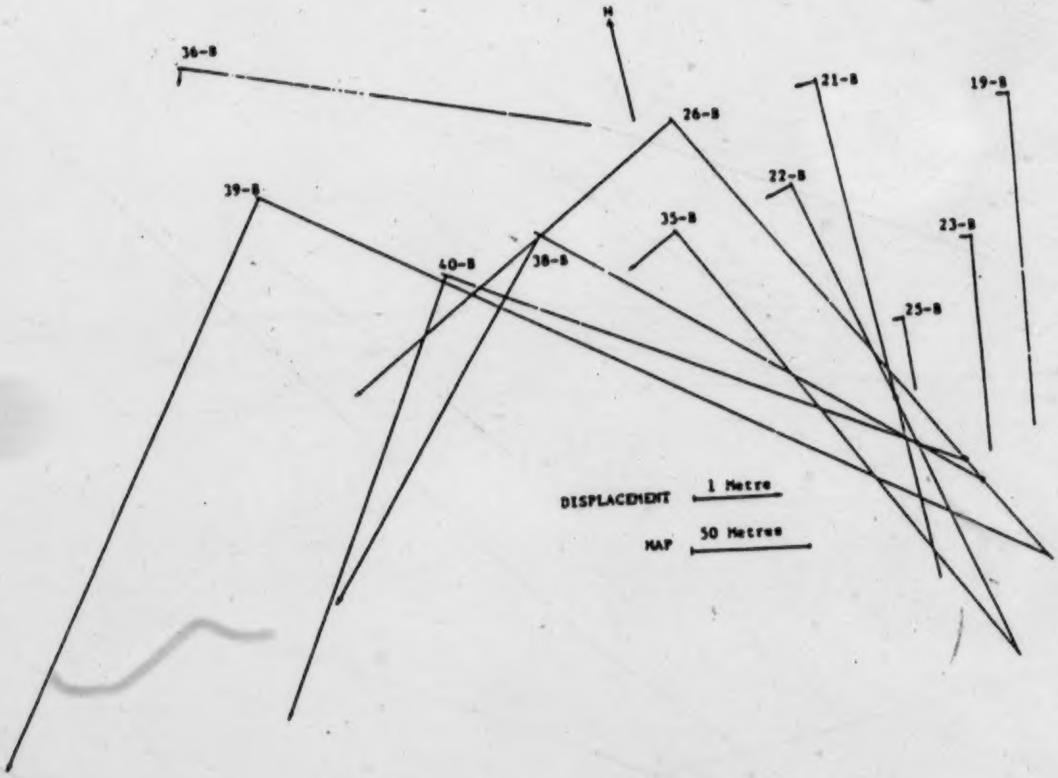
N
36-B
21-B
19-B
26-B
22-B
39-B
35-B
23-B
40-B
38-B
25-B
DISPLACEMENT
1 Metre
MAP
50 Metres

Figure 3.6 The resultants of the displacement vectors and centers of rotation on the common plane of movement at 5:00 P.M November 10th 1979

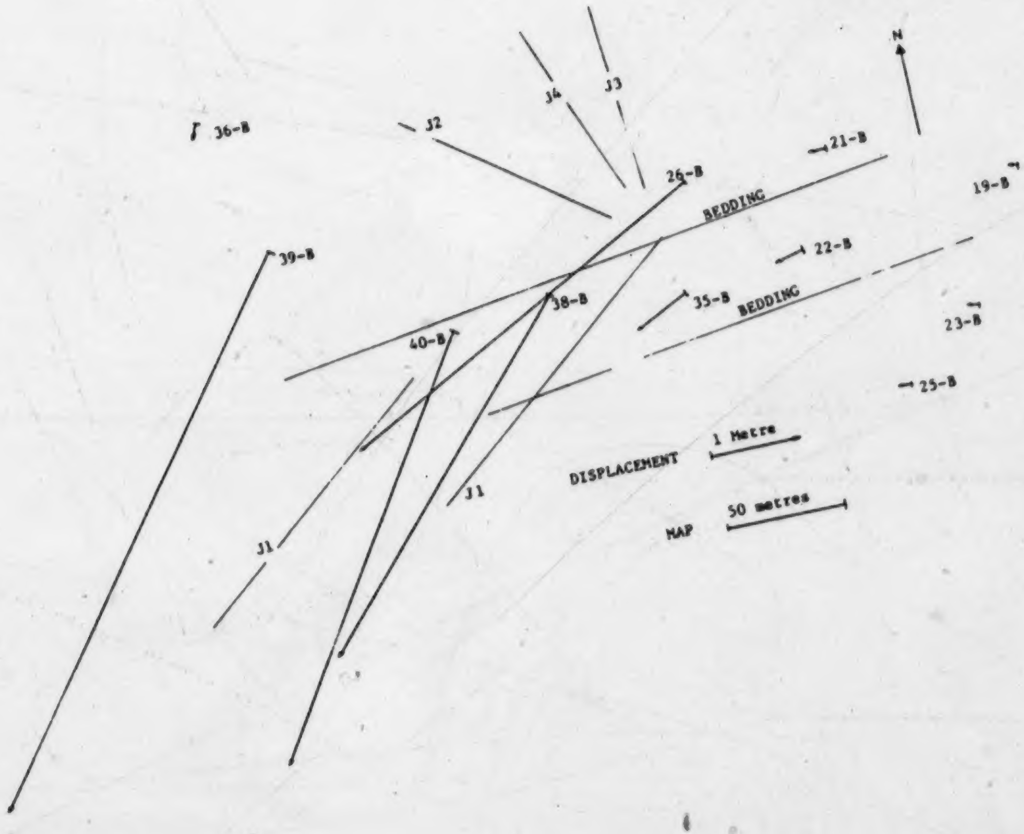
36-B
J2
J4
J3
N
21-B
26-B
19-B
BEDDING
39-B
22-B
35-B
BEDDING
38-B
23-B
40-B
25-B
1 Metre
DISPLACEMENT
J1
J1
50 metres
MAP

Figure 3.7 The resultants of the displacement vectors and traces of discontinuities on the common plane of movement at 5:00 P.M November 10th 1979

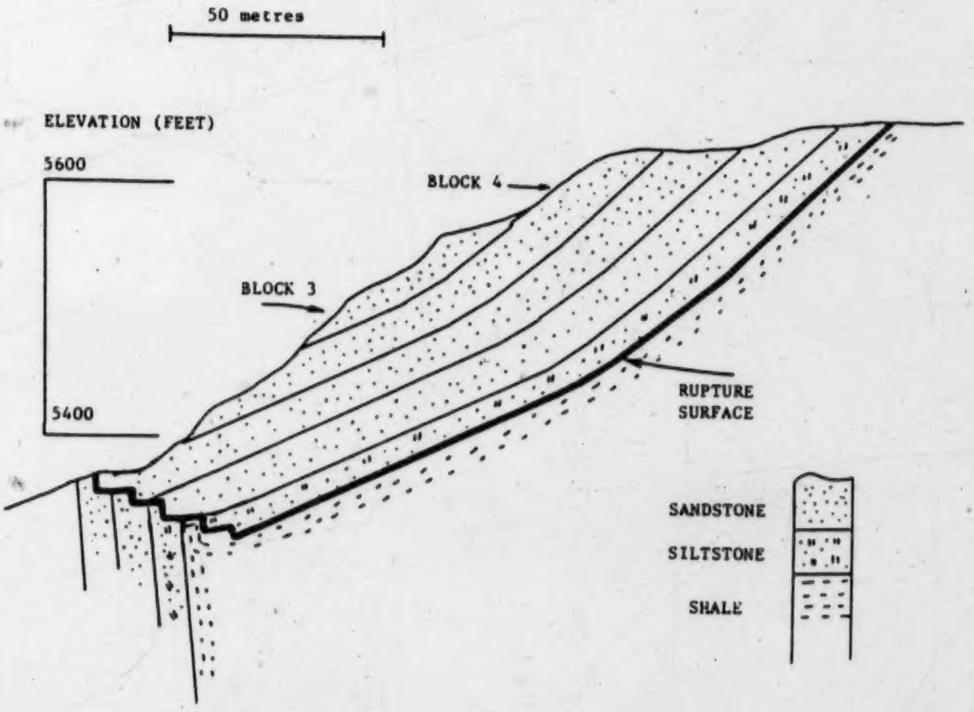
50 metres
ELEVATION (FEET)
5600
5400
BLOCK 4
BLOCK 3
RUPTURE SURFACE
SANDSTONE
SILTSTONE
SHALE

Figure 3.8 Cross section (B-B) in Figure 2.4 proposed by S.Masoumzadeh

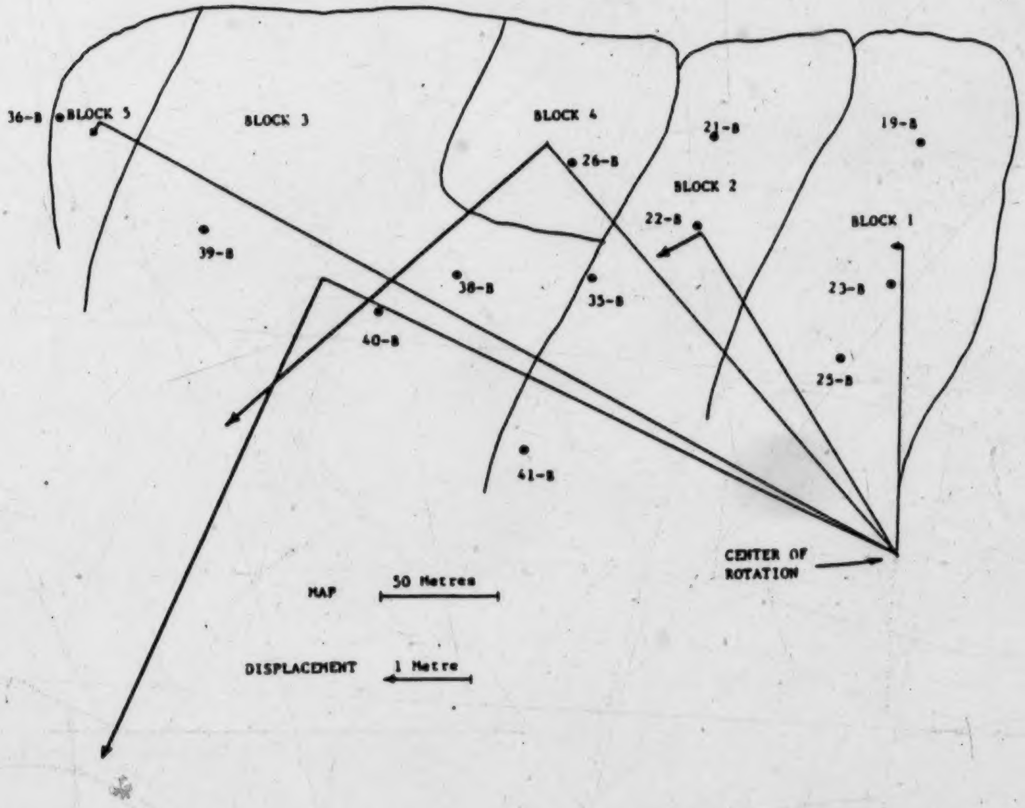
36-B
BLOCK 5
BLOCK 3
BLOCK 4
26-B
21-B
19-B
BLOCK 2
22-B
BLOCK 1
39-B
38-B
35-B
23-B
40-B
25-B
41-B
CENTER OF ROTATION
MAP
50 Metres
DISPLACEMENT
1 Metre

Figure 3.9 Simplified plan of the moving blocks at 5:00 P.M November 10th 1979

the bedding. Section 3.3.2 discusses in details the processes involved in these movements. Finally the third block , characterized by the 36-B , 38-B , 39-B , 40-B and 41-B prisms , occupies the west end of the slide. It moved down the dip direction of the bedding. Departure from this will be discussed in Section 3.3.2.

3.3.2.2 Second Hypothesis

This hypothesis involves two blocks. The first block is identical to that of the first hypothesis. It contains the 19-B , 21-B , 23-B and 25-B prisms , which toppled away from J3 and J4 joint sets. The second block includes the remaining prisms and it rotated around an axis of rotation. The common plane of movement is shown in Figure 3.1. This plane was constructed by passing the best great circle through the direction of the resultants of the displacement vectors shown in Figure 3.1. All of the vectors are , within ±10° of this plane and the projections of the vectors on this plane represent the magnitudes of the vectors. The angles subtended around a point by the projections of the vectors on this plane are equal. An axis of rotation passes through this point. The axis of rotation is perpendicular to the plane of movement. This axis is shown in Figure 2.3.

3.3.2.3 Third Hypothesis

This hypothesis consists of two blocks. The first block consists of the 19-B , 21-B , 23-B and 25-B prisms and is identical to that of the second hypothesis. This block toppled away from J3 and J4 joint sets. The second block embodies the remaining prisms. It slid as a translating wedge. This wedge is formed by J1 and bedding. J3 and J4 control the lateral and upper extent of the wedge.

In order to allow the application of Hocking's rule , the dip angle of the bedding is taken just a few degrees (i.e. 4°) less than that of the slope (Figure 3.2). Hocking's (1976) condition for sliding is kinematically satisfied , because the line of intersection of J1 and bedding , I_1 , lies between the line of intersection of J1 and the upper slope , I_2 , and the line of intersection of J1 and the lower slope , I_3. The upper slope is assumed horizontal , as shown in figure 3.8. The dip direction of the bedding is the same as the slope. When the dip direction of the bedding is 1° to the west of that of the slope , Hocking's rule states that sliding down the dip direction of the bedding is possible. On the other hand , when the dip direction of the bedding is 1° to the east of that of the slope , Hocking's rule states that sliding down the line of intersection of J1 and bedding is possible.

3.3.3 Working Movement Hypothesis

The first hypothesis mentioned above , with some modifications , can be applied for movement interpretation.

This will be demonstrated through a discussion about Figures 3.1 to 3.7. The first hypothesis involved 3 blocks. However , it will be shown that 5 blocks can be identified.

Although , the 22-B , 26-B , 35-B , 36-B , 38-B , 39-B , 40-B and 41-B prisms all displaced in one common plane of movement shown in Figures 3.1 and 3.5 , they do not , however , as shown in Figures 3.3 and 3.6 , have identical centers and angles of rotation. Thus , they can not , in contrast with the second hypothesis , be represented as one block.

Orientations of the displacement vectors for the above prisms , shown in Figures 3.1 to 3.7 , have an approximate range of 50°. The range for the magnitudes of the vectors is about 1 metre at 9:00 A.M and 7 metres at 5:00 P.M. Therefore , the requirements for the third hypothesis , i.e. identical orientation and magnitude of the vectors , are not satisfied.

As mentioned earlier , the first hypothesis with some modifications can be applied to the data. At 9:00 A.M , the angles subtended by the displacement vectors were measured from Figure 3.3. Five blocks were identified based on the measured angles ;

BLOCK 1 contains the 19-B , 21-B , 23-B and 25-B prisms which moved parallel to each other and as Figures 3.1 and 3.4 show they toppled away from the J3 joint set. Figure 2.3 shows the eastern extent of blocks 3 and 4. The bearing of this line varies between 010°

and 029°. The intersection between J1 and the high wall trends at 222° , making an angle of 13° to 32° with the eastern extent of blocks 3 and 4 , shown in Figure 2.3. The strike of J1 makes an angle of 22° with the north east extent of block 4 , shown in Figure 2.3. Therefore , J1 cannot be regarded as the only joint set which controlled the eastern extent of blocks 3 and 4. It is assumed that a combination of J1 and J3 joint sets provided an almost vertical plane , with 80° dip , making the eastern edge of blocks 3 and 4. This plane was identified in field by tension cracks and it is named here as the lateral margin. As mentioned before the bearing of the intersection of the lateral margin and the high wall , measured from Figure 2.3 , varies between 010° and 029°. The strike of this surface is 010° , as its intersection with horizontal plane trends at 010° on the eastern margin of block 4. The strike of the surface is 022° , as its intersection with the high wall trends at 180+029=209° on the eastern margin of block 3. This surface provided a free surface for toppling away from J3. Taking an average of 16° for the direction of the strike of the plane of separation at the eastern margin of the slide , Goodman's kinematic test (1980) shows that the pole to J3 is located in the region of possible toppling (Figure 3.1). The lateral margin was first constructed with the dip/dip direction of 080/286. The friction angle acting along sandstone joints is assumed to be 35°. Then , another plane (045/286) which dips 35° less than that of the lateral margin and with the same strike is constructed. The region shown in Figure 3.1 is confined to the great circle of the 045/286 plane and the vertical small circles 30° from the dip direction of the lateral margin.

BLOCK 2 contains the 22-B and 35-B prisms each with an angle of rotation of 6°. This block represents a transitional stage , both in direction and magnitude , between blocks 1 and 3. The resultants of the displacement vectors are produced by two independent movements. The first movement is a result of toppling away from J3. It is similar to the movement of the first block. The second movement is a result of sliding down the dip direction of the bedding. It is similar to the movement of block 3.

BLOCK 3 contains the 38-B , 39-B , 40-B and 41-B prisms with angles of rotation , obtained from Figure 3.2 , in the range of 8° to 11°. This block moved down the dip direction of the bedding. Figures 3.1 shows that the directions of the 38-B , 39-B , 40-B and 41-B prisms are within 20° of one another. Therefore , they can be represented as one block. The bearing of the vectors are within 10° of the dip of the bedding

, indicating movement down the dip direction of the bedding. However , all plunge less than the dip angle of the bedding , indicating dilation or variations in the local curvature of the bedding. AS mentioned in section 3.3.2.3 , Hocking's rule states that the sliding of a wedge , controlled by bedding and J1 , is possible. Therefore , block 3 slid as a wedge. This wedge moved down the dip direction of the bedding and dilated at the toe. Figure 3.8 shows the cross section B-B of Figure 2.3. The 40-B and 41-B prisms moved less than 10° to the horizontal , indicating the dilation of the bedding on the "step" structure at the toe. The perpendicular joints to the bedding , J2 , J3 and J4 provided the "step" structure shown at the toe of the slide. The 39-B prism moved at 30° to the horizontal , indicating movement along the dip direction of the bedding.

BLOCK 4 The 26-B prism moved in a way similar to that of block 2 , but with larger displacements.

BLOCK 5 The 36-B prism moved in a way similar to that of block 3 but with smaller displacements.

At 5:00 P.M , the five blocks mentioned above , using figures 3.4 to 3.6 , were identified. The angles subtended by the resultants of the displacement vectors were increased to 43° for block 3 and unchanged for block 1 , block 2 and block 5. Block 4 displaced a similar magnitude to block 3. The displacement records for the 41-B prism are not available at 5:00 P.M. The eastern failure limit shown in Figure 2.3 represents that the 41-B prism did not move with block 3 during the most rapid sliding. Therefore , it moved as an independent block , marking the sixth block. As the data is not available for block 6 , this block is not shown in Figure 3.9. Figure 3.9 shows the simplified plan of the moving blocks at 5:00 P.M .

3.3.4 Piezometric Levels

As part of the monitoring program in this portion of the pit , several nests of standpipes were installed in the north wall. The location of these nests is shown in Figure 2.3.

Readings of the water levels were taken at least once a week and correlated with initial wall movements and rates of pumping from the walls. Observations of changes in water elevations are not presented here but are on record at Cardinal River Coals Ltd. The main observations were as follows ;

1. Following the major displacement in the north wall standpipe 7B showed an abrupt decrease in water elevation.
2. Because of attitude of bedding , i.e. , essentially parallel to the wall , the dewatering wells were not totally efficient in causing drawdown across bedding.

3.4 Remedial Measures

After a major movement on November 10 , 1979 , remedial action , reported by Milligan and Hebil (1980) , was begun. This consisted of establishing three dewatering wells above the zone , and the construction of a buttress berm 14 metres high and 46 metres wide along the length of the failure. Pumping of the dewatering wells was to alleviate pore pressures in the rocks which were thought to contribute to the wall failure. Other wells were subsequently drilled at the east of the pit. However , in January 1980 , because of cold weather problems , they were not pumping. Figure 2.3 shows the location of the dewatering wells that were drilled at that time.

The construction of the buttress , as Munn (1983) reported , took two months and was completed while under continuous displacement monitoring of the wall and the dump itself using EDM equipment. The wall movement continued at the rate of 6 millimetres per day for five weeks then slowed to 3 millimetres per day and stopped moving on January 20 , 1980 upon completion of the buttress. The total movement of the failure was 6.9 metres horizontally and 3.9 metres vertically over an eight-month period. During this period , there was only one day of production lost with no loss of coal in the pit.

According to Johnson (1982) the immediate impact of this failure on survey costs was the expense of monitoring. This consisted of two contract survey crews , working a

24-hour day (12 hour shifts) , 7 days a week , for 2 months , at a cost of $72,500.

Munn (1983) stated that potentially , the consequences of this failure could have been severe. The final access ramp was designed to traverse this wall. Warning of the failure through monitoring permitted a relocation of the final access ramp to the opposite wall so that the buttress could be constructed to stabilize the movement.

In January 1980 further recommendations were made by Milligan and Hebil (1980) as follows :

1. Because of the possibility of overturned beds at deeper levels at the east end of the pit , this area of the pit be mapped as the excavation proceeded. Additional prisms and a slope inclinometer were recommended to be installed in this area.
2. Backfilling of the mined out areas of the pit be undertaken as soon as possible following the completion of mining.

3.5 Factor Of Safety Determination

Milligan and Hebil (1980) determined the factor of safety of the slide. The analysis and visual observation of the wall (i.e. , no sign of seepage at the toe) indicated that the geological structure had the main influence in controlling stability. Therefore , it was recommended that the remedial measure involving the placement of the toe berm be adopted. However , to reduce the possibility of a build-up of groundwater at the back of the wall , it was further recommended that the existing dewatering wells be employed to their optimum extent. This would entail connecting up the wells to a common collecting system and making sure that the wells would be essentially maintenance free.

A stability analysis was undertaken to determine the optimum dimensions for the stabilizing berm. The configuration used to examine this aspect is shown in Figure 3.10. Using the strength parameters and groundwater conditions as shown in Figure 3.10 , Table 3.3 summarizes the results from the stability analysis.

Table 3.3 Stabilizing toe berm effect in factor of safety

BERM WIDTH	FACTOR OF SAFETY
30 Metres	0.907
46 Metres	1.092

From this , it is seen that the minimum berm width was recommended to be 46 metres. The berm would at least be 42 metres high which would necessitate the berm completion around an elevation of 5500 feet. This berm width could be achieved along most of the toe of the failure surface ,

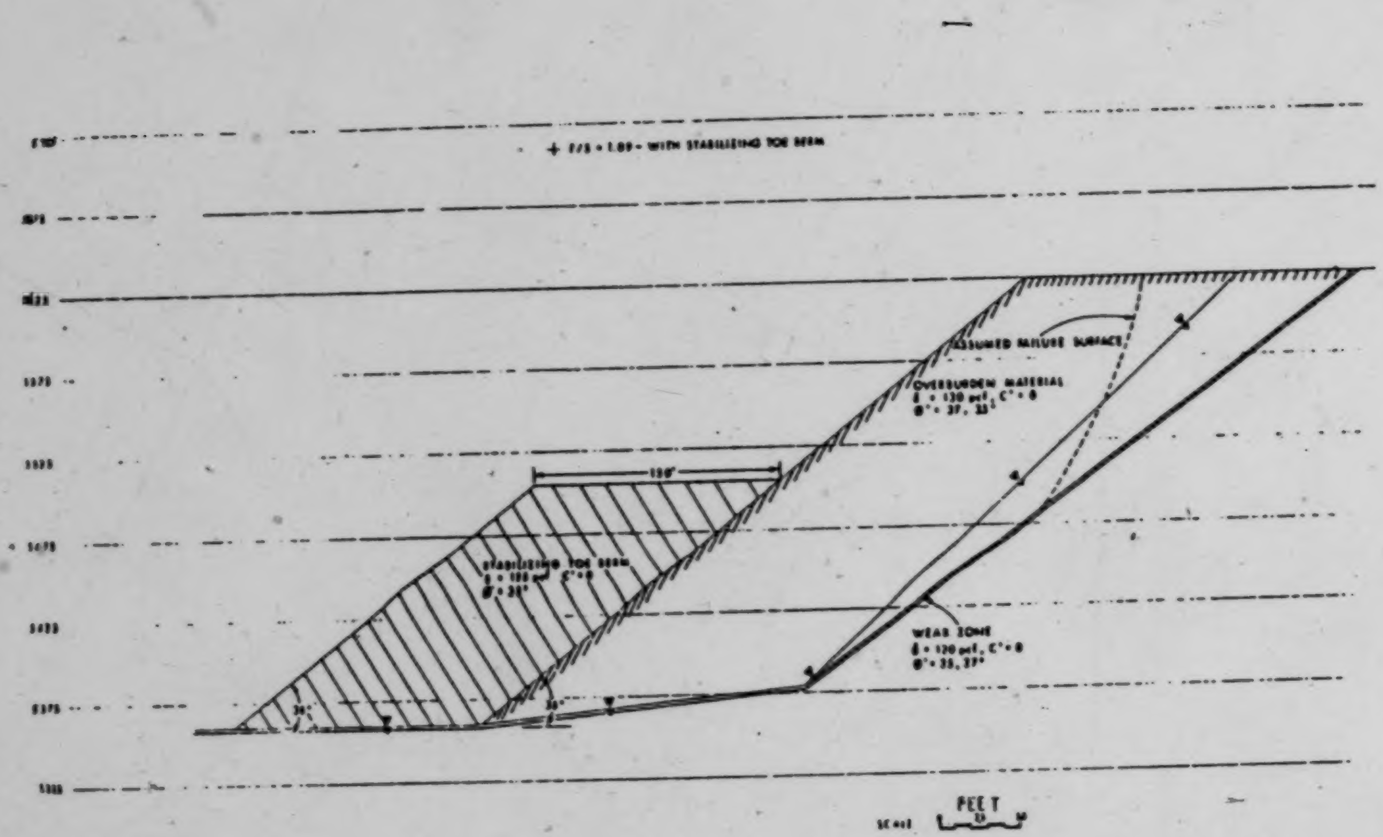
+ F/S = 1.09 - WITH STABILIZING TOE BERM
ASSUMED FAILURE SURFACE
OVERBURDEN MATERIAL
γ = 120 pcf, C' = 0
φ' = 37, 33°
130'
STABILIZING TOE BERM
γ = 120 pcf, C' = 0
φ' = 30°
30°
WEAR ZONE
γ = 120 pcf, C' = 0
φ' = 35, 37°
SCALE
FEET

Figure 3.10 Stability analysis for north wall and stabilizing toe berm in 51-B-2 pit

without covering the coal. This was especially true at the west end of the wall above the prism movements indicated the maximum movements had occurred. At the east end of the failure , the berm width would have to be reduced to about 30 metres to prevent covering the coal in this part of the pit. However , the reduction in berm width at this end of the slide surface would not affect the stability of the wall.

Chapter 4

LITERATURE REVIEW

4.1 Introduction

This chapter reviews various relations for analyzing displacement curves. Conventional displacement or creep curves are described. The following four laws , and , their applications through case studies results are given ;

1. Saito relation
2. Exponential law
3. Power law
4. Zavodni and Broadbent's law

A detailed formulation of these laws , describing all parameters , are presented. The application of these laws to 51-B-2 pit displacement data will be discussed in the next chapter.

4.2 Conventional Creep Curves

Creep curves show the relation between time and displacement at a particular constant load or stress (Varnes , 1982). An ideal creep curve may contain the following sequence of deformation;

a. instantaneous deformation or elastic response.

b. rapid deformation during decelerating creep.

c. constant displacement rate during steady-state creep.

d. accelerating creep.

e. rupture.

Varnes (1982) described several common characteristics derived from past research on creep at various levels of stress. The following is a summary (Figure 4.1) ;

1. If an inflection occurs , in which a curve that initially is concave downward becomes concave upward , then generally ultimate failure is inevitable if the load is maintained.
2. Changes in exterior conditions of load or temperature or of internal structure or composition during the process may either delay or halt the progress rupture and produce a curve with irregular shape.
3. There is usually a critical stress above which , other conditions being constant , long-term tests result in concave upward curves. This is often taken as the measure of long-term strength.
4. The strain at which inflection occurs has been found to be more or less constant among tests run on the same material at various levels of stress.

Field displacement data have been plotted in a manner similar to those shown in Figure 4.1. Munn (1979) stated that in order to use monitoring to successfully decide when operations may , or may not , continue below a moving slope , the movement data must be correctly and rapidly interpreted. He showed a method of displaying movement data as a plot of cumulative slope movement against time

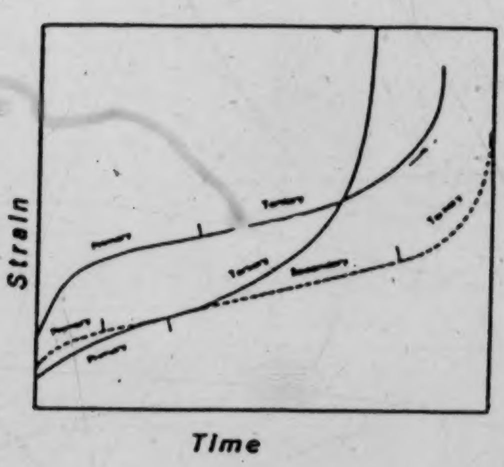

Figure 4.1 Typical creep curves

Figure 4.2 Typical shape of movement/time plot preceding failure

Figure 4.2 was removed because of the unavailability of copyright permission. This Figure is Figure 6.9 of Wyllie and Munn (1979). Figure 4.2 shows typical shape of movement/time plot preceding failure.

illustrated in Figure 4.2. This graph would readily show any increase in the rate of movement that would be indicative of deteriorating stability conditions. On the other hand it is seen that several episodes of acceleration may occur before failure and that the total displacement is usually substantial.

4.3 Saito-Type Relations

Servi and Grant (1951) expressed the relationship between the minimum strain rate , at the point of inflection of the ϵ-t curve , or during the quasisteady state , and the time remaining before failure as:

$$\dot{\epsilon}_m=E_0/(t_f-t) \tag{4-1}$$

where $\dot{\epsilon}_m$ is the minimum creep rate , (t_f-t) is the time to failure , t_f is the time of failure , t is the time of observation and E_0 is a constant. Monkman and Grant (1956) analyzed available data on rupture life versus minimum creep rate of a large number of pure metals and alloys and found that these materials obeyed a generalized version of Equation 4-1 in the form:

$$\log(t_f-t)+m\log\dot{\epsilon}_m=c \tag{4-2}$$

where m and c are constants.

Saito (1969) extended equation 4-2 to cover not only the relation between minimum creep rate and time to failure but also the creep rate during the whole period of accelerating creep. This results in;

$$\dot{\epsilon}=C/(t_f-t)^n \tag{4-3}$$

where ϵ is strain or displacement , t is time of observation , t_f is the time of failure , and C and n are constants. Equation 4-3 indicates that the rate of strain approaches infinity as t approaches t_f; also that the rate is finite at t=0. Varnes (1982) named the relation 4-3 as "pure Saito" , when n , as in many cases observed , was near to or equal to 1 , and as "generalized Saito" when $n \neq 1$.

Saito (1980) examined experimental data and concluded that the steady state creep rate and creep-rupture life plot of soil might be considered widely applicable to any type of soil and to any region on the earth. He further stated that the displacement $\Delta\epsilon$ and remaining time to rupture $(t_f - t)$ would make a straight line on a semi-logarithmic graph , if rupture life , t_f , could be chosen adequately. This relationship , being equivalent to "pure Saito" form , provided a way for finding rupture life on a semi-logarithmic graph.

The Saito relations are simple ones of possible wide application. They have been independently discovered and used in various forms by a number of investigators of failure processes in different countries. Four such studies were briefly described by Varnes (1982) as follows:

Schumm and Chorley (1964) analyzed movement observations on a section of sandstone cliff at Chaco Canyon National Monument , New Mexico , and determined that:

$$\log(k-\epsilon) = p \log(t_f - t) + q \qquad (4\text{-}4)$$

where $(k-\epsilon)$ is the distance the cliff section had yet to move before it fell , t is the time of observation , (t_f-t) is the time remaining before fall , and q is a constant. This is equivalent to the generalized Saito form , Equation 4-3 , with $n<1$.

Dobes and Milicka (1976) analyzed experimental data on a number of metals and alloys and showed that:

$$\log((t_f-t)/\epsilon_c)+m_1 \log\dot{\epsilon}_s=C \qquad (4\text{-}5)$$

where (t_f-t) is time to failure by fracture , ϵ_c is total creep deformation , $\dot{\epsilon}_s$ is minimum creep rate , and m_1 and C are constants. This , too , is equivalent to the generalized Saito form in which $n<1$ and the final strain just prior to fracture is finite.

Iken (1977) analyzed the movement of a large mass of glacier ice moving into a lake and breaking off. She found that:

$$\dot{\epsilon}=B/(t_A-t)^d + \dot{\epsilon}_1 \qquad (4\text{-}6)$$

where $\dot{\epsilon}_1$ is velocity of the ice mass , t_A is essentially the time of failure , t the time of observation , and $\dot{\epsilon}$, B , and d are constants. This is a generalized Saito form (equation 4-3) with the addition of a constant velocity , or viscous term , $\dot{\epsilon}_1$. The exponent d appears from Iken's graphs to be less than 1.

Sandstorm and Kondyr (1980) analyzed tertiary creep data for Mo and CrMo steels under constant load at 500°-600° C. They found that after removal of instantaneous strain and strain due to primary creep the tertiary creep followed the relation:

$\dot{\epsilon} = A \exp(B\epsilon)$ (4-7)

in which e is the base of natural logarithms and A and B are constants. Equation 4-7 is equivalent to the pure Saito form in equation 5-5. These authors also showed that the tertiary creep rate is consistent with the mechanics of creep damage.

4.4 Exponential Form

This may be expressed in various equivalent ways (After Varnes , 1982) :

$\epsilon = k[\exp(T/a)-1]$ (4-8)

$\ln\dot{\epsilon} = \ln(k/a) + T/a$ (4-9)

$\dot{\epsilon} = k/a + \epsilon/a$ (4-10)

This form is easily tested by seeing if plots of logarithm of rate versus time or rate versus strain are linear.

4.5 Power of Time Form

This may be expressed as (After Varnes , 1982) :

$\epsilon = aT^n + b$ (4-11)

$\dot{\epsilon} = naT^{n-1}$ (4-12)

$\log\dot{\epsilon} = \log(na) + (n-1) \log T$ (4-13)

if b=0

$\log \epsilon = \log a + n \log T$ (4-14)

This form is easily tested by plotting log rate versus log time.

4.6 Simultaneous Creep Stages

In working with curves showing both decelerating and accelerating creep , Varnes (1982) found that the accelerating portion often could not be analyzed satisfactorily by itself because the process responsible for primary creep continued beyond the point of inflection. This required that the mathematical relations for the primary process also be examined. As should have been expected , analysis of the primary portion of creep curves then indicated that the process governing accelerating creep commonly began well prior to the time inflection , i.e. the t versus $dt/d\epsilon$ curve was not a straight line during the decelerating creep. In these cases , the two processes had to be considered together and the times at which the accelerating process began and the decelerating process ended usually could be determined only by close examination of various transformations of a smooth ϵ-t curve into linear forms.

Many types of functions have been proposed for ϵ-t relations in primary creep. Varnes (1982) found the power law most useful for analyzing the primary portion of creep curves :

for $c<0$:

$$\dot{\epsilon} = a(t + b) \qquad (4\text{-}15)$$

which integrated for the case $c \neq -1$ gives :

$$\epsilon = a\,(t + b)^{c+1}/(c + 1) + \text{constant} \qquad (4\text{-}16)$$

and for $c=-1$, the logarithmic form :

$$\epsilon = a \ln(t + b) + \text{constant} \qquad (4\text{-}17)$$

Varnes (1982) indicated a close relation between the processes of logarithmic decelerating and Saito accelerating creep (equation 5-3). If the exponent c in Equation 4-15 is -1 then :

$$\dot{\epsilon} = t/a + b/a \qquad (4\text{-}18)$$

and a plot of the reciprocal rate versus time , both on arithmetic scales is linear. The reciprocal of rate can be recognized as the "time resistance" introduced by Janbu (1969) .

4.7 Case Studies Results

Varnes (1982) tabulated the results of some analyses on creep curves of various materials. He stated that where two processes were shown in succession , there was a definite change in one of the linear plots even though the ϵ-t curve was almost always smooth. Also , if two successive processes were of the same form , there was a change in numerical value of the coefficients or parameters in the equations. He derived the following conclusions for different materials :

1. Field , Rock or Soil

   Most examples followed a pure or generalized Saito form for at least part of the creep duration. One wholly exponential form and two power forms were also observed. Only the accelerating parts were analyzed of curves for slope movements that involved seasonal fluctuations , such as the topple reported by Brawner and Stacey (1979) and the slide at Tablachaca Dam , Peru , which was under study by Novosad. Most slope failures appeared eventually to follow a generalized Saito form.

2. Laboratory Rock

The laboratory tests on a few rock materials appeared to involve rather complex mixes of primary and tertiary forms acting concurrently or in succession. All involved pure or generalized Saito forms , but in tuff , alabaster and carnallite the primary process appeared to persist to the end of the test and the tertiary process began at the beginning of the test.

4.8 Zavodni and Broadbent's Fit

Zavodni and Broadbent (1980) described efforts that had been made to quantify parameters associated with slide movement , and compared the displacement records of several large scale open pit porphyry copper slope failures. They defined the term "excess force" which was usually related to an external event such as a blast , earthquake , rain , temperature change , ground water pressure change , or excavation of buttress rock. Two principal failure stages were recognized in the typical slope failure leading to total collapse (Figure 4.3) :

a. Regressive stage during which the failing mass would re-stabilize if some disturbance(s) external to the rock (i.e. excess force) and structure was(were)

Figure 4.3 was removed because of the unavailability of copyright permission. This Figure is Figure 1 of Zavodni and Broadbent (1980). Figure 4.3 shows typical displacement rate versus time record of a large scale rock failure proceeding to collapse. Liberty pit failure No.1.

removed ; the overall average velocity in this stage could slightly accelerate , remain constant , or decelerate.

b. progressive stage during which the failure would displace at an accelerating rate to the point of total collapse unless active control measures were taken. A large portion of total displacement was always monitored in this stage rather than in the regressive stage.

Overall displacement records in both failure stages were apparently of simple exponential form with a definite break occurring at the onset of failure point (Figure 4.3). All data were recorded on displacement rate versus days prior to total collapse. Semi-log plots and bi-linear curve fits were demonstrated for most slides that proceeded to collapse (Figure 4.3).

Zavodni and Broadbent (1980) revealed a semi-quantitative empirical relationship for failure collapse prediction. They , in conjunction with a semi-log plot such as in Figure 4.3 , were able to estimate the number of days untill total collapse , once the failure onset point was reached and the progressive stage of displacement rate pattern was established from the monitoring record.

$$\dot{\epsilon}_{md}/\dot{\epsilon}_0 \cong K \qquad (4-19)$$

where in Figure 4-3 :

$\dot{\epsilon}_{md}$ = velocity of mid-point in the progressive failure stage

$\dot{\varepsilon}_0$ = velocity at onset of failure point

K = constant (avg.=7.21 , range=4.6-10.4 , σ=2.11)

Knowing that the general equation for a semi-log straight line fit has the form ;

$$\dot{\varepsilon} = c\ e^{st} \tag{4-20}$$

where

$\dot{\varepsilon}$ = velocity in mm/min

s = slope of line log(mm/min)/min

c = constant

t = time minutes

e = base of natural logarithm

and assuming t=0 at the collapse onset point , Equation 4-20 takes the following form for the progressive failure stage ;

$$\dot{\varepsilon}=\dot{\varepsilon}_0\ e^{st} \tag{4-21}$$

From this equation and the empirical relationship of Equation 4-19 , Zavodni and Broadbent (1980) could determine the velocity at the collapse point $\dot{\varepsilon}_f$ as :

$$\dot{\varepsilon}_f = K^2\ \dot{\varepsilon}_0 \tag{4-22}$$

Broadbent and Ko (1971) illustrated that , in both regressive and progressive failure stages creep curves followed the behavior of a Kelvin or Voigt rheologic model. This model employed both elastic and viscous properties.

Zavodni and Broadbent (1980) after examination of major slope failures in open pit mines stated that a displacement rate above 0.035 mm/min indicated that a failure was probably in the progressive stage and that total collapse could occur within 0-48 days.

Chapter 5

EVALUATION OF t_f (TIME OF FAILURE) PREDICTION METHODS

5.1 Introduction

In general all methods of predicting the time to failure , t_f , can be divided into two main groups. In the first group the origin of time axis , T_0 , is known (Figure 5.1). T_0 in a creep test is the moment that load ceases to be added to a specimen. In the second group the origin of time axis , T_0 , is not known. In the case of a natural slope , shear movements along bedding planes and joints take place during geologic times (i.e. millions of years). A displacement measurement shows the position of a point , i.e. at time t_1 with respect to t_0 where t_0 is the time when the first measurements were recorded. Therefore , the time span X shown in Figure 5-1 is unknown.

5.2 Failure Definition

Since this chapter discusses the time of failure , the term "failure" needs to be explained. There are ambiguities in the definition of failure in the literature. The mathematical model proposed by Saito (1969 , 1980) in the previous chapter , Equation 4-3 , suggests an infinite rate of displacement at the time of failure , as the denominator approaches zero. The infinite displacement rate is physically impossible. The mathematical relations for accelerating creep expressed by the exponential and power of

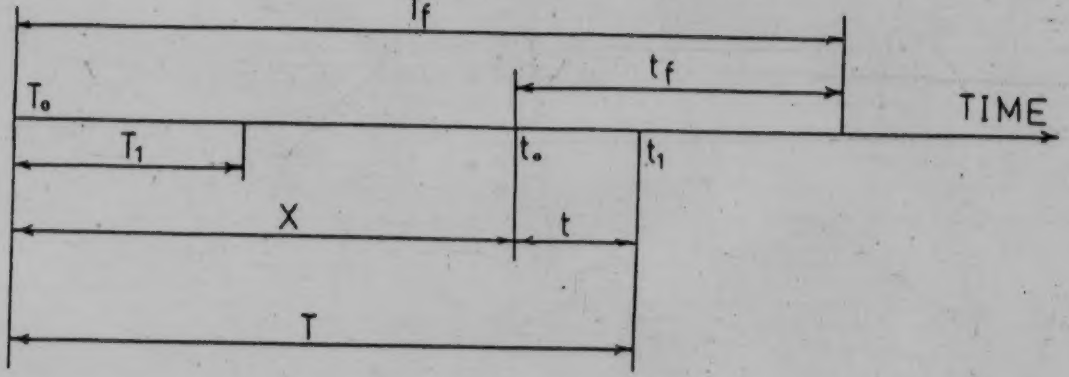
T_f
t_f
TIME
T_o
T_1
t_o
t_1
X
t
T

Figure 5.1 Times definitions

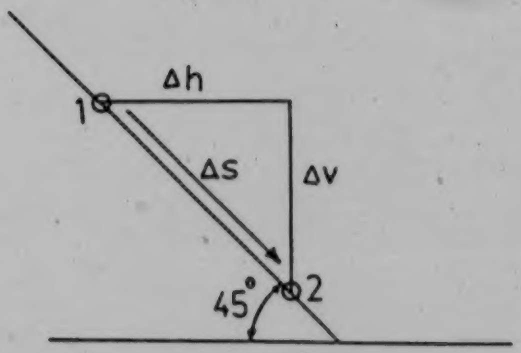
Δh
1
Δs
Δv
2
45°

Figure 5.2 Displacement vector and its components

time forms (Varnes , 1982) show that the velocity increases as the time goes on , and the time of failure is not determined. Zavodni and Broadbent (1980) reported a velocity range of 0.04 to 1.04 mm/min at the time of failure. MacRae (1982) , Wyllie and Munn (1979) introduced a critical slide velocity of 0.5 mm/min for evacuation of pit personnel and equipment under the moving mass a few hours before failure. Munn (1983) defined failure as excessive wall movement which may cause rock to fall into the active mine area. He further stated that the term "failure" can not be defined as a cataclysmic event but just as another mining problem.

Another ambiguity in the definition of the term "failure" is the path of movement of a point within the moving rock (i.e. , rock specimen , rock slope). A velocity vector is tangential to the path of movement. Any component of the velocity of a point has a magnitude less than the speed (velocity magnitude) of that point. For instance , it is zero in a direction perpendicular to the velocity vector. For example the velocity component of a point in a rock slope moving along the dip direction of strata with 45° dip angle , in a horizontal direction perpendicular to the strike , has a magnitude 30% less than the speed of that point (Figure 5.2).

In summary , local conditions at the work place , such as efficiency in protection of men and equipment , can greatly influence failure definition. Failures are not usually catastrophic events. They can be defined as rapid movements. The allowable limit velocity of these movements is determined by local personnel and experience in coping with failure consequences. In setting such an allowable limit velocity , the direction of movement needs to be considered.

5.3 General Procedure

Transformation of data obtained from creep curves or field measurements into linear plots is necessary to determine the form of mathematical relations that creep data obey. This allows linear regression methods be used , t_f predictions to be more convincing , and slopes and intercepts of lines to be more easily determined. Preferably two or more linear plots derived from the same basic equation , shown in Table 5.1 , need to be analyzed for mutual confirmations (Varnes , 1982). Graphical differentiation methods can be applied to transform the creep data into linear forms. Since this method requires graphical calculations by hand , it would increase the work of linearization. A disadvantage of this method is that the displacement rates needs to be computed by drawing tangents to creep curves. However , in a numerical analysis with the help of a computer the actual values of displacement and time obtained from field measurements can be used directly. Long time intervals may reduce the accuracy of estimates of the displacement rates.

If logarithmic axes such as $\log\epsilon$ and $\log t$ are used, zero quantities cannot be plotted. The use of displacement rate instead of displacement provides plots which are independent of the zero point of displacement measurements. Although displacement rate analysis avoids the zero point of displacement the calculation of the rate itself may be difficult. The limitations in the application of graphical and numerical differentiation methods have already been mentioned.

5.4 T_0 Known Case

The origin of the time axis, T_0, is known for all conventional laboratory creep tests. Varnes (1982) explained in five steps a procedure for determination of creep mathematical relations. Figure 5-3 shows the principal types of graphs used for analysis of creep curves. For calculation of t_f value, the time of failure, the Saito relations were used. First an estimation of t_f was made through use of reciprocal rate versus time plot (Figure 5.3-B). Then by linearization of a plot of displacement or log rate versus $\log(t_f-t)$, as shown in Figures 5.3-D and 5.3-E, "fine tuning" of the t_f approximation was possible.

Knowing T_0, all the proposed creep relations in the preceding chapter can be linearized. Equations 4-9, 4-10, 4-13 and 4-14 show linear forms of exponential and power laws. Equation 4-20 can be written in the linear form of :

$$\ln\dot{\epsilon} = \ln c + st \qquad (5\text{-}1)$$

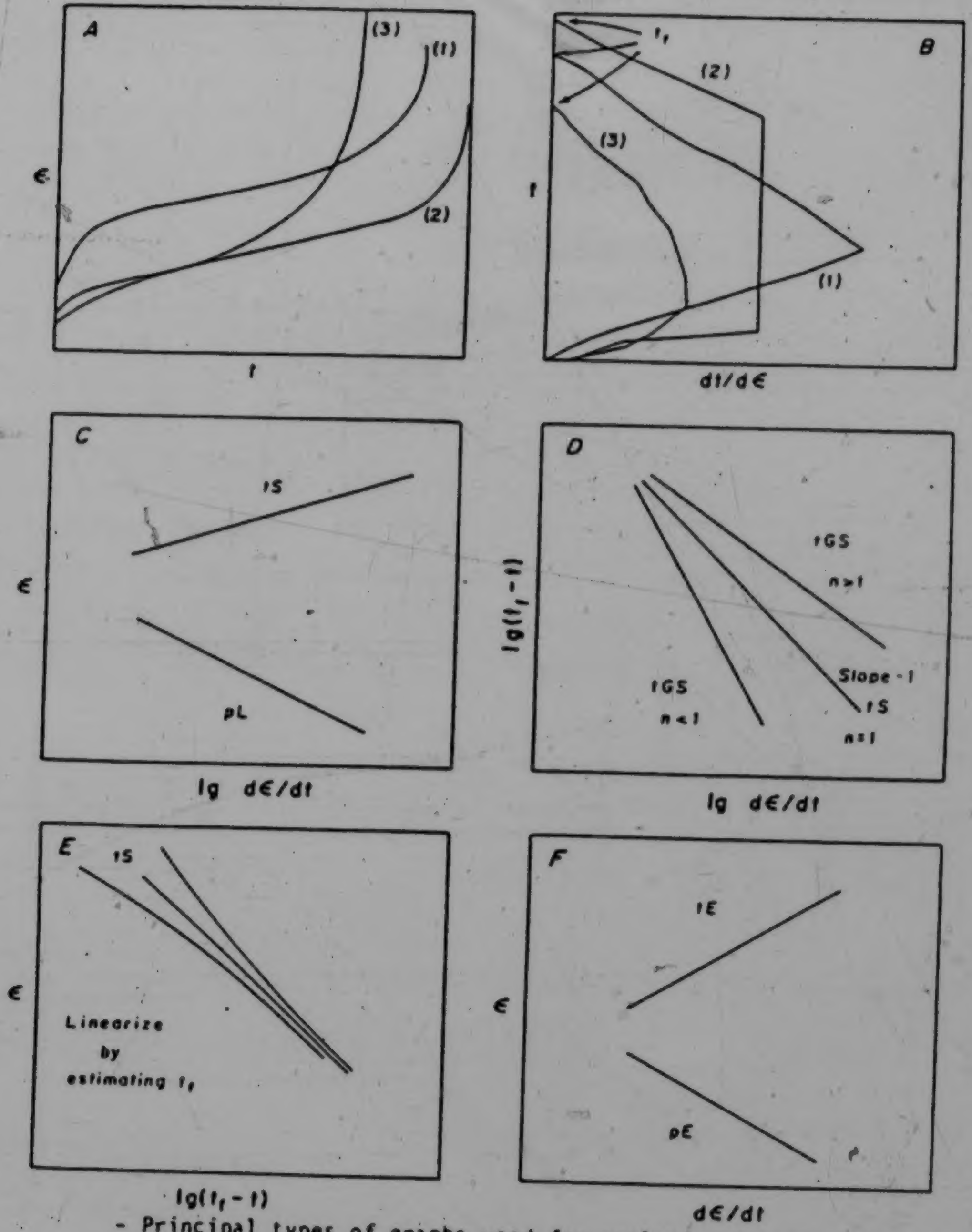

- Principal types of graphs used for analysis of creep curves. Symbols indicate type of creep. Tertiary: tS, pure Saito; tGS, generalized Saito; tE, exponential. Primary: pL, logarithmic; pE, exponential. Time of failure, t_f.

Figure 5.3 Principal types of graphs used for analysis of creep curves

$c \simeq \dot{\epsilon}_f$

Some linear relations between ϵ , rate , time , $(t_f - t)$ and their logarithms can be derived from Equation 4-3 as follows:

$\log \dot{\epsilon} = \log C - n \log (t_f - t)$ pure or generalized Saito (5-2)

$1/\dot{\epsilon} = t_f/C - t/C$ pure Saito(5-3)

$\epsilon = C_1 - C \ln(t_f - t)$ pure Saito(5-4)

$\epsilon = C_1 - \ln C^{C} + C \ln \dot{\epsilon}$ pure Saito(5-5)

$\log(1/\dot{\epsilon}) = -\log C + n \log(t_f - t)$ pure or generalized Saito (5-6)

Table 5.1 summarizes some possible line parameters for various types of creep relations .

5.5 T_0 Unknown Case

For reasons mentioned at the beginning of this chapter , the origins of time , T_0's , for all field data obtained from north wall of 51-B-2 pit are unknown.

The time variable , T , for power and exponential laws indicates the time since the creep process started. These laws may be written as :

$\epsilon = k[\exp((X+t)/a) - 1]$ (5-7)

$\epsilon = a(X+t)^n + b$ (5-8)

The constant X shows that the creep activities prior to the first measurements at time t_0 are unknown. Therefore , any plot involving total time and displacement , t and ϵ , may not be linear. A relation , between velocity $\dot{\epsilon}$,

RELATION	Y	X	INTERCEPT	SLOPE
PURE OR GENERALIZED SAITO $\dot{\varepsilon}=C/(t_f-t)^n$	$\log\dot{\varepsilon}$	$\log(t_f-t)$	$\log C$	$-n$
	$\log\frac{1}{\dot{\varepsilon}}$	$\log(t_f-t)$	$-\log C$	n
PURE SAITO $\dot{\varepsilon}=C/(t_f-t)$	ε	$\log(t_f-t)$	C_1	$-C$
	ε	$\ln\dot{\varepsilon}$	$C_1-\ln C^C$	C
	$1/\dot{\varepsilon}$	t	t_f/C	$-1/C$
	$1/\dot{\varepsilon}$	(t_f-t)	0.0	$1/C$
EXPONENTIAL LAW $\varepsilon=k\ (\exp(T/a)\ -1)$	$\ln\dot{\varepsilon}$	T	$\ln(k/a)$	$1/a$
	$\dot{\varepsilon}$	ε	k/a	$1/a$
POWER LAW $\varepsilon=a\ T^n+b$	$\log\dot{\varepsilon}$	$\log T$	$\log(na)$	$n-1$
	$\log\varepsilon$	$\log T$	$\log a$	n
ZAVODNI AND BROADBENT'S FIT $\dot{\varepsilon}=C\exp(st_f-st)$	$\ln\dot{\varepsilon}$	t_f-t	$\ln C$	s
	$\ln\dot{\varepsilon}$	t	$\ln C+st_f$	$-s$

Table 5.1 Line parameters for creep relations

acceleration $\ddot{\epsilon}$ and time t , derived from the power law is proposed as follows :

$$\dot{\epsilon} = an(X+t)^{n-1} \tag{5-9}$$

$$\ddot{\epsilon} = an(n-1)(X+t)^{n-2} \tag{5-10}$$

$$\dot{\epsilon}/\ddot{\epsilon} = (X+t)/(n-1) \tag{5-11}$$

This is a line with the slope of 1/(n-1) and intercept of X/(n-1) . X , a and n values can be determined and linear forms of power law tested.

Using a , n and X constants the $\dot{\epsilon}$ value corresponding to T=t+X may be calculated. Then , the time of failure , based on a defined displacement rate , can be calculated. In the case of an exponential law being followed , the following relations can be developed to show that the ratio between velocity and acceleration is a constant :

$$\dot{\epsilon} = (k/a)\ \exp(t/a) \tag{5-12}$$

$$\epsilon = (k/a^2)\ \exp(t/a) \tag{5-13}$$

$$\dot{\epsilon}/\ddot{\epsilon} = a \tag{5-14}$$

Both Equations 5-11 and 5-14 can not be applicable at the same time. The analysis of the data will probably show that either Equation 5-11 or 5-14 is applicable.

It is shown that Saito relations , power law and Zavodni and Broadbent's equation are essentially similar in form.

Saito relation can be written as :

$$\dot{\epsilon} = C\ t_f^{-n}(1-t/t_f)^{-n} \tag{5-15}$$

$$\log\dot{\epsilon} = \log C - n\ \log[t_f(1-t/t_f)] \tag{5-16}$$

and if $t \ll t_f$:

$$\log \dot{\epsilon} = \log C - n \log t_f + n(t/t_f) \qquad (5\text{-}17)$$

power law can be written as :

$$\dot{\epsilon} = an(X+t)^{n-1} \qquad (5\text{-}18)$$

$$\log \dot{\epsilon} = \log an + (n-1)\log[X(1+t/X)] \qquad (5\text{-}19)$$

and if $t<<X$:

$$\log\dot{\epsilon} = \log(an) + (n-1)\log X + (n-1)(t/X) \qquad (5\text{-}20)$$

Zavodni and Broadbent's equation can be written as :

$$\ln \dot{\epsilon} = \ln C + s(t_f-t) \qquad (5\text{-}21)$$

It can be seen that Equations 5-17 , 5-20 and 5-21 all would relate linearly $\log\dot{\epsilon}$ to t as long as the observation time t is not too close to the time of failure (Table 5-2).

The exponential law can be written as :

$$\ln \dot{\epsilon} = \ln k + (X+t)/a \qquad (5\text{-}22)$$

Therefore , exponential law is also identical to other preceding creep relations. The similarity between exponential law and Zavodni and Broadbent's relation is not dependent on $t<<X$.

5.6 Analysis Of The Data

5.6.1 Computer Programs

A Fortran-4 program written by Cruden (1969) was used to fit the power and exponential laws. This program had to be modified so that the strain data were replaced by displacement in the input file. One or two components of the resultants of the displacement vectors can be entered.

POWER LAW	$\dot{\varepsilon}/\ddot{\varepsilon} = (X+t)/(n-1)$
	$\log\dot{\varepsilon} = \log(an) + (n-1)\log X + (n-1)(t/X)$
SAITO RELATION	$\log\dot{\varepsilon} = \log C - n\log t_f + n(t/t_f)$
EXPONENTIAL LAW	$\dot{\varepsilon}/\ddot{\varepsilon} = a$
ZAVODNI AND BROADBENT'S FIT	$\ln\dot{\varepsilon} = \ln C + s(t_f - t)$

Table 5.2 A comparison of laws

Furthermore , strain rates were replaced by displacement rates. Finally a program was derived to examine the Saito relation. Within a given range of t_f , this program calculates fit parameters and as soon as the Durbin Watson statistic reaches a preset value the computation will stop and a graph is produced. On the other hand , programs for the analysis of power law , exponential law and velocity to acceleration ratio were developed. Listings of these programs together with the definition of input parameters , examples of input and output are presented in the Appendix. Flow diagrams of the programs are illustrated in Figures 5.4 to 5.8.

5.6.2 Criteria For Goodness of Fit

As a test for serial correlation the Durbin Watson statistic , dw , was used. If the residuals are positively serially correlated , dw will tend to be small. If the residuals are negatively serially correlated , dw will tend to be large. Durbin and Watson (1951) tabulated two groups of critical values for dw against n , the number of observations ; an upper value of dw , which , if not exeeded , suggests that positive serial correlation of the residuals might exist in the observations , and a lower value of dw , which , if not exeeded , suggests that positive serial correlation exists in the data (Cruden 1971).

Non-zero means of the residuals reflect departure from randomness of the residuals.

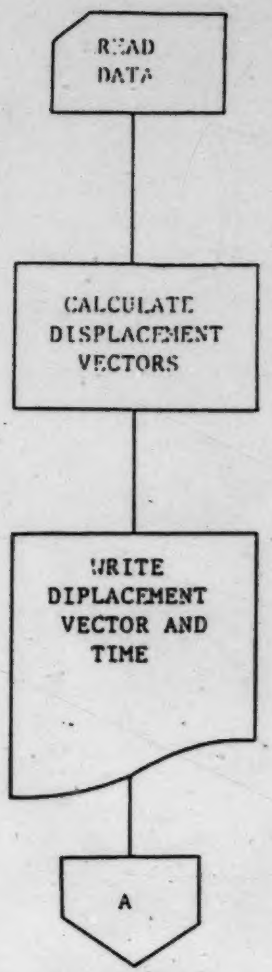
READ DATA
CALCULATE DISPLACEMENT VECTORS
WRITE DIPLACEMENT VECTOR AND TIME
A

Figure 5.4 Saito fit flow diagram for the time of failure prediction

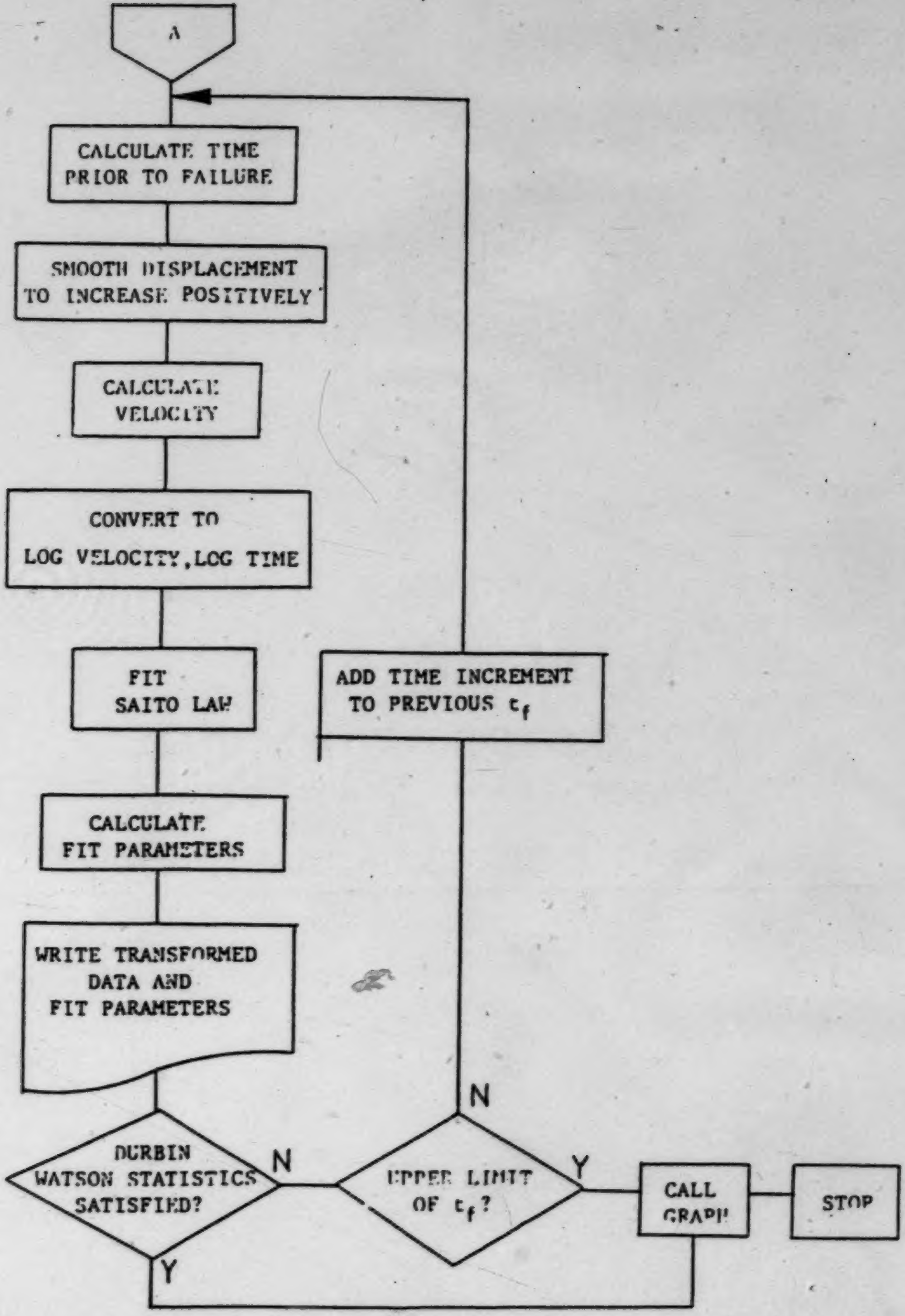
A
CALCULATE TIME PRIOR TO FAILURE
SMOOTH DISPLACEMENT TO INCREASE POSITIVELY
CALCULATE VELOCITY
CONVERT TO LOG VELOCITY,LOG TIME
FIT SAITO LAW
CALCULATE FIT PARAMETERS
WRITE TRANSFORMED DATA AND FIT PARAMETERS
DURBIN WATSON STATISTICS SATISFIED?
N
Y
UPPER LIMIT OF t_f?
N
Y
ADD TIME INCREMENT TO PREVIOUS t_f
CALL GRAPH
STOP

Figure 5.5 Saito fit flow diagram for the time of failure prediction cont.

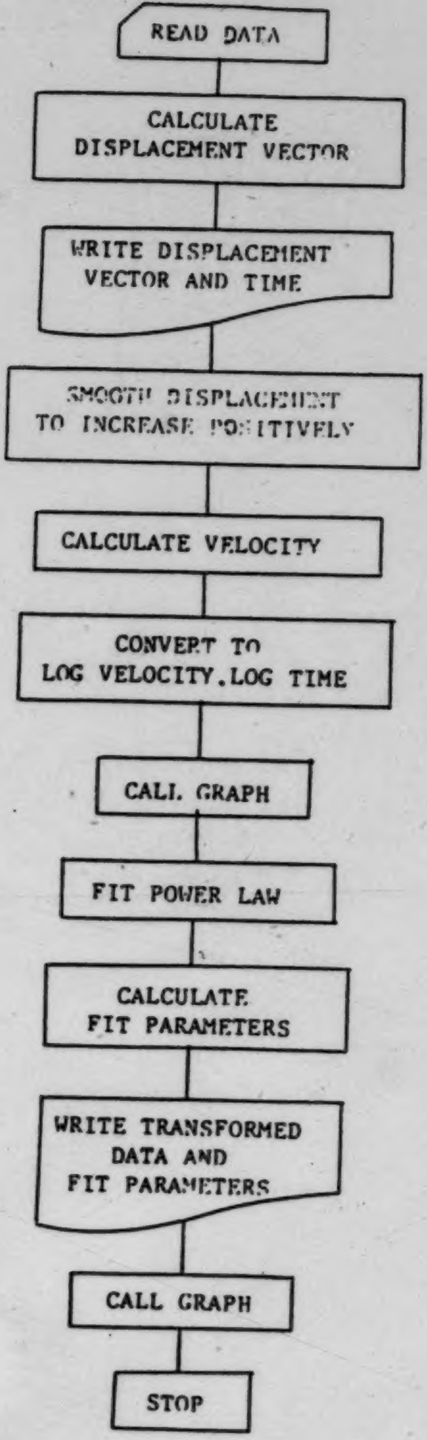
READ DATA
CALCULATE DISPLACEMENT VECTOR
WRITE DISPLACEMENT VECTOR AND TIME
SMOOTH DISPLACEMENT TO INCREASE POSITIVELY
CALCULATE VELOCITY
CONVERT TO LOG VELOCITY.LOG TIME
CALL GRAPH
FIT POWER LAW
CALCULATE FIT PARAMETERS
WRITE TRANSFORMED DATA AND FIT PARAMETERS
CALL GRAPH
STOP

Figure 5.6 Power law flow diagram

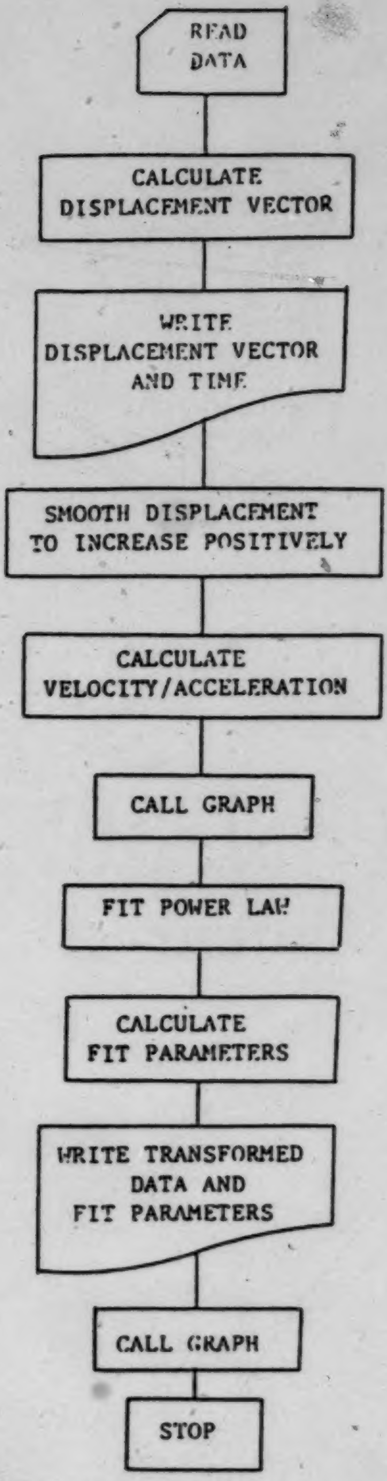
READ DATA
CALCULATE DISPLACEMENT VECTOR
WRITE DISPLACEMENT VECTOR AND TIME
SMOOTH DISPLACEMENT TO INCREASE POSITIVELY
CALCULATE VELOCITY/ACCELERATION
CALL GRAPH
FIT POWER LAW
CALCULATE FIT PARAMETERS
WRITE TRANSFORMED DATA AND FIT PARAMETERS
CALL GRAPH
STOP

Figure 5.7 Power law(velocity/acceleration) flow diagram

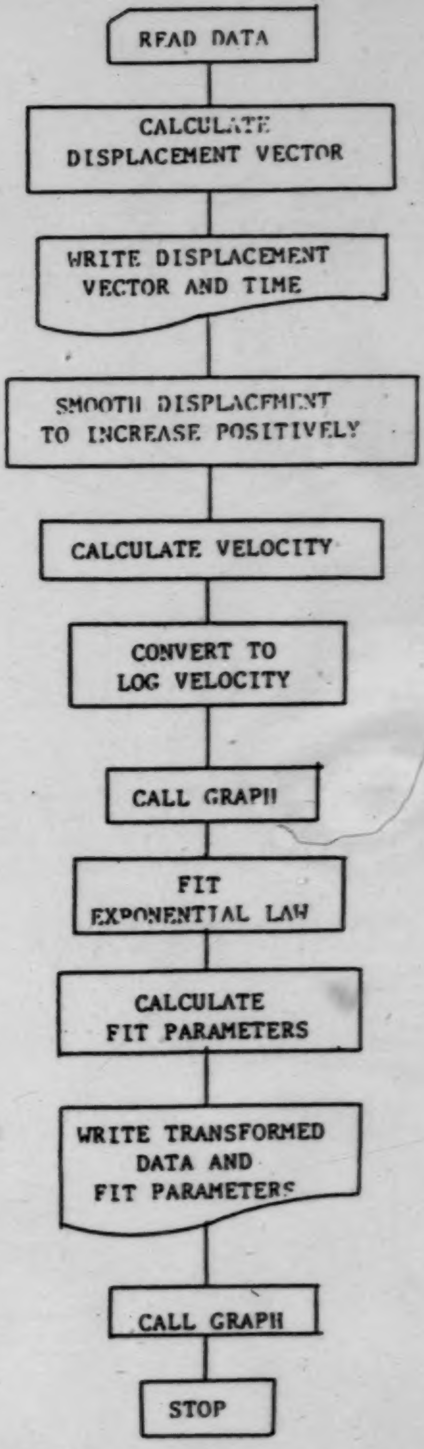
READ DATA
CALCULATE DISPLACEMENT VECTOR
WRITE DISPLACEMENT VECTOR AND TIME
SMOOTH DISPLACEMENT TO INCREASE POSITIVELY
CALCULATE VELOCITY
CONVERT TO LOG VELOCITY
CALL GRAPH
FIT EXPONENTIAL LAW
CALCULATE FIT PARAMETERS
WRITE TRANSFORMED DATA AND FIT PARAMETERS
CALL GRAPH
STOP

Figure 5.8 Exponential law flow diagram

The test of slope significance examines the hypothesis that the fitted line does not have a slope significantly different from zero , a hypothesis equivalent to suggesting that the data might be as well represented by a constant , and that the fitted line has not picked out any significant variation (Cruden , 1971). The test of slope significance statistic , can be referred to F-tables with one and (n-2) degrees of freedom.

Another criterion analyzes variations in the slope and intercept of a fitted line (Benjamin and Cornell , 1970). If $a_1+\beta_1 X$ is the estimated regression line , $(1-a)$ two-sided confidence interval for the slope and intercept will be :

$\beta_1 \pm t_{\alpha/2, n-2}\ S_B$

$a_1 \pm t_{\alpha/2, n-2}\ S_A$

based on a value from a table of the t distribution , $t_{\alpha/2, n-2}$, S_B and S_A , the estimates of the standard deviation of the slope and intercept.

In the output of computer programs the degree of freedom for F-tables and t distribution tables is written as 'weighting' , and for Durbin Watson tables as the 'transformed data number'.

5.6.3 Selection Of Data

Measurements before the slide and after January 28th , 1979 were used for analyses of the resultants of the displacement vectors and cumulative horizontal and vertical displacements. For slope distance analysis some measurements taken before January 28th were also included. The data obtained before the above time show slight decrease in displacement ,in the range of instrument error , with time. Measurements recorded after the time of slide , at and after 5:00 P.M 10th November , 1979 , do not represent the accelerating creep process.

In the analysis of the resultants of the displacement vectors and cumulative horizontal displacements of the 26-B prism , the data points which did produce high weighting factors were eliminated from the data file to examine their effect on Durbin Watson statistics. These data were produced within the accuracy of measuring instruments. Local fluctuations in ground water level might have also provided these data.

An estimation of the time of most rapid sliding , t_f , based on MacRae (1983) was as November 10th , 1979 at 12:45 p.m. However , in analyses of the slope distance data and the resultants of the displacement vectors for 26-B prism , t_f variations were tested.

5.6.4 Units

Except for slope distance analysis all units for time are in minutes and for displacement in millimetres. The time units for slope distance analysis were in days. Because the maximum number of digits stored in computer memory in a single precision mode is 7 , some errors of the order of 1 to 2 minutes would arise if the input data were in days for time variable.

5.6.5 Spring Ahead And Fall Back Daylight Times

With the exception of slope distance data , the time records were corrected by taking into account the spring ahead and fall back daylight time. Spring ahead daylight time arrived at 2:00 a.m Sunday , 29th April 1979 when clocks were set ahead for an hour. Fall back daylight time ended at 2:00 a.m Sunday , 28th October 1979 when clocks were set back one hour. 60 minutes were subtracted from time values recorded between May 2nd and October 22nd. 60 minutes were added to the time values recorded during and after October 29th.

5.6.6 16 Prisms Displacement Analysis

16 prisms were analyzed for pure or generalized Saito relations. Table 5.1 shows the intercept and slope of the Saito line with its axes as log velocity versus log time prior to failure. Results are shown in Tables 5.3 to 5.6. Although no values for Durbin Watson statistics are given below 15 transformed data , these results are also presented. Durbin Watson statistics for 15 transformed data are shown in parentheses. A slope of -1 represents pure Saito relation being followed. Because of the limited capabilities of the computer program in early stages , only the cumulative horizontal displacements have been used. Corrections for the direction of movements have not been

included and data with high weighting factor were not excluded. The Analysis shows that not all prisms represent linear relations. The 19-B , 20-B , 25-B , 26-B , 35-B , 39-B , 40-B and 42-B prisms satisfy pure or generalized Saito relations. The 21-B , 23-B , 36-B , 38-B , 41-B , 43-B and 44-B prisms did not follow the Saito relation. Test of slope significance was not satisfied for the above prisms , indicating that no significant movement took place. Test of slope significance was satisfied for the 22-B prism ; however , the Durbin Watson statistic was not satisfied. Therefore , the 22-B prism displacements did not represent the Saito relation.

Variations of the Saito relation parameters were used as a criterion for block movement analysis. Knowing the slopes and intercepts of the fitted lines , C and n constants were calculated from the line parameters given in Table 5.1 for the generalized Saito relation. Figures 5.9 to 5.12 show the 90% two-sided confidence limits for C and n constants. It can be seen that prisms may be divided into two groups based on common confidence limits. The 19-B , 20-B , 22-B and 25-B prisms represent one group with their C and n constants less than 0.3 and 0.5 , respectively. The second group involves the 26-B , 35-B , 39-B , 40-B and 42-B prisms with their C and n constants more than 1 and 0.5 , respectively. The fitted lines for the first group had negative intercepts , indicating low C values. High C and n values indicate that the second group moved more than the first one. Therefore , the 26-B , 35-B , 39-B , 40-B and 42-B prisms moved more than other prisms , and , the 26-B prism had the highest movements. The confidence limits for the 39-B and 40-B prisms are very close to each other , representing that they moved simultaneously.

90% two-sided confidence interval for the slope and intercept are greater than 0.1 and 0.7 , variations from ±1 minute and ±10 millimetres measurement errors. This indicates that measurement and instrument errors are not the only causes of data scatter. This subject will be discussed in more depth in Chapter 6.

5.6.7 26-B Prism Displacement Analysis

The displacement records obtained from 26-B prism were analyzed in 3 different forms , i.e. , slope distance , cumulative horizontal displacements and the resultants of the displacement vectors.

5.6.7.1 Slope Distance Analysis

The slope distance , the distance between the EDM station and any prism , and time measurements were used to test the fit of log($\dot{\epsilon}$) versus log(t) , log($\dot{\epsilon}$) versus t and $\dot{\epsilon}$ versus log(t). None of the above fits were linear. This shows that power , exponential and Zavodni and Broadbent's laws are not applicable (Table 5.7).

The Saito relation and also the effect of the time of slide , t_f , on linearity were tested. Tables 5.8 to 5.10 summarize the results of regression analyses for

Table 5.3 Results of cumulative horizontal displacement analysis

PRISM	19-B	20-B	21-B	22B
LAW	SAITO	SAITO	SAITO	SAITO
DATA	ALL	ALL	ALL	ALL
INTERCEPT	-4.95	-4.34	-5.68	-2.86
±INTERCEPT 90%	2.264	2.45	2.24	1.68
SLOPE	-0.289	-0.36	-0.195	-0.402
±SLOPE 90%	0.20	0.21	0.20	0.15
DW CALCULATED	2.903	2.067	2.281	1.284
DW FROM TABLE 5%	(1.08)	(1.08)	1.18-1.39	1.24-1.43
TSS CALCULATED	5.661	7.74	2.473	18.54
TSS FROM TABLE 5%	4.13	4.14	4.07	4.08
RESIDUALS	-0.000058	0.000102	0.000360	0.000083
WW-2	33.9	33	39.4	39.6
TRANSFORMED DATA	10	9	19	23

DW=DURBIN WATSON STATISTICS
TSS=TEST OF SLOPE SIGNIFICANCE
WW-WEIGHTING

Table 5.4 Results of cumulative horizontal displacement analysis cont.

PRISM	23-B	25-B	26-B	35-B
LAW	SAITO	SAITO	SAITO	SAITO
DATA	ALL	ALL	ALL	ALL
INTERCEPT	-6.334	-4.479	7.758	2.496
±INTERCEPT 90%	2.02	1.18	1.732	5.47
SLOPE	-0.173	-0.307	-1.277	-0.842
±SLOPE 90%	0.178	0.11	0.16	0.61
DW CALCULATED	2.616	3.392	2.356	2,46
DW FROM TABLE 5%	1.08-1.36	(1.36)	1.34-1.48	(1.36)
TSS CALCULATED	2.553	22.27	184.81	6.192
TSS FROM TABLE 5%	4.10	4.17	4.07	4.67
RESIDUALS	0.000191	0.00002	-0.00216	-0.000008
WW-2	34.8	30.5	42	17
TRANSFORMED DATA	16	9	30	13

DW=DURBIN WATSON STATISTICS
TSS=TEST OF SLOPE SIGNIFICANCE
WW=WEIGHTING

Table 5.5 Results of cumulative horizontal displacement analysis cont.

PRISM	36-B	38-B	39-B	40-B
LAW	SAITO	SAITO	SAITO	SAITO
DATA	ALL	ALL	ALL	ALL
INTERCEPT	-2.14	3.626	3.494	3.351
±INTERCEPT 90%	4.04	6.59	2.98	3.98
SLOPE	-0.288	-0.803	-0.717	-0.739
±SLOPE 90%	0.47	0.74	0.34	0.46
DW CALCULATED	1.799	2.624	2.197	2.691
DW FROM TABLE 5%	(1.36)	(1.36)	(1.36)	(1.36)
TSS CALCULATED	1.221	3.784	14.259	8.392
TSS FROM TABLE 5%	4.96	4.75	4.67	4.67
RESIDUALS	0.000058	0.00001	0.000013	-0.000007
WW-2	12	12	13	12.9
TRANSFORMED DATA	10	12	14	10

DW=DURBIN WATSON STATISTICS
TSS=TEST OF SLOPE SIGNIFICANCE
WW-WEIGHTING

Table 5.6 Results of cumulative horizontal displacement analysis cont.

PRISM	41-B	42-B	43-B	44-B
LAW	SAITO	SAITO	SAITO	SAITO
DATA	ALL	ALL	ALL	ALL
INTERCEPT	-2.637	0.729	-16.204	-14.926
±INTERCEPT 90%	6.21	0.95	13.63	17.14
SLOPE	-0.146	-0.463	1.204	0.9
±SLOPE 90%	0.70	0.11	1.58	2.08
DW CALCULATED	3.336	1.844	3.44	3.268
DW FROM TABLE 5%	(1.36)	(1.36)	(1.36)	(1.36)
TSS CALCULATED	0.138	74.058	4.881	0.824
TSS FROM TABLE 5%	4.75	5.99	10	5.99
RESIDUALS	0.000044	0.000028	0.000037	0.000066
WW-2	11.9	6	3.5	5.9
TRANSFORMED DATA	8	7	4	3

DW=DURBIN WATSON STATISTICS
TSS=TEST OF SLOPE SIGNIFICANCE
WW=WEIGHTING

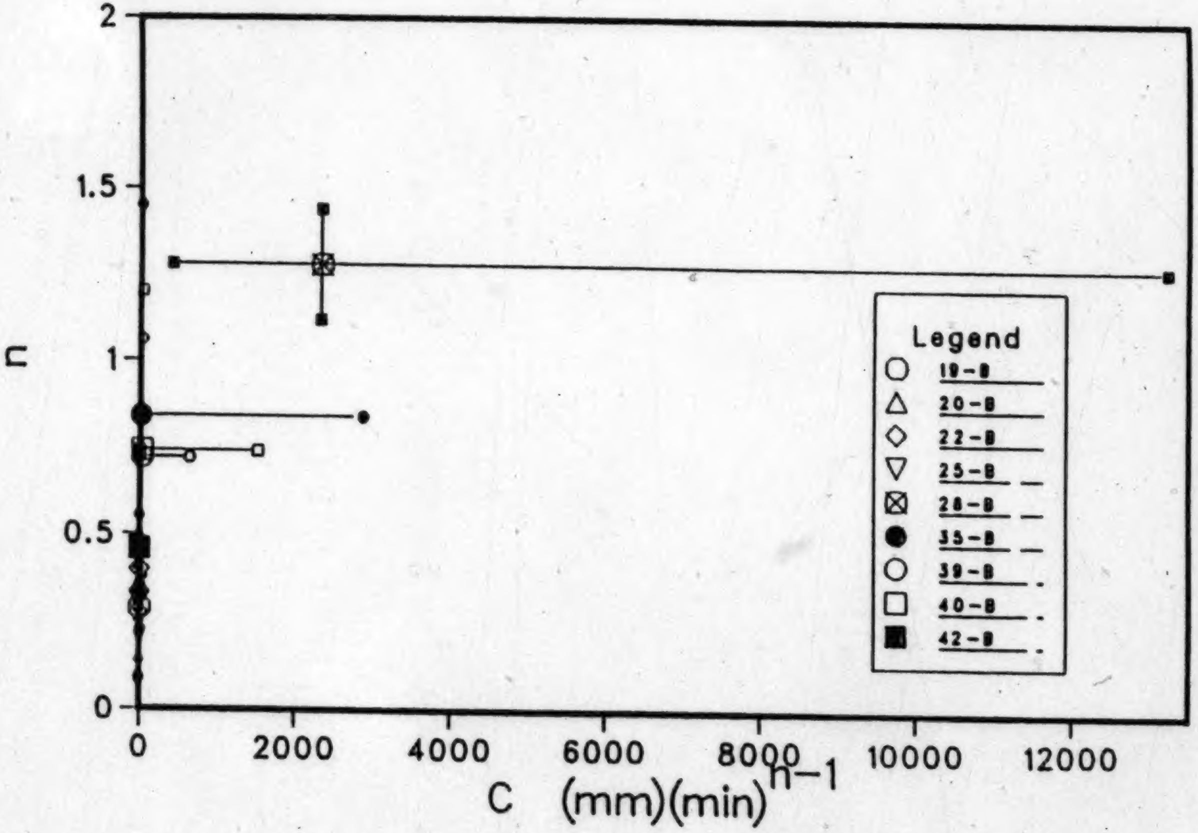

Figure 5.9 90 percent confidence limit for the Saito relation parameters

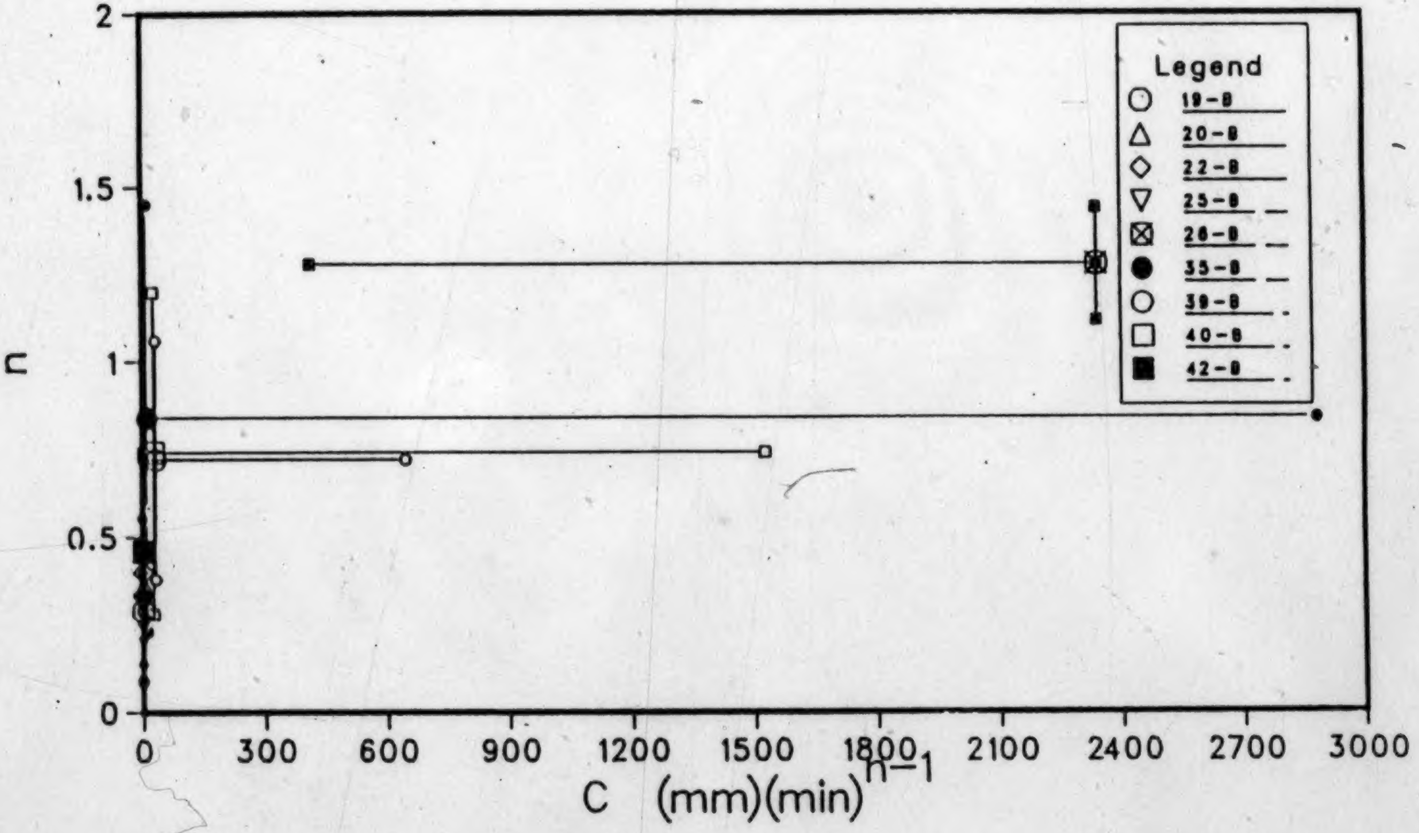

Figure 5.10 90 percent confidence limit for the Saito relation parameters

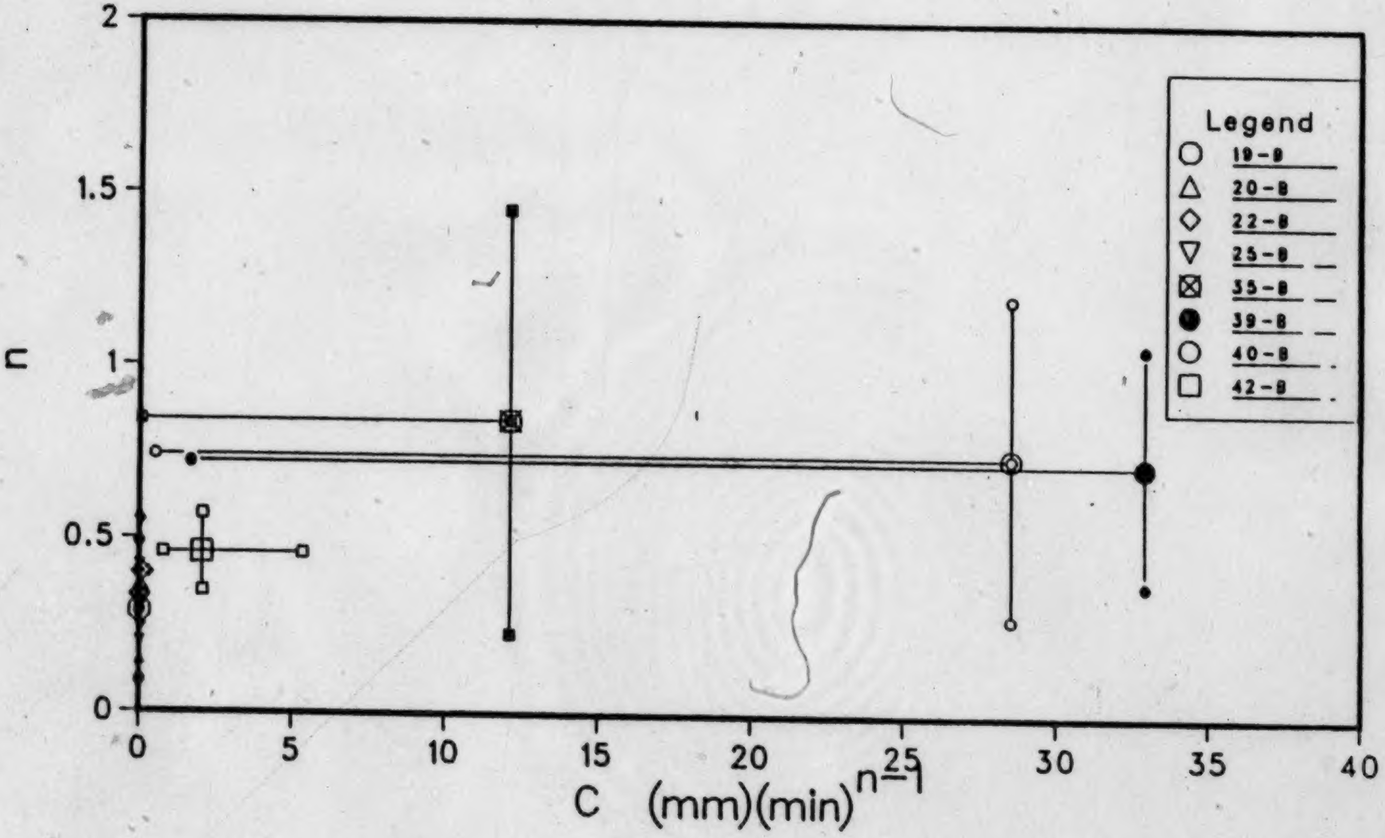

Figure 5.11 90 percent confidence limit for the Saito relation parameters

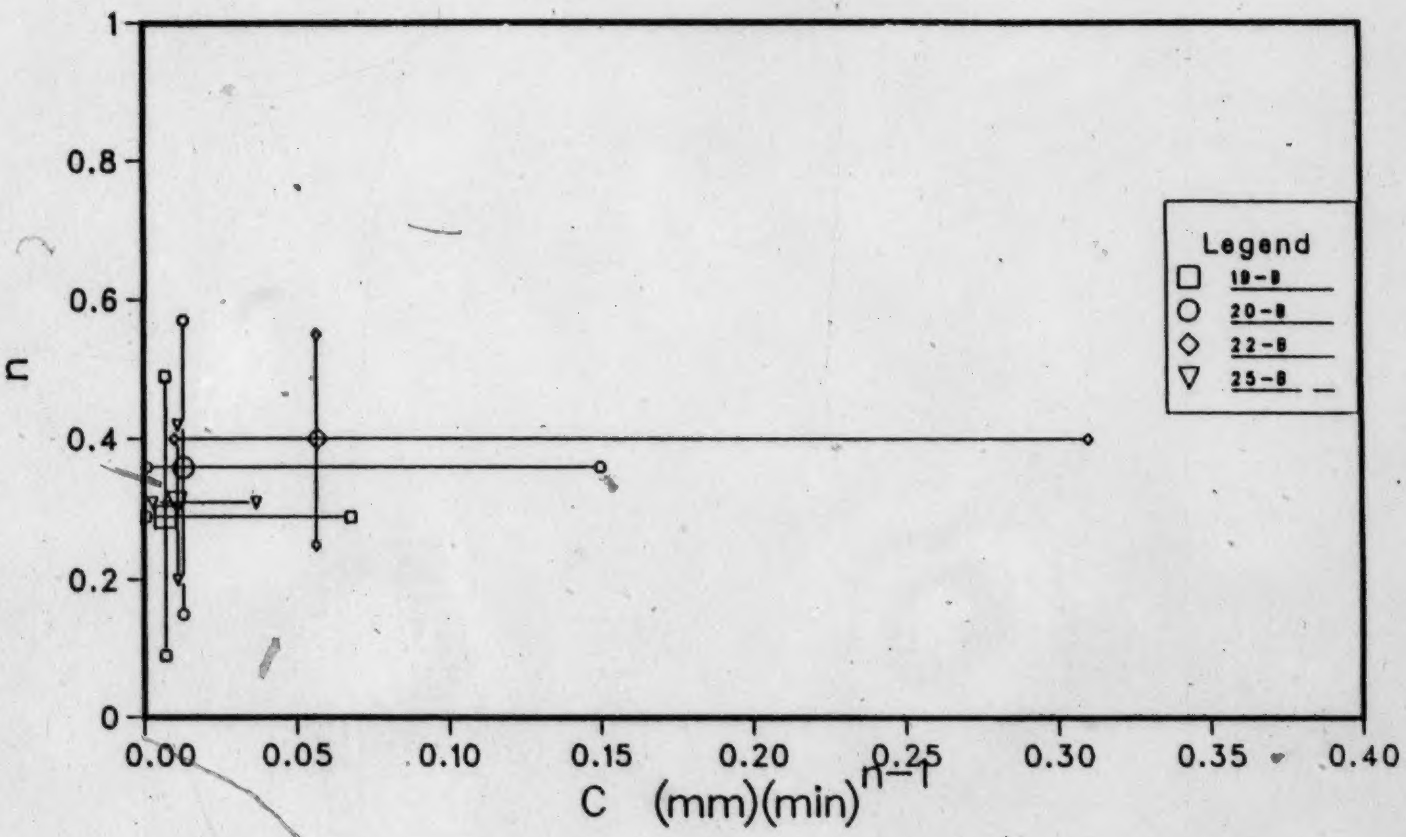

Figure 5.12 90 percent confidence limit for the Saito relation parameters

different t_f's. For all analyses , the data sets were identical. The data set contained all measurements taken before 10:00 A.M November 10th , 1979.

As the time of slide was increased the Durbin Watson statistics were increased. When the t_f value represented 16:30 hours November 10th 1979 , the Durbin Watson statistic was 1.447 , just above the upper bound of the critical value at 5% confidence level. Therefore , significant possitive serial correlation did not exist.

The data recorded before May 2nd 1979 produced a high weighting factor in the computer transformed data. When these were excluded from the analysis , the Durbin Watson statistics increased and n value , the power constant in the Saito relation , reduced from 1.43 to 1.2.

5.6.7.2 Horizontal Displacement Analysis

Cumulative horizontal displacements , without correction for the direction of movement , were used to examine four different laws. This was done in two stages. The first stage involved the analysis of the complete set of data (see section 5.6.3). In the second stage , the data set was divided into two parts. Part one contained the measurements taken before 22nd of October.

1. Complete Data Set

   The plot of $\log(t_f - t)$ versus $\log(\dot{\varepsilon})$ (Figure 5.13) shows that the Saito relation is being followed. Table 5.11 summarizes all parameters.

Table 5.7 Slope distance analysis results

PRISM	26-B	26-B	26-B
LAW	POWER	EXPONENTIAL	$\dot{\varepsilon}$ - LOG(t)
DATA	ALL	ALL	ALL
INTERCEPT	-16.902	-5.001	-2194.22
±INTERCEPT 90%	4.6	1.04	3785.2
SLOPE	3.188	0.0203	469.57
±SLOPE 90%	0.86	0.003	706.6
DW CALCULATED	0.468	0.627	1.012
DW FROM TABLE 5%	1.24-1.43	1.24-1.43	1.24-1.43
TSS CALCULATED	39.02	83.4	1.252
TSS FROM TABLE 5%	4.08	4.08	4.08
RESIDUALS	0.00008	0.000667	-0.070313
WW-2	41	41	41
TRANSFORMED DATA	22	22	22

DW=DURBIN WATSON STATISTICS
TSS=TEST OF SLOPE SIGNIFICANCE
WW=WEIGHTING

Table 5.8 t_f effect in slope distance analysis results

PRISM	26-B	26-B	26-B	26-B
LAW	SAITO	SAITO	SAITO	SAITO
t_f AT NOV,10	10.00	10.30	11.00	11.30
DATA	ALL	ALL	ALL	ALL
INTERCEPT	5.862	5.888	5.9124	5.9368
±INTERCEPT 90%	0.748	0.749	0.750	0.751
SLOPE	-1.407	-1.4121	-1.4171	-1.4219
±SLOPE 90%	0.16	0.161	0.161	0.161
DW CALCULATED	1.351	1.36	1.368	1.376
DW FROM TABLE 5%	1.24-1.43	1.24-1.43	1.24-1.43	1.24-1.43
TSS CALCULATED	222.39	223.54	224.63	225.69
TSS FROM TABLE 5%	4.08	4.08	4.08	4.08
RESIDUALS	0.00015	0.000201	0.000141	0.000122
WW-2	40	40	40	40
TRANSFORMED DATA	22	22	22	22

DW=DURBIN WATSON STATISTICS
TSS=TEST OF SLOPE SIGNIFICANCE
WW=WEIGHTING

Table 5.9 t_f effect in slope distance analysis results cont.

PRISM	26-B	26-B	26-B	26-B
LAW	SAITO	SAITO	SAITO	SAITO
t_f AT NOV,10	12.00	12.30	13.00	13.30
DATA	ALL	ALL	ALL	ALL
INTERCEPT	5.9603	5.9832	6.0059	6.0278
±INTERCEPT 90%	0.752	0.753	0.753	0.754
SLOPE	-1.4266	-1.4312	-1.4356	-1.4399
±SLOPE 90%	0.161	0.161	0.161	0.162
DW CALCULATED	1.384	1.392	1.400	1.407
DW FROM TABLE 5%	1.24-1.43	1.24-1.43	1.23-1.43	1.24-1.43
TSS CALCULATED	226.689	227.65	228.58	229.46
TSS FROM TABLE 5%	4.08	4.08	4.08	4.08
RESIDUALS	0.000107	0.000117	0.000157	0.000184
WW-2	40	40	40	40
TRANSFORMED DATA	22	22	22	22

DW=DURBIN WATSON STATISTICS
TSS=TEST OF SLOPE SIGNIFICANCE
WW=WEIGHTING

Table 5.10 t_f effect in slope distance analysis results cont.

PRISM	26-B	26-B	26-B	26-B
LAW	SAITO	SAITO	SAITO	SAITO
t_f AT NOV.10	14.00	14.20	15.00	16.30
DATA	ALL	ALL	ALL	ALL
INTERCEPT	6.0492	6.0633	6.0909	6.1505
±INTERCEPT 90%	0.755	0.758	0.757	0.760
SLOPE	-1.4442	-1.4470	-1.4525	-1.4642
±SLOPE 90%	0.162	0.162	0.162	0.163
DW CALCULATED	1.414	1.419	1.428	1.447
DW FROM TABLE 5%	1.24-1.43	1.24-1.43	1.24-1.43	1.24-1.43
TSS CALCULATED	230.31	230.86	231.92	234.12
TSS FROM TABLE 5%	4.08	4.08	4.08	4.08
RESIDUALS	0.000175	0.000113	0.000186	0.000175
WW-2	40	40	40	40
TRANSFORMED DATA	22	22	22	22

DW=DURBIN WATSON STATISTICS
TSS=TEST OF SLOPE SIGNIFICANCE
WW=WEIGHTING

The power law was tested in two ways. A plot of $\dot{\varepsilon}/\ddot{\varepsilon}$ versus t illustrated that the slope of the line was quite sensitive to the X value. Slope values less than or equal to zero , representing the inadequacy of power law , were obtained.

On the other hand the X value was increased for plots of log($\dot{\varepsilon}$) versus log(t) , in approximate intervals of 10,000 minutes , from 10,000 to 6,000,000 minutes. The Durbin Watson statistics were increased from 0.618 to 0.876 , i.e. , power law could not be applied. In all cases there were significant slopes , different from zero (Table 5.12).

For evaluation of exponential law , as the X values were increased from 0.0 to 1,000,000 minutes in plots of log($\dot{\varepsilon}$) versus t , the Durbin Watson statistical values were constant at 0.886. There was a slope significantly different from zero.

2. Divided Data

As mentioned before the data was divided into two parts. Part one contained the measurements taken before 29th of October , when increase in acceleration was begun. Table 5.13 summarizes the results for the power and exponential laws. All 4 plots in this table are linear. However , the test of slope significance was low for part one data , indicating that the displacements before October

Table 5.11 Results of cumulative horizontal displacement analysis

PRISM	26-B
LAW	SAITO
DATA	ALL
INTERCEPT	6.15
±INTERCEPT 90%	1.69
SLOPE	-1.1
±SLOPE 90%	0.165
DW CALCULATED	1.943
DW FROM TABLE 5%	1.30-1.46
TSS CALCULATED	128.4
TSS FROM TABLE 5%	4.26
RESIDUALS	-0.000231
WW-2	24
TRANSFORMED DATA	26

DW=DURBIN WATSON STATISTICS
TSS=TEST OF SLOPE SIGNIFICANCE
WW=WEIGHTING

Table 5.12 X effect in power law statistics

X Minutes	DURBIN WATSON STATISTIC	TEST OF SLOPE SIGNIFICANCE
10,000	0.618	17.616
20,000	0.640	20.075
50,000	0.679	23.900
60,000	0.688	24.800
100,000	0.715	27.281
120,000	0.726	28.207
150,000	0.739	29.350
170,000	0.746	30.000
200,000	0.756	30.835
220,000	0.762	31.322
250,000	0.770	31.967
300,000	0.780	32.868
350,000	0.790	33.606
400,000	0.797	34.222
450,000	0.803	34.746
500,000	0.809	35.198
550,000	0.814	35.591
600,000	0.818	35.937
700,000	0.825	36.516
800,000	0.831	36.985
900,000	0.836	37.371
1,000,000	0.840	37.694
1,100,000	0.843	37.972
1,200,000	0.846	38.205
1,500,000	0.853	38.754
2,000,000	0.860	39.346
2,500,000	0.865	39.723
3,000,000	0.868	39.982
4,000,000	0.872	40.324
5,000,000	0.874	40.532
6,000,000	0.876	40.674

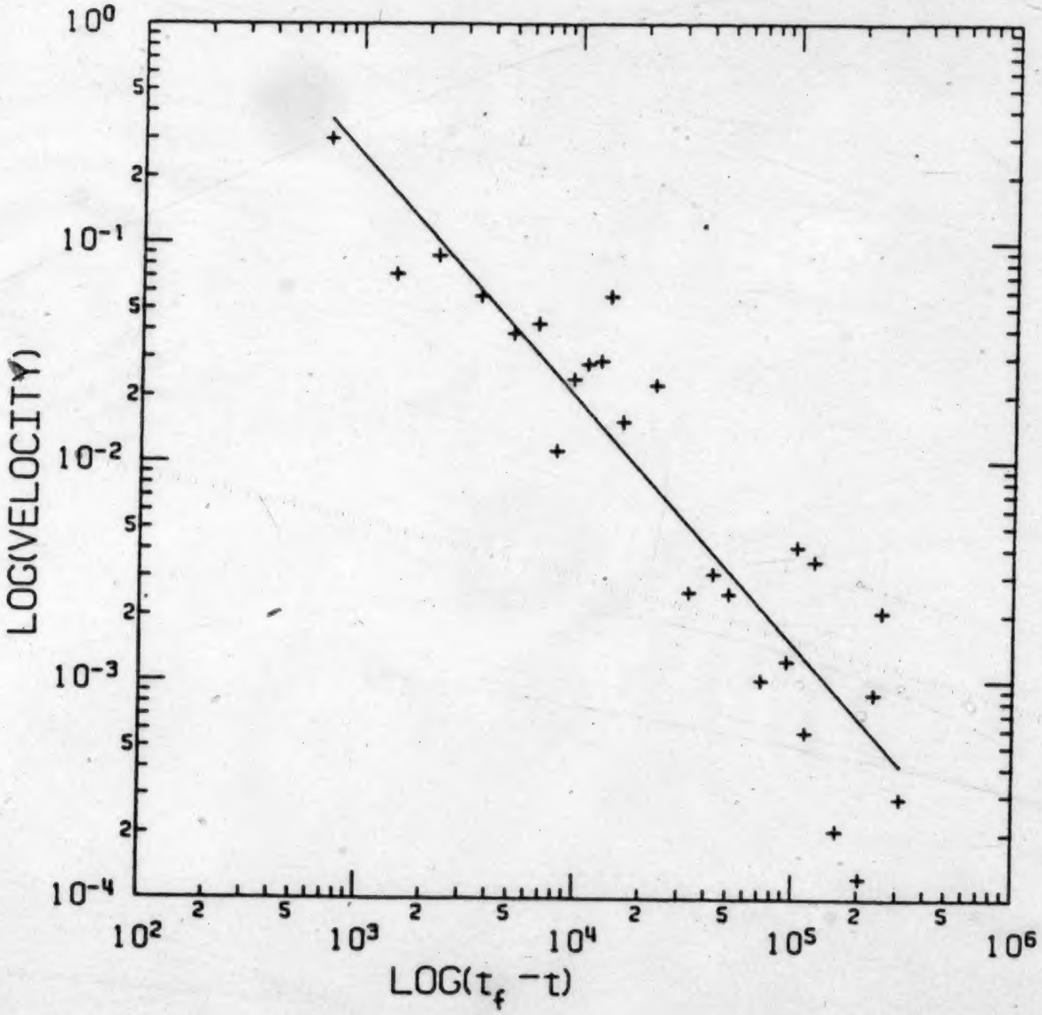

Figure 5.13 Saito fit to cumulative horizontal displacements (velocity in mm/min , time in min)

29th were not significant. the exponential law proves that the Zavodni and Broadbent's equation may be applicable.

5.6.7.3 Displacement Vector Resultant Analysis

A displacement vector resultant was calculated from its vertical and horizontal components. Upward vertical components , though in the range of instrument error , and data points that produced high weighting factors were eliminated for the following complete and divided data sets. No data was omitted for t_f variation analysis. It was also assumed that all displacement vectors had identical orientations. The procedure used here is similar to that of horizontal displacement analysis.

1. Complete Data Set

Results showed that pure Saito relation is applicable. Power and exponential laws do not fit the data. The $\dot{\epsilon}/\ddot{\epsilon}$ versus t plot had a negative slope. Table 5.14 summarizes the results. Figures 5.14 to 5.17 illustrate the corresponding plots.

2. Divided Data

The data was divided into 2 parts. Part 2 contained measurements taken after 29th October 1979 , when MacRae's (1982) observations confirmed drastic acceleration in displacements.

Both parts of the data showed that Saito , power and exponential laws were applicable. Because of the use of the resultants of the displacement

Table 5.13 Results of cumulative horizontal displacement analysis - divided data

PRISM	26-B	26-B	26-B	26-B
LAW	EXPONENTIAL	EXPONENTIAL	POWER	POWER
DATA	PART 1	PART 2	PART 1	PART 2
INTERCEPT	-8.394	-32.527	-9.69	-372.14
±INTERCEPT 90%	1.528	19.037	3.809	243.18
SLOPE	0.000007	0.000084	0.238	28.901
±SLOPE 90%	0.0000067	0.000054	0.321	19.04
DW CALCULATED	2.206	1.532	1.786	1.524
DW FROM TABLE 5%	(1.36)	(1.36)	(1.36)	(1.36)
TSS CALCULATED	3.607	7.637	1.809	7.451
TSS FROM TABLE 5%	4.96	4.84	4.96	4.84
RESIDUALS	0.0000069	0.000507	0.000072	0.000072
WW-2	10	11	10	11
TRANSFORMED DATA	12	13	12	13

DW=DURBIN WATSON STATISTICS
TSS=TEST OF SLOPE SIGNIFICANCE
WW-WEIGHTING

vectors more displacement quantities are available than those of horizontal or slope distance analyses.

The plots of $\dot{\epsilon}/\ddot{\epsilon}$ versus t have positive slopes , however they do not have a slope significantly different from zero. Tables 5.15 and 5.16 summarize the results. Figures 5.18 to 5.25 show all plots. These results will be discussed in detail in Section 5.6.8 and Chapter 6.

3. t_f Variation

Table 5.17 shows the effect of the choice of t_f in linearity. Except for the analysis results shown in the first line of the table , in which high weighting factors were avoided , all data points were used. The peak Durbin Watson statistical value of 2.069 was observed at 365560 minutes , a time about 5 days after the actual time of slide. It reduced to 1.403 , below the upper bound of the critical value at 5% confidence level , indicated significant positive serial correlation (Figure 5.26). On the other hand , the test of slope significance statistics showed slopes different from zero. Figure 5.27 shows the variations of the Saito fit statistics with the time of failure. The parallel variations of the test of slope significance with Durbin Watson statistics is illustrated.

Table 5.14 Results of analysis of the resultants of the displacement vectors

PRISM	26-B	26-B	26-B	26-B
LAW	POWER	EXPONENTIAL	SAITO	$\dot{\varepsilon}/\dot{\varepsilon}$ - t
DATA	ALL	ALL	ALL	ALL
INTERCEPT	-51.4	-10.4	6.460	11637
±INTERCEPT 90%	16.9	1.57	2.022	56690
SLOPE	3.7	0.0000194	-1.116	-0.038
±SLOPE 90%	1.352	0.0000055	0.197	0.188
DW CALCULATED	0.742	0.915	1.605	1.809
DW FROM TABLE 5%	1.30-1.46	1.30-1.46	1.30-1.46	1.29-1.45
TSS CALCULATED	22.2	35.8	94.52	o.118
TSS FROM TABLE 5%	4.26	4.26	4.26	4.28
RESIDUALS	0.003	0.0003	-0.000222	-0.289
WW-2	24	24	24	23
TRANSFORMED DATA	26	26	26	25

DW=DURBIN WATSON STATISTICS
TSS=TEST OF SLOPE SIGNIFICANCE
WW-WEIGHTING

Table 5.15 Results of analysis of the resultants of the displacement vectors - part 1 data

PRISM	26-B	26-B	26-B	26-B
LAW	POWER	EXPONENTIAL	SAITO	$\dot{\varepsilon}/\ddot{\varepsilon}$ - t
DATA	PART 1	PART 1	PART 1	PART 1
INTERCEPT	-20.427	-8.2	3.849	-38819
±INTERCEPT 90%	19.32	1.9	10.584	79650
SLOPE	1.124	0.0000071	-0.906	0.237
±SLOPE 90%	1.577	0.0000081	0.911	0.381
DW CALCULATED	1.506	1.58	1.623	1.368
DW FROM TABLE 5%	(1.36)	(1.36)	(1.36)	(1.36)
TSS CALCULATED	1.638	2.514	3.193	1.649
TSS FROM TABLE 5%	4.84	4.84	4.84	4.96
RESIDUALS	0.000258	0.000099	0.000001	-0.5
WW-2	11	11	11	10
TRANSFORMED DATA	13	13	13	12

DW=DURBIN WATSON STATISTICS
TSS=TEST OF SLOPE SIGNIFICANCE
WW=WEIGHTING

Table 5.16 Results of analysis of the resultants of the displacement vectors - part 2 data

PRISM	26-B	26-B	26-B	26-B
LAW	POWER	EXPONENTIAL	SAITO	$\dot{\varepsilon}/\dot{\varepsilon}$ - t
DATA	PART 2	PART 2	PART 2	PART 2
INTERCEPT	-534.07	-44.81	3.251	-524098
±INTERCEPT 90%	246.02	25.36	2.710	1632555
SLOPE	41.59	0.000119	-0.731	1.45
±SLOPE 90%	19.26	0.000071	0.313	4.65
DW CALCULATED	1.698	1.708	2.531	2.388
DW FROM TABLE 5%	(1.36)	(1.36)	(1.36)	(1.36)
TSS CALCULATED	8.775	8.874	17.90	0.326
TSS FROM TABLE 5%	4.96	4.96	4.96	5.12
RESIDUALS	0.00759	0.00043	0.000014	4.0039
WW-2	10	10	10	9
TRANSFORMED DATA	12	12	12	11

DW=DURBIN WATSON STATISTICS
TSS=TEST OF SLOPE SIGNIFICANCE
WW=WEIGHTING

Table 5.17 An examination of the Saito relation

$t_{f1} - t_{f2}$ Minutes	DURBIN WATSON STATISTIC	TIME INTERVAL Minutes
358390-358980	1.562-1.654	15
354360 - 356160	1.677 - 1.876	30
356260 - 363760	1.894 - 2.066	100
363760 - 356560	2.066 - 2.069	300
365560 - 386260	2.069 - 1.956	300
389260 - 405260	1.937 - 1.847	1000
405000 - 600000	1.824 - 1.462	5000
600000 - 700000	1.462 - 1.403	5000

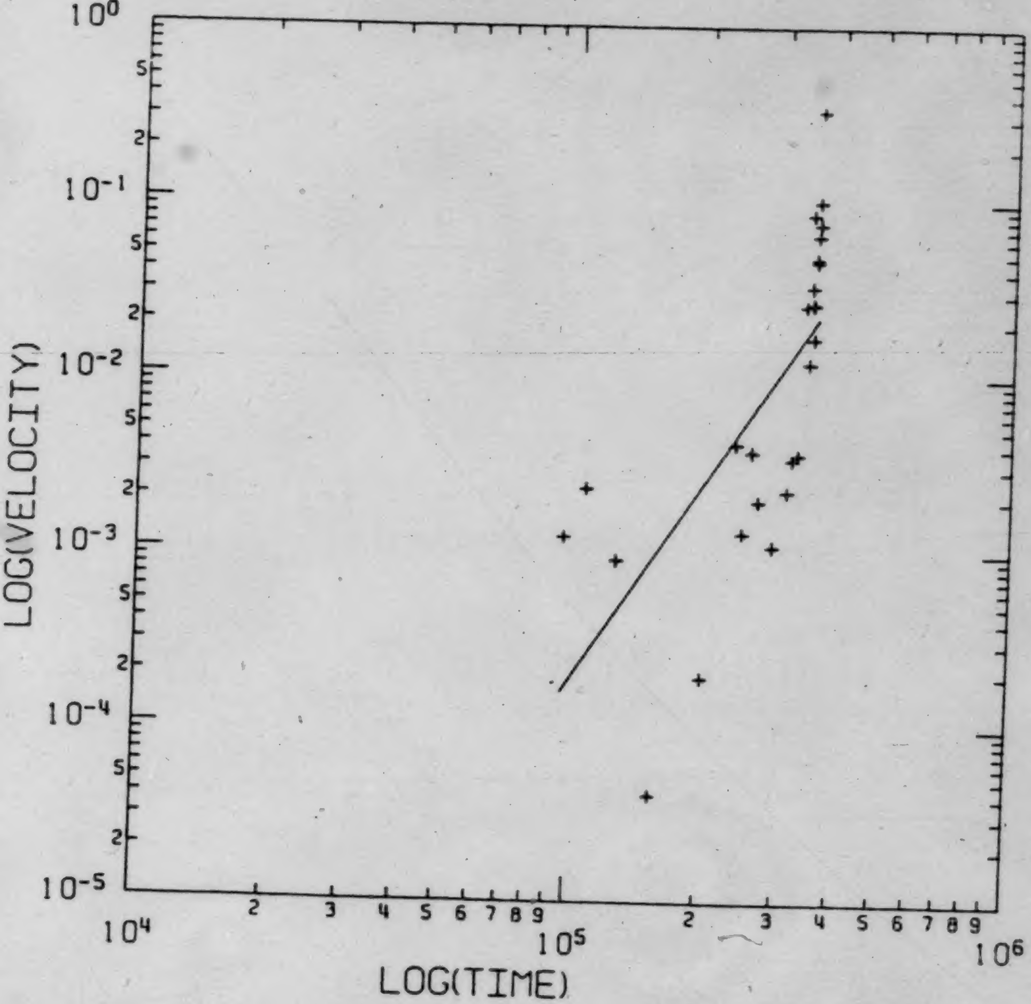

Figure 5.14 Power law fit to the resultants of the displacement vectors (velocity:mm/min , time:min)

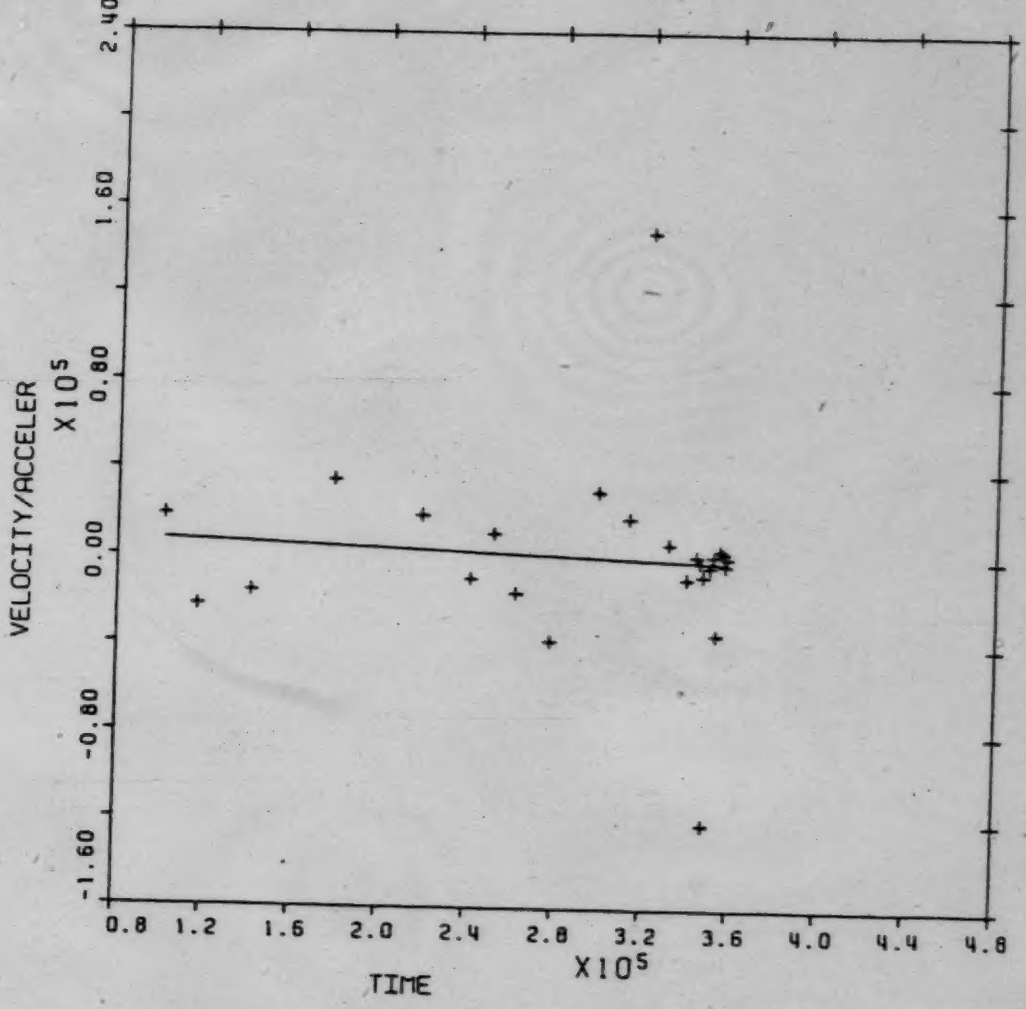

Figure 5.15 Power law fit to the resultants of the displacement vectors (velocity/acceleration:min , time:min)

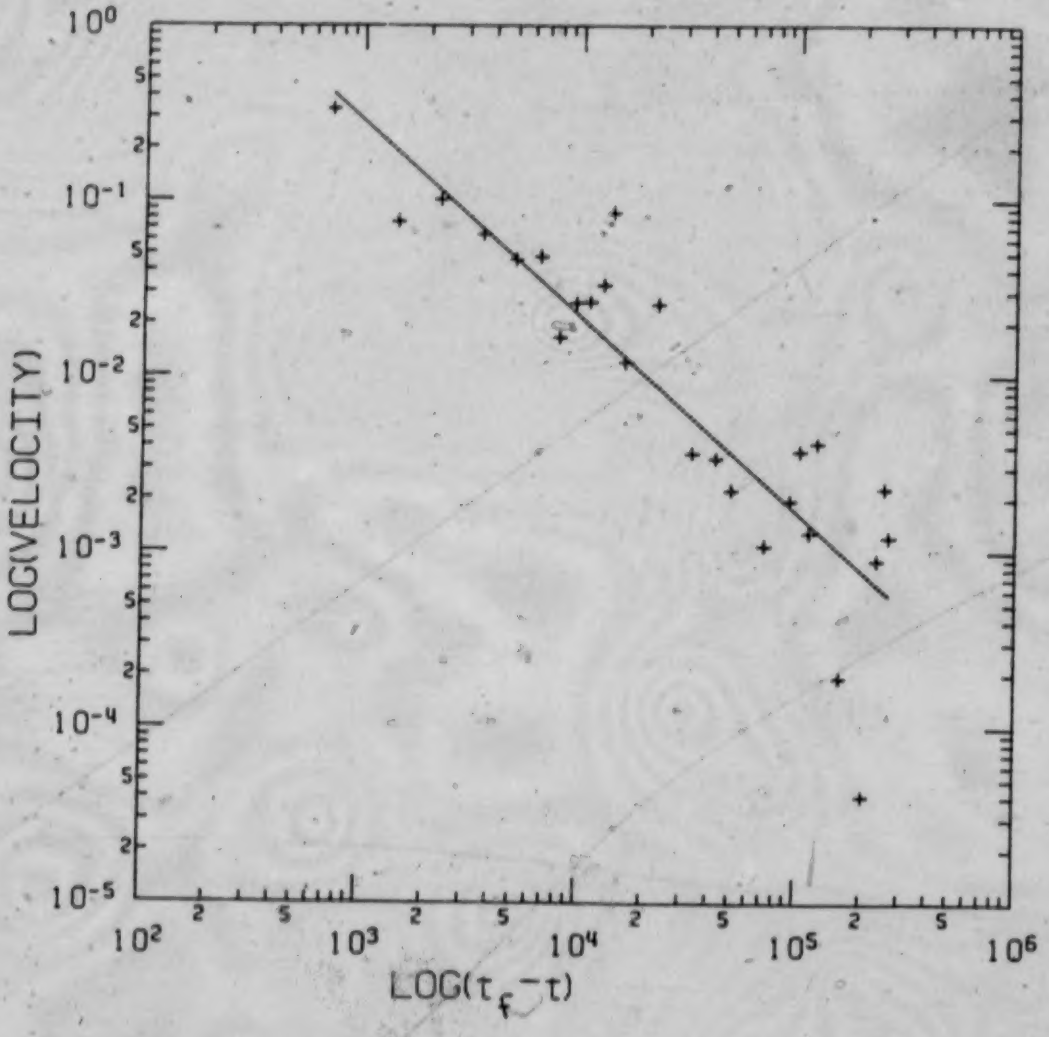

Figure 5.16 Saito fit to the resultants of the displacement vectors (velocity:mm/min , time:min)

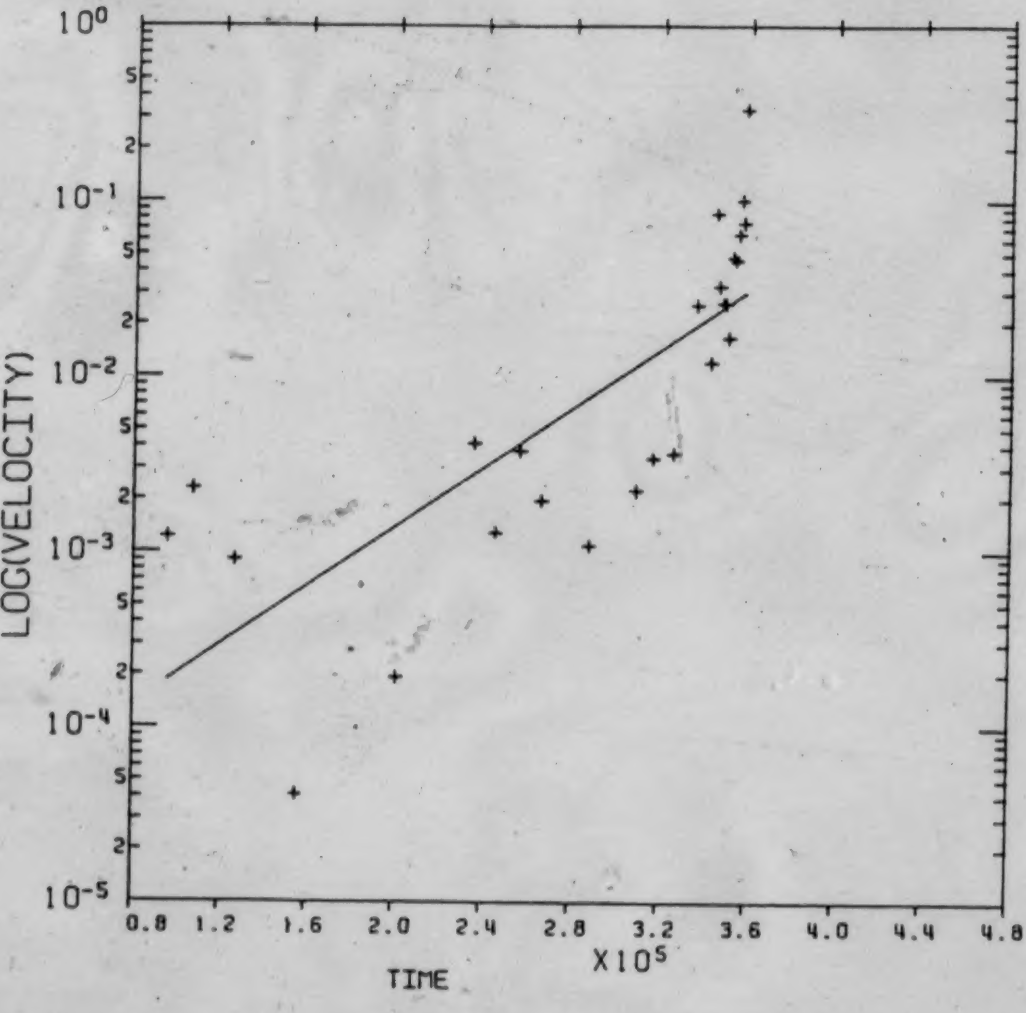

Figure 5.17 Exponential law fit to the resultants of the displacement vectors (velocity:mm/min , time:min)

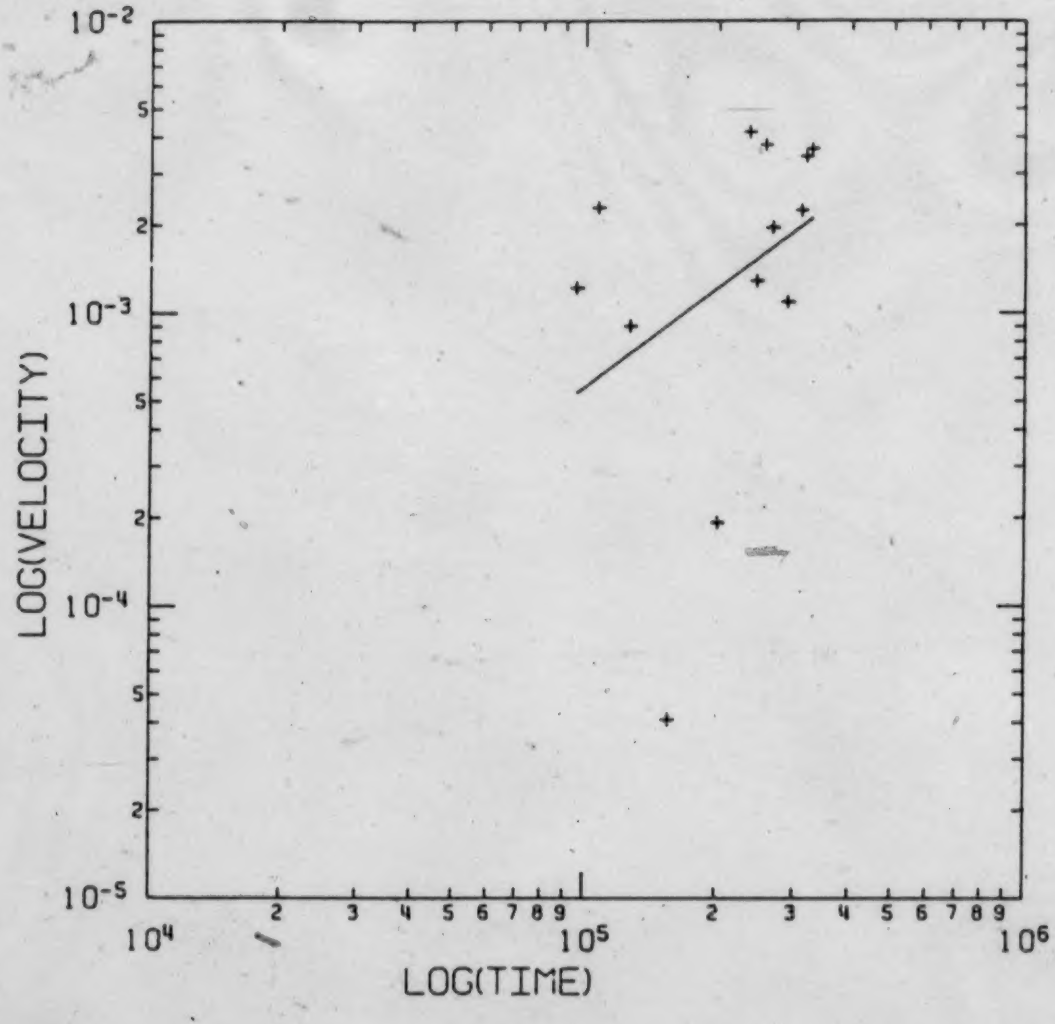

Figure 5.18 Power law fit to the resultants of the displacement vectors - part 1 data(velocity:mm/min , time:min)

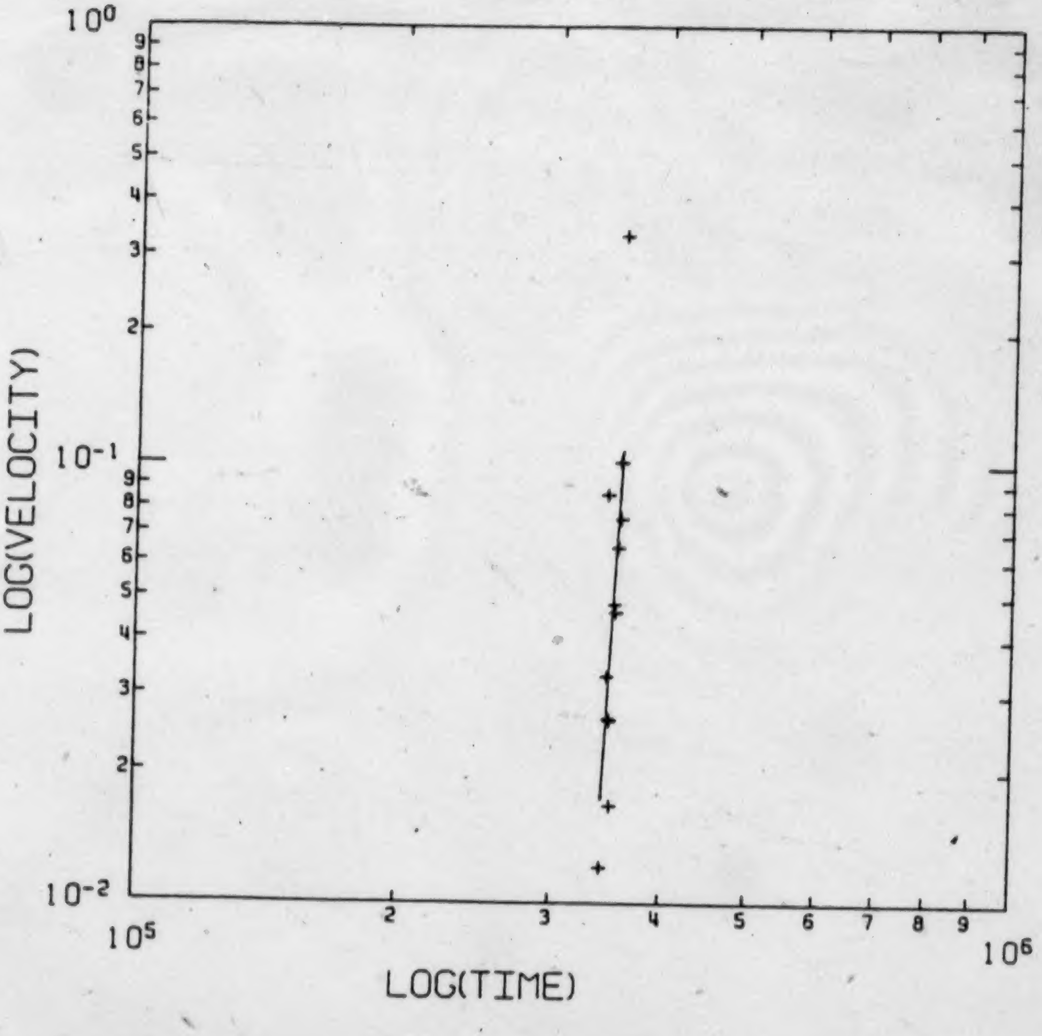

Figure 5.19 Power law fit to the resultants of the displacement vectors - part 2 data(velocity:mm/min , time:min)

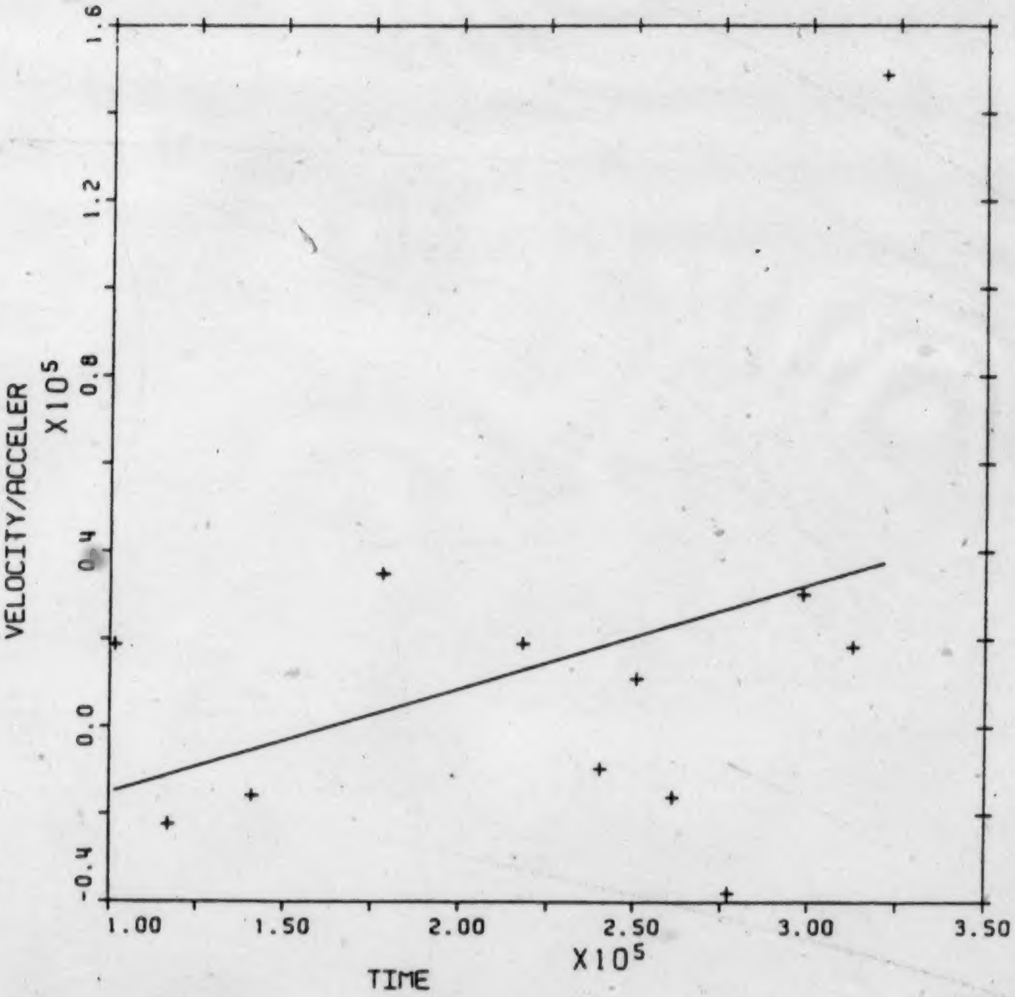

Figure 5.20 Power law fit to the resultants of the displacement vectors - part 1 data(velocity/acceleration:min , time:min)

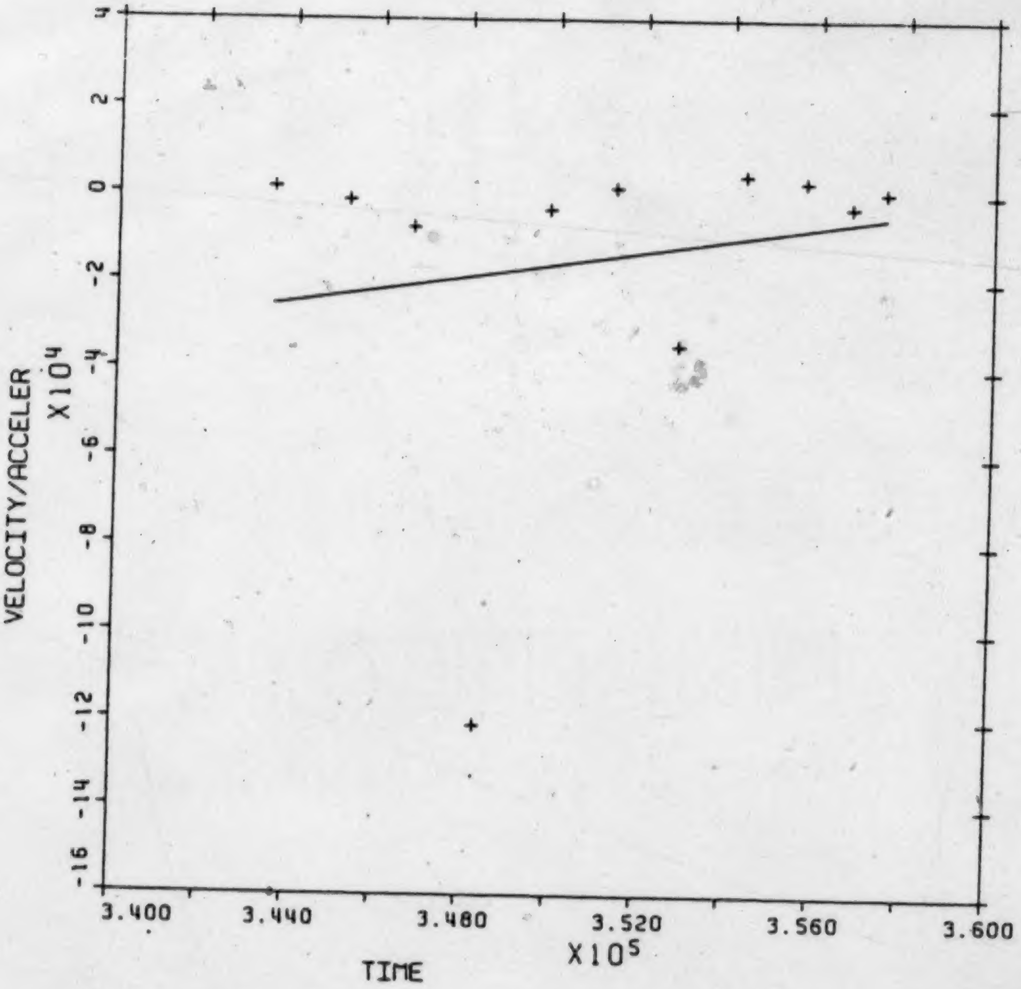

Figure 5.21 Power law fit to the resultants of the displacement vectors - part 2 data(velocity/acceleration:min , time:min)

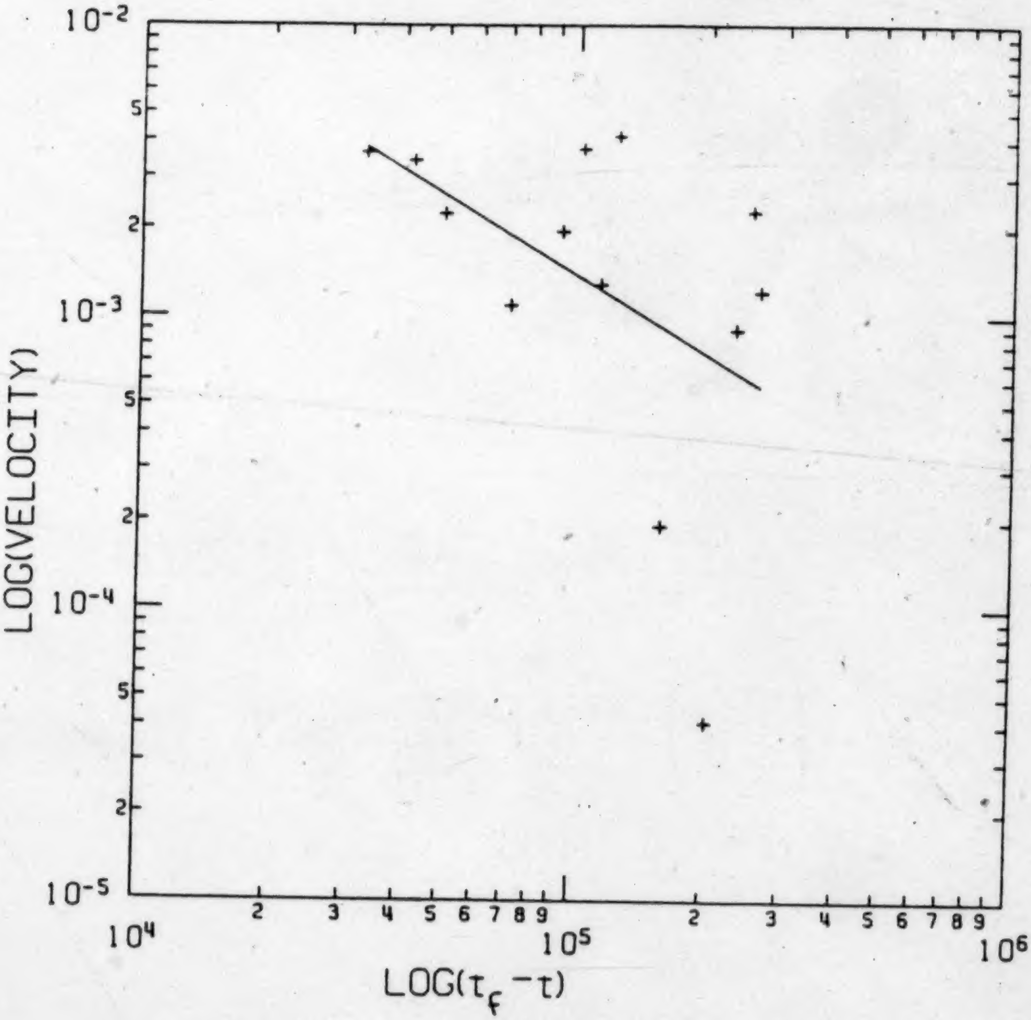

Figure 5.22 Saito fit to the resultants of the displacement vectors - part 1 data(velocity:mm/min , time:min)

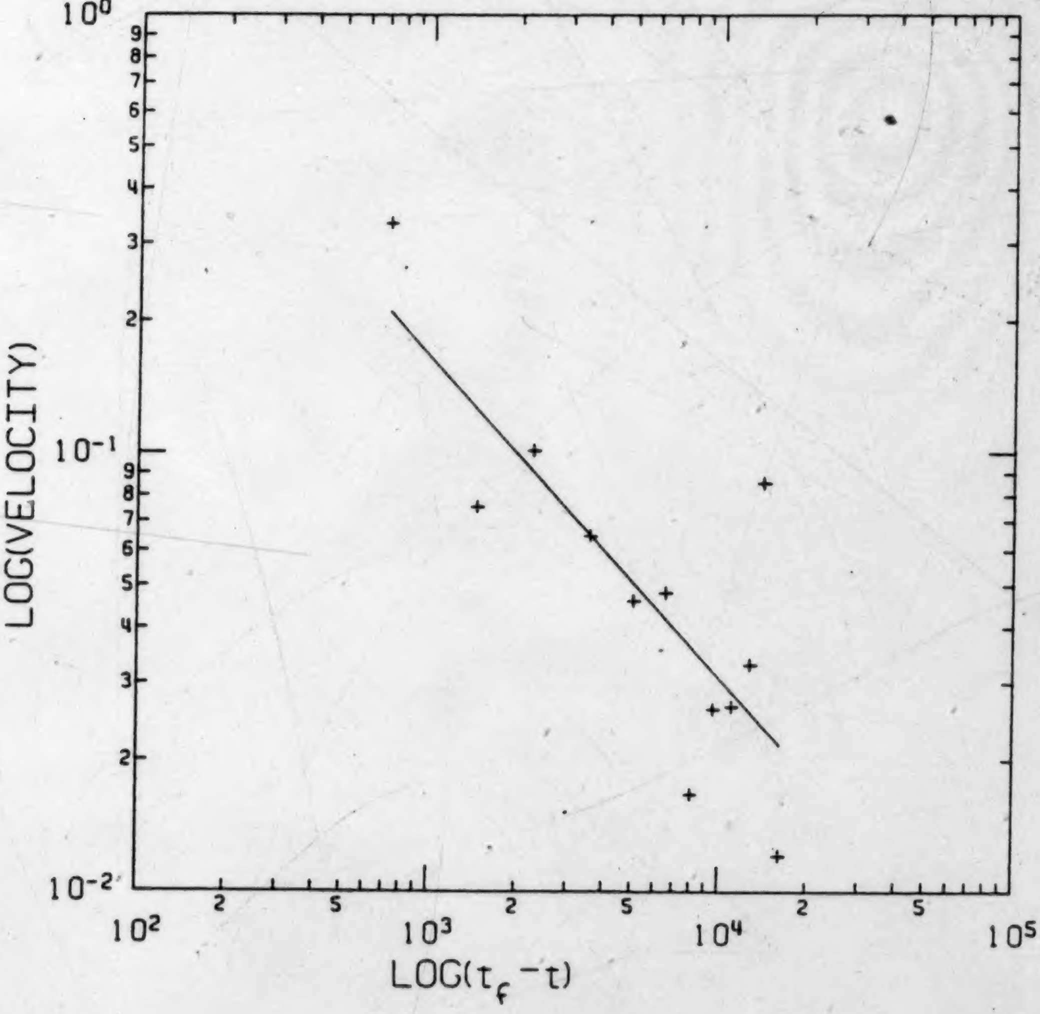

Figure 5.23 Saito fit to the resultants of the displacement vectors - part 2 data(velocity:mm/min , time:min)

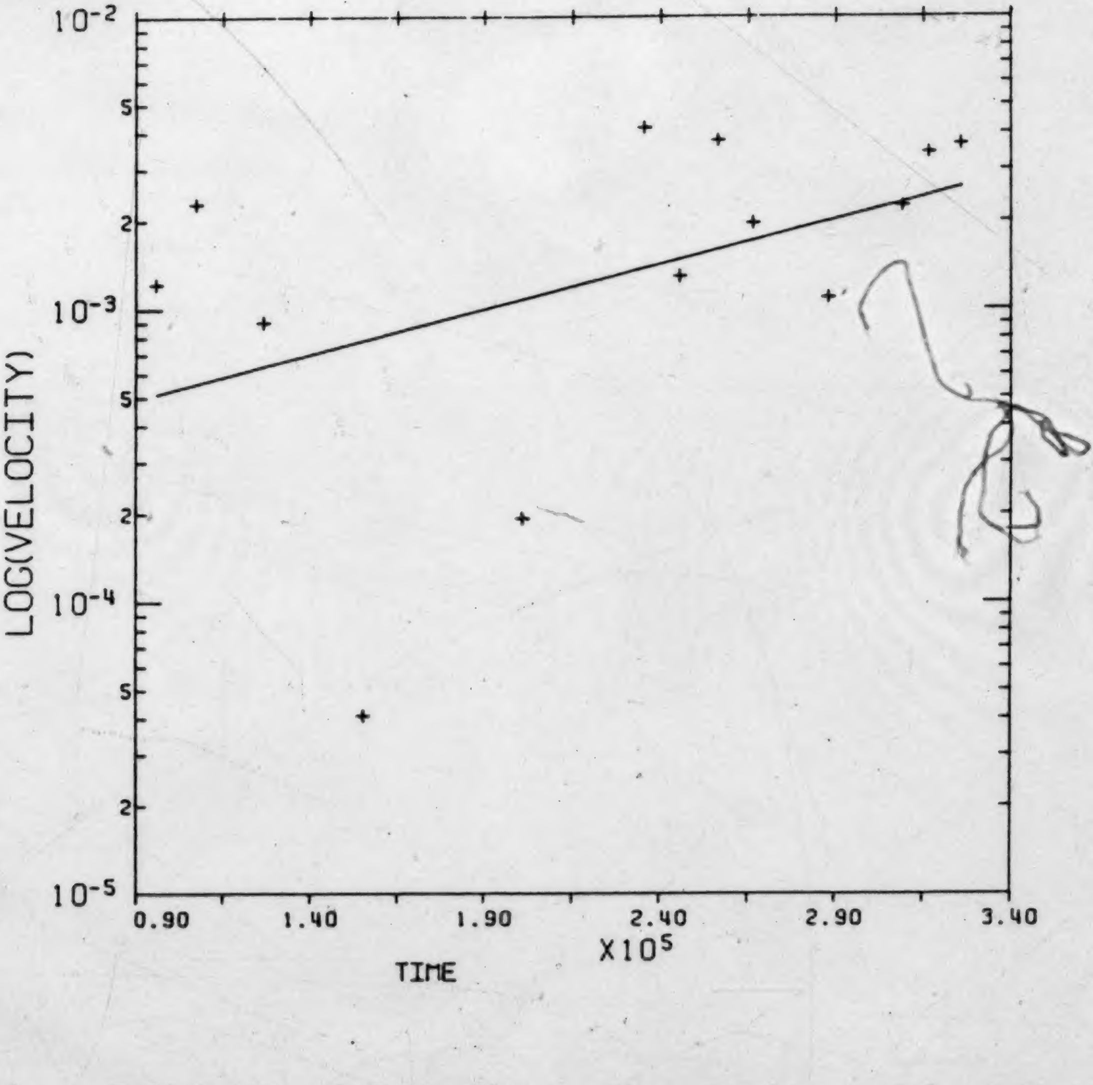

Figure 5.24 Exponential law fit to the resultants of the displacement vectors - part 1 data (velocity:mm/min , time:min)

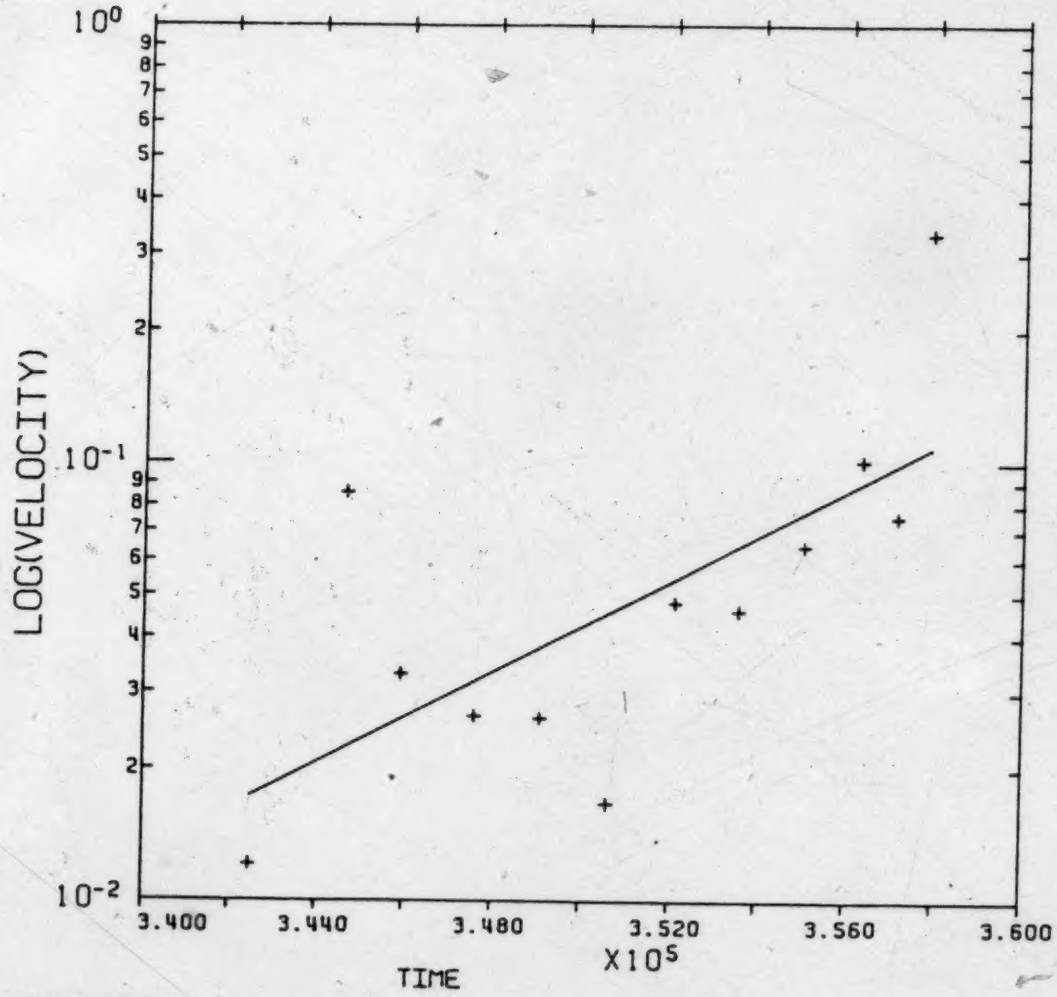

Figure 5.25 Exponential law fit to the resultants of the displacement vectors - part 2 data (velocity:mm/min , time:min)

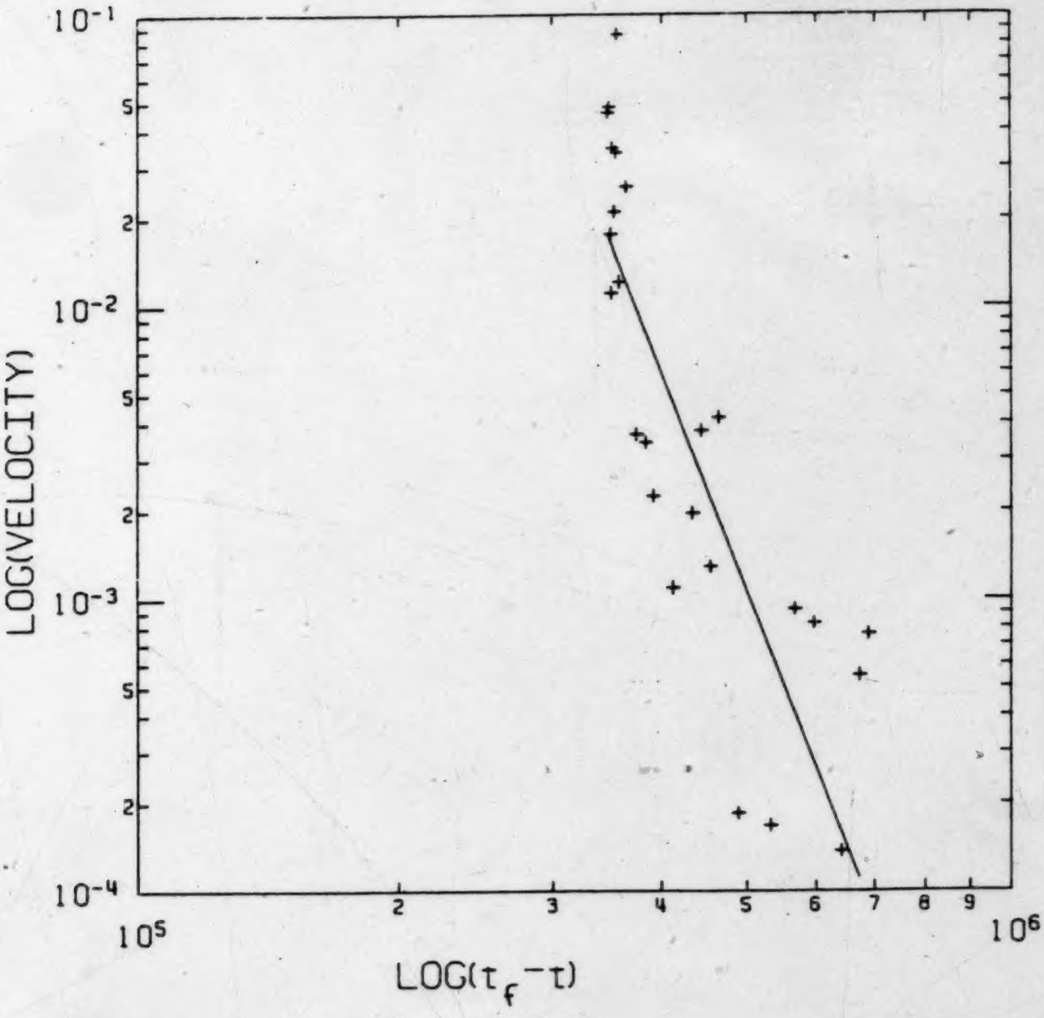

Figure 5.26 Saito fit to the resultants of the displacement vectors when t =700,000 minutes (velocity:mm/min , time:min)

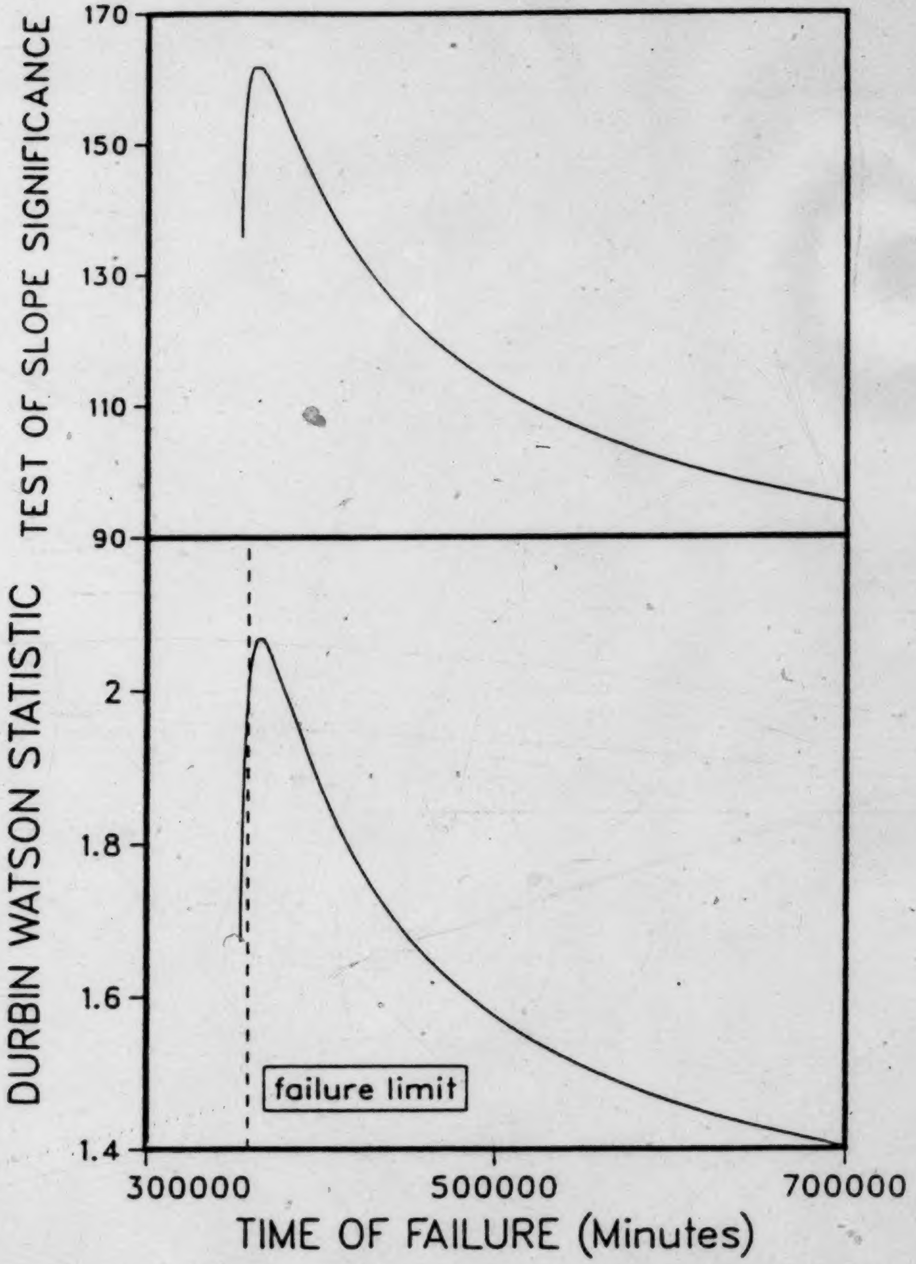

Figure 5.27 Saito fit statistics - time of failure effect

5.6.8 Discussion

5.6.8.1 Power Law

The plots of $\dot{\epsilon}/\ddot{\epsilon}$ versus t (see Figure 5.15 , Table 5.14 and section 5.6.7.2) had either a negative or approximately zero slope and negative X values , when the whole data set was analyzed. This indicated that the power law was not applicable to the complete period of accelerating creep. The same plots had positive slopes for both parts , when the data set was divided into 2 parts (Tables 5.15 and 5.16). In all cases the Durbin Watson statistics were more than the upper limit , and , the test of slope significance statistics were less than those at 5% confidence level , indicating that there was not a slope significantly different from zero.

The n values obtained from $\dot{\epsilon}/\ddot{\epsilon}$ versus t plots for parts one and two of the data were 5.16 and 1.68 with corresponding negative X values of 161746 and 356387 minutes respectively as opposed to n values of 2.12 and 42.59 obtained from $\log(\dot{\epsilon})$ versus log(t) plots. Using the n values of the latter lines , the slope of the former lines would be in the range of 0.02 to 0.89. This range is very small and is manifested as the low test of slope significance statistics.

The negative X values may indicate that the processes represented by the power law were started after the measurements had started.

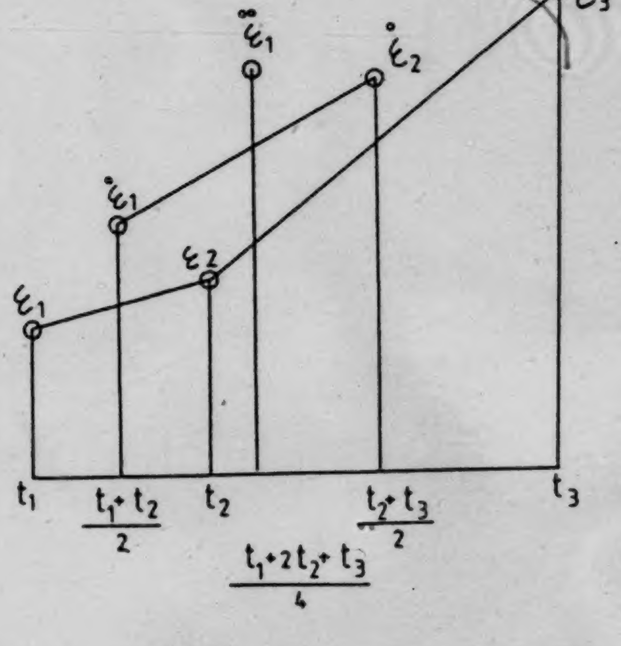
$\ddot{\varepsilon}_1$
$\dot{\varepsilon}_2$
ε_3
$\dot{\varepsilon}_1$
ε_2
ε_1
t_1
$\frac{t_1+t_2}{2}$
t_2
$\frac{t_2+t_3}{2}$
t_3
$\frac{t_1+2t_2+t_3}{4}$

Figure 5.28 Computation of velocity and acceleration

Apart from human and instrument errors and external forces of rain , snow , earthquake , blasting , etc , approximate numerical calculation of velocity and acceleration contributes to the above discrepancies. Figure 5.28 shows the numerical technique used to compute velocity and acceleration.

It can be seen that linear interpolation was used to compute velocity and acceleration. Any pair of velocity and acceleration , calculated for determination of any velocity to acceleration ratio , should correspond to identical time values. Taking this into account , the resultants of the displacement vectors and cumulative horizontal displacements were used to fit the power law. In this case both velocity and acceleration were calculated at time $(t_1+2t_2+t_3)/4$. For further details refer to the documentation and listing of the program POW2 in the Appendix.

As the curvature of the displacement versus time curve increases , departure from linearity increases , and , the linear interpolation method becomes less valid. Because of this error involved near to the time of failure , the n value was very low for part 2 data.

5.6.8.2 Zavodni And Broadbent's Fit

From the analyses carried out for the fit of the resultants of the displacement vectors , and , taking t_f=358605 minutes , equations for exponential law may be written as:

For part 1 , i.e. , regressive stage ;

$\dot{\epsilon} = 0.00276\ e^{-0.000007(t_f - t)}$

For part 2 , i.e. , progressive stage ;

$\dot{\epsilon} = 0.093\ e^{-0.000004(t_f - t)}$

The collapse velocity at the time of slide is 0.09 mm/min. This velocity is far less than reality. Records and plots of log($\dot{\epsilon}$) versus t (Figures 5.17 and 5.25) show that on the morning of November 10 , there was a drastic increase in displacement. This increase can be regarded , despite Zavodni and Broadbent's 2-line theory , as a third line with steeper slope after t_0=357150 minutes and $\dot{\epsilon}_0$=0.074 mm/min. Taking a typical k=7 value , a collapse velocity of $(7^2)(0.074)$=3.6 mm/min is obtained. This velocity is more than seven times of that suggested by MacRae (1982) and Wyllie and Munn (1979) as the critical slide velocity.

5.6.9 Practical Applications

The data set was analyzed in two ways ; whole and partial.

When the whole data set was analyzed , the least squares method parameters were not satisfied for power and exponential laws. However , they were satisfied for the Saito fit. Estimation of velocities at times beyond the last measurements is a function of t_f for the Saito fit. It was shown that a range of t_f was acceptable. The upper limit for t_f was 241395 minutes after the actual time of the most rapid movement , and , the lower limit was a few minutes after the last measurements. In contrast with what Varnes (1982) and Saito (1969 , 1980) stated , the exact prediction , "fine tuning" , of the time of failure is not possible. At t=358440 minutes , velocities of 2.09 and 0.02 mm/min were obtained when t_f was 358605 and 600,000 minutes , respectively. Hence , the choice of t_f has greatly influenced the prediction of velocities before failure.

The power , Saito , exponential and Zavodni and Broadbent's laws were all applicable when partial data were used. The first portion of data , taken before 29th of October 1979 , did not show large movements. However , the second portion , showed drastic displacements. All accelerating creep relations for part 2 data may be compared with one another. Figure 5.29 compares these relations beyond 165 minutes to failure. This figure was drawn from the fitted lines parameters written in Table 5.16 by using Table 5.1. It is seen that power , exponential and Zavodni and Broadbent's 2-line theories greatly underestimate velocities close to the time of failure. They show velocities less than 0.13 mm/min , in contrast with the critical slide velocity of 0.5 mm/min introduced by MacRae (1982) and Wyllie and Munn (1979). These low velocities were obtained when 2 accelerating creep stages were assumed. It will be demonstrated that higher velocities can be obtained by taking into account the third accelerating creep stage. On the other hand , the Saito relation yields

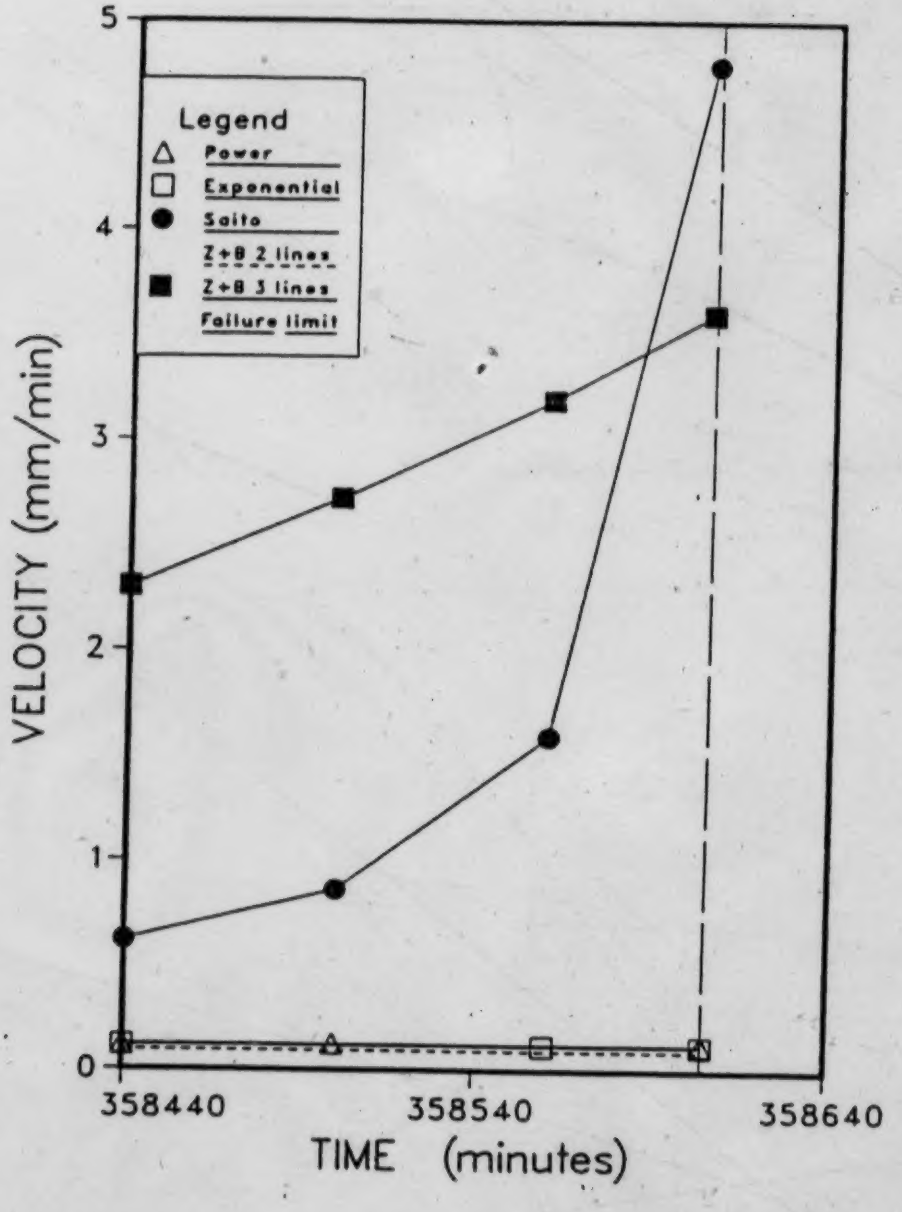

Figure 5.29 Comparison of laws beyond 165 minutes prior to failure

velocities in excess of the suggested critical value , with the time of failure chosen as 358605 minutes. This relation also suggests that the critical slide velocity of 0.5 mm/min was obtained at 9:05 A.M , on November 10th 1979 , 3 hours and 40 minutes before the time of failure. A close examination of the Saito relation is not possible , since the latest available recorded velocity is 0.33 mm/min at t=357885 minutes , a time 12 hours before the time of the most rapid movement.

As mentioned in the discussion of the fit (Section 5.6.8.2) of Zavodni and Broadbent's function , because of high velocities near to failure , it was necessary to assume a third line after $\dot{\varepsilon}_0$=0.074 mm/min and t_0=357150 minutes. This line , shown in Figure 5.29 , gives velocities over 2 mm/min and a finite velocity of 3.6 mm/min at the time of failure. The critical slide velocity of 0.5 mm/min was predicted 12.3 hours before failure. If data near to failure time were available , the validity of this line could be tested.

A practical procedure for t_f prediction is not possible. However , a criterion can be set for prediction of the time of critical slide velocity. The last velocities , plotted in Figures 5.19 and 5.25 , show that there was a drastic increase in velocity from 0.1 to 0.33 mm/min , at t=357885 minutes. This increase can be regarded as the initiation of the third stage of accelerating creep process. The power , exponential and Saito relations show that velocity reached a threshold value of 0.1 mm/min 34 , 23.3 and 33.2 hours before failure , respectively. This threshold velocity of 0.1 mm/min indicates the boundary between the second and third accelerating creep stages. There are only three displacement measurements available after the threshold value of 0.1 mm/min had been reached and before the moment of failure. A satisfactory test of the Durbin Watson statistic requires a minimum number of 16 measurements. However , a rough estimation of velocity prior to failure , using the last three available displacement measurements , can be made. From these data , 2 velocities and their corresponding times are calculated. By passing power and exponential lines through these 2 points , velocities before failure may be estimated. The critical slide velocity of 0.5 mm/min corresponded to 8 hours and 23 minutes before failure for the power law , and , 8 hours and 38 minutes for the exponential line. Velocities at the time of failure were also calculated as 1.35 and 1.43 mm/min for the power and exponential laws , respectively.

As mentioned before , prediction of the time of the threshold velocity can be made by the use of the second accelerating creep stage. Displacement records show that this stage started at t=340680 minutes , equivalent to 2:00 P.M October 29 , 1979. The power law fit showed that this stage ended at t=356560 minutes , a time 34 hours before failure. The total time span of this stage is 11 days. The threshold velocity of 0.02 mm/min marks the initiation of the second accelerating creep stage. The low available number of data does not allow satisfactory prediction of the threshold velocity of 0.1 mm/min. If displacement readings were taken every 8 hours after the time when velocity had reached 0.02 mm/min , the prediction of the time of the threshold velocity of 0.1 mm/min would be satisfactorily possible 6 days in advance.

In conclusion , determination of the time of failure was not possible. For this reason , the Saito and Zavodni and Broadbent's relations are impractical. The power and exponential laws represented 3 accelerating creep stages. Using the third stage , the critical slide velocity was approximately predicted 8.5 hours before failure.

5.6.10 Consideration Of The Decelerating Creep

An examination of the data shows that the 26-B , 38-B , 39-B and 40-B prisms moved more than 3 metres after the slide occurred on November 10th. Other prisms moved a few centimetres. The 40-B prism showed more displacements than the others. Figure 5.30 illustrates the power law fit to the resultants of the displacement vectors for the 40-B prism. Fit parameters are written in Table 5.18. The fitted line shows that the velocity decreases to less than 0.03 mm/min on January 20 , when the buttress construction was completed.

Table 5.18 Results of analysis of the resultants of the displacement vectors for decelerating creep of the 40-B prism

PRISM	40-B
LAW	POWER
DATA	ALL
INTERCEPT	-0.547
±INTERCEPT 90%	0.840
SLOPE	-0.264
±SLOPE 90%	0.086
DW CALCULATED	1.867
DW FROM TABLE 5%	1.63
TSS CALCULATED	26.54
TSS FROM TABLE 5%	4.0
RESIDUALS	-0.000733
WW-2	63
TRANSFORMED DATA	64

DW=DURBIN WATSON STATISTICS
TSS=TEST OF SLOPE SIGNIFICANCE
WW=WEIGHTING

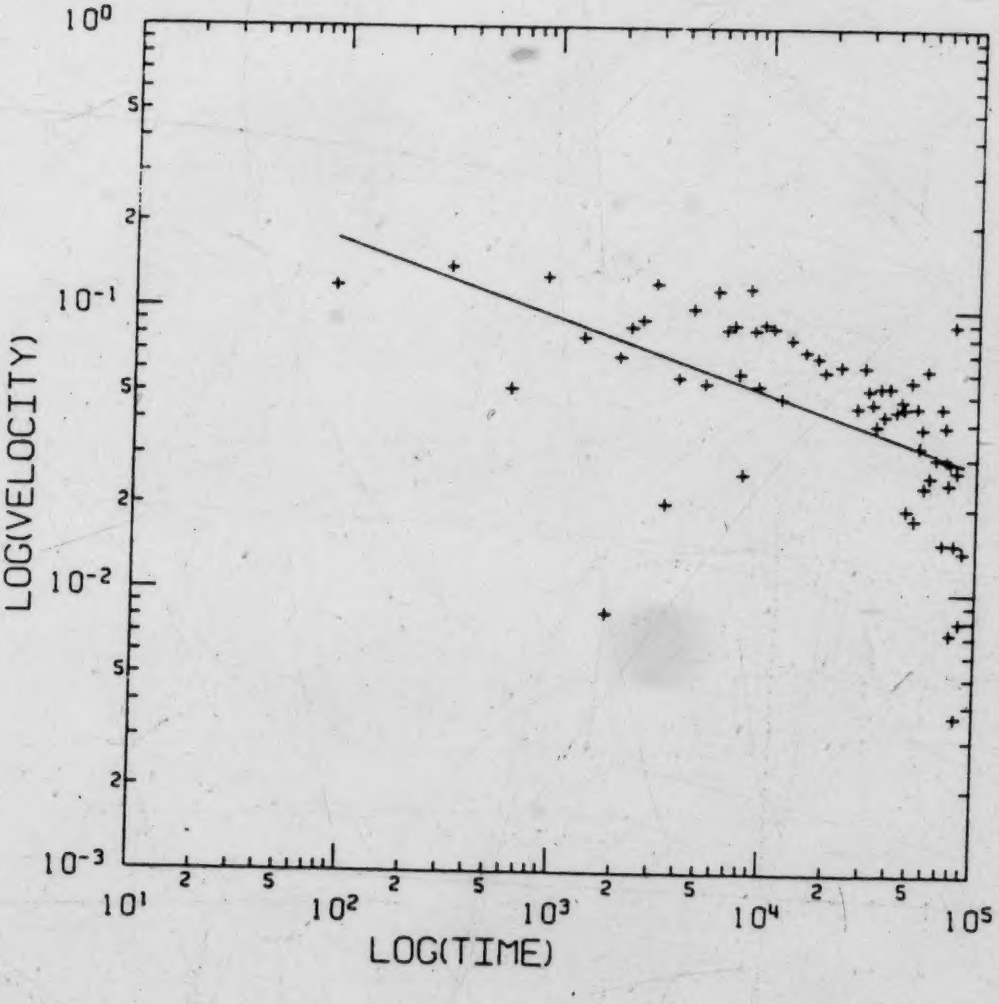

Figure 5.30 Power law fit to the resultants of the displacement vectors for decelerating creep of the 40-B prism (velocity:mm/min , time:min)

Chapter 6

CONCLUSIONS AND RECOMMENDATIONS

In this chapter , conclusions derived from the displacement analyses of 16 prisms in general and 26-B prism in particular , and recommendations for further expansion of this research program , are presented.

6.1 Conclusions

6.1.1 Power and Exponential Laws

1. The power and exponential laws were found to be the most practical relations for the prediction of the critical slide velocity , approximately 7 days in advance , as an indication of the impending failure. The application of the power law leads to a slightly more conservative design and therefore it is recommended (Section 5.6.9).
2. The power and exponential laws , when 2 accelerating creep stages were considered , compared to Saito relation , underestimate acceleration , particularly at times close to the time of the most rapid movement (Section 5.6.9).
3. When 3 accelerating creep stages were considered , an operational procedure was adopted for prediction of the time of the critical slide velocity , when evacuation of pit personnel and equipment should begin. Just before the initiation of the third accelerating creep stage , the threshold velocity of 0.1 mm/min was observed ,

approximately 34 hours before failure. Few available data in this stage showed that the critical slide velocity of 0.5 mm/min corresponded to 8.5 hours before failure. On the other hand , the threshold velocity of 0.02 mm/min was observed just before the initiation of the second accelerating creep stage. The prediction of the third accelerating creep stage was possible 6 days in advance , when measurements were taken every 8 hours upon the initiation of the second stage (Section 5.6.9).

4. Three numerical approximations are included in $\dot{\epsilon}/\ddot{\epsilon}$ term. First and second are the linear interpolations for the calculation of velocity and acceleration. Third is the incorrect assumption that the calculated velocity and acceleration belong to the same time (Section 5.6.8.1).

6.1.2 Saito Relation

1. Four different laws were analyzed and pure and generalized Saito laws found to be the most prevailing ones , when all data set was included for the 26-B prism and t_f was known (Section 5.6.7.3). Data for 16 prisms were analyzed. Half of the prisms did not follow Saito relation (Section 5.6.6).
2. A procedure for t_f prediction was presented (Section 5.6.1). t_f can be a variable within a given range of time. A preset upper limit Durbin Watson statistic may be given. The program will stop computation as soon as the upper limit of either Durbin Watson statistic or t_f is

reached. For the 26-B prism data , t_f at 5% confidence level could not be precisely , as opposed to what Saito (1969 , 1980) stated , determined. However , a range of acceptable values was obtained. The upper limit for t_f was 168 days after the actual time of the most rapid sliding (Sections 5.6.7.3 and 5.6.9) . Factors influencing this procedure will be discussed in Section 6.2.

3. The critical slide velocity , using the Saito fit parameters , was obtained 3.6 hours prior to failure. Velocity increased to 4.8 mm/min , 10 minutes before failure (Section 5.6.9).

6.1.3 Zavodni and Broadbent's fit

1. Zavodni and Broadbent's fit may be applicable , when t_f is known. However , instead of their proposed two , three accelerating creep stages were observed (Sections 5.6.8.2 and 5.6.9) .
2. Taking into account the third accelerating creep stage , the velocity reached to its critical value of 0.5 mm/min , 12.4 hours prior to failure (Section 5.6.9).

6.1.4 Movement Hypothesis

Five moving blocks were identified. Block 1 toppled away from the J3 joint set. The movement of blocks 2 and 4 is composed of two independent movements ; toppling away from the J3 joint set and sliding down the dip direction of the bedding. Blocks 3 and 5 moved along the dip direction of the bedding. Block 3 slid as a wedge , controlled by the J1 joint set and bedding (Section 3.3.3).

6.1.5 Other Conclusions

1. In the time long before the time of rupture , all laws may be applicable (Section 5.5).
2. Power and Saito relations have similar forms. They both represent displacement as a function of time to a power of n. However , the time variable for the power law , T , starts from the beginning of the accelerating creep process and the time variable for Saito relation , t_f-t , starts from the end of the accelerating creep process. The time variable in the power law shows the time after the initiation of the creep processes , and in Saito relation , the time before the termination of the creep processes (Sections 4.3 and 4.5).
3. All prisms neither moved in the same direction nor accelerated simultaneously. The ultimate time of slide for every or a group of prisms may be different from others (Sections 3.3.1 and 3.3.2).
4. Exponential and Zavodni and Broadbent's fit are identical in origin. However , the latter may be composed of 2 or more consecutive exponential lines (Sections 4.4 , 4.8 , 5.6.8.2 and 5.6.9).
5. Use of the resultants of the displacement vectors , instead of their components such as slope distance or cumulative horizontal displacement , can better represent

creep processes (Section 5.6.7).

6. The elimination of data which produced high weighting factors by human or instrument error resulted in higher values for Durbin Watson statistics (Section 5.6.7.1).

6.1.6 Limitation of application

The conclusions and recommendations outlined in this Chapter are applicable to the 51-B-2 pit conditions. However , they may be extended to other coal mines in the Rockies providing that geology is similar and slopes are drained. Low water elevations were reported by MacRae (1982) and Milligan and Hebil (1980) (Sections 3.3.1.1 and 3.3.4).

6.2 Recommendations

1. The time intervals of displacement monitoring should be reduced to 30 minutes , as soon as the velocity of 0.1 mm/min marks the initiation of the third accelerating creep stage. This allows a more accurate and reliable prediction of the time of the critical slide velocity approximately 18 hours in advance.
2. The time intervals of displacement monitoring should be reduced to 8 hours , as soon as the velocity of 0.02 mm/min marks the initiation of the second accelerating creep stage. This allows the prediction of the initiation of the third accelerating creep stage approximately 6 days in advance.
3. Ways to improve t_f prediction precision may be divided

into 2 groups.

Firstly , variations of ±10 millimetres in displacement and ±1 minute in time , can provide changes , ±0.1 in slope and ±0.7 in intercept of the Saito line. Therefore , the use of survey instruments with higher accuracy is valuable. The best application of the instruments is made , when successive measurements do not exceed the instruments accuracy. So , the use of short time intervals is recommended.

Secondly , external forces created by a blast , earthquake , rain , temperature change , ground water pressure change and excavation of buttress rock must be taken into consideration. These factors can greatly speed up or slow down the creep processes , and consequently affect t_f prediction precision. A record of the above activities needs to acompany displacement records. Ideal displacement records do not reflect the above external forces.

4. MacRae (1982) , plotted cumulative bearing versus time. It was seen that the 37-B , 38-B , 39-B and 40-B prisms moved simultaneously ; therefore , they may represent a moving block. With the use of displacement contours , areas with displacement concentration may be identified and analyzed as a block.

The change of distance between a pair of prisms with time indicates that they are moving on separate blocks. A computer program can be written to plot the variations of these distances with time. Therefore , the kinematics of the blocks and its variation with time can be better understood.

5. Alternative forms of linear relations , as presented in Tables 5.1 and 5.2 may be tested for mutual confirmation of the results.
6. Any kind of relation which may produce infinite displacement or displacement rate at the time of failure can be compared with the Saito relation , i.e. ; $\dot{\epsilon} = K/(e^{(t_r-t)}-1)^n$.
7. The resultants of the displacement vectors were analyzed. The direction of all vectors was assumed to be identical. Corrections for this should be included. Therefore , the use of displacement vectors instead of their resultants is recommended.
8. Data near to the time of slide were not available for the analyses of cumulative horizontal displacements and displacement vectors resultants. The inclusion of these data would be useful to the analyses.

BIBLIOGRAPHY

Benjamin , J.R. , and Cornell , C.A. , 1970. Probability , Statistics , and Decision for Civil Engineers. McGraw-Hill Book Company , 684 p.

Brawner , C.O. , and Stacey , P.F. , 1979. Hogarth Pit Slope Failure , Ontario , Canada , in Voight , B. , ed. , Rock Slides and Avalanches , 2 , pp. 699 - 707.

Broadbent , C.D. , and Ko , K.C. , 1971. Rheologic Aspects of Rock Slope Failures. Proceedings , 13th U.S. Symposium on Rock Mechanics , University of Illinois , Urbana , pp. 573 - 593.

Cruden , D.M. , 1969. A Laboratory Study of the Strain Behaviour and Acoustic Emission of Stressed Rock. Ph.D thesis , London University , 522 p.

Cruden , D.M. , 1971. The Form of the Creep Law for Rock under Uniaxial Compression. International Journal of Rock Mechanics and Mining Science , 8 , pp. 105 - 126.

Dobes , F. , and Milicka , K. , 1976. The Relation Between Minimum Creep Rate and Time to Fracture. Metal Science , 10 , pp. 382 - 384.

Durbin , J. , and Watson , G.S. , 1951. Testing for Serial Correlation in Least Squares regression - II. Biometrika 38 , pp. 159 - 176.

Goodman , R.E. , 1980. Introduction to Rock Mechanics , John Wiley & Sons , 478 p.

Hebil , K.E. , 1980. Report on Structural Mapping of Pit Walls at the Cardinal River Coals Ltd. , Luscar Ltd. , 24 p.

Hedley , D.G.F. , 1969. Triangulation and Trilateration Methods of Measuring Slope Movement. Canadian Department of Energy , Mines and Resources , Mines Branch ; Mining Research Center , Internal Report 72/69.

Hill , K. , 1980. Thesis on The Structural and Stratigraphy of the Cadomin Area , Masters thesis , University of Alberta , 191 p.

Hocking , G. , 1976. A Method for Distinguishing between Single and Double Plane Sliding of Tetrahedral Wedges. International Journal of Rock Mechanics and Mining Science and Geomechanics. Abstracts, 13 , Pergamon Press. pp. 225 - 226.

Iken , A. , 1977. Movement of a Large Ice Mass Before

Breaking Off. Journal of Glaciology , 19 , pp. 595 - 605.

Janbu , N. , 1969. The Resistance Concept Applied to Deformations of Soils. Proceedings , *In* 7th International Conference on Soil Mechanics and Foundation Engineering , Mexico City , Mexico , 1 , pp. 191 - 196.

Johnson , R.S. , 1982. Slope Stability Monitoring. *In* 4th Canadian Symposium on Mining Surveying and Deformation Measurements , Banff , Alberta , Canadian Institute of Surveying , pp. 363 - 379.

MacRae , A.M.R. , 1982 . Case Histories of Deformation Measurements in Canadian Surface Mines. *In*4th Canadian Symposium on Mining Surveying and Deformation Measurements , Banff , Alberta , Canadian Institute of surveying , pp. 255 - 278.

MacRae , A.M.R. , 1983. Personal communications.

McLean , J.R. , 1982. Lithostratigraphy of the Lower Cretaceous Coal-Bearing Sequence , Foothills of Alberta. Geological survey of Canada , Paper 80-29 , pp. 1 - 46.

Milligan , M.F. , and Hebil , K.E. , 1980. Report on the Geotechnical Investigation of the North Wall of 51-B-2 Pit. Project No. E209 , Luscar Ltd. , 27 p.

Monkman , F.C. , and Grant , N.J. , 1956. An Empirical Relationship Between Rupture Life and Minimum Creep Rate in Creep-Rupture tests. Proc. American Society for Testing Materials, 56 , pp. 593 - 605 , with discussion , pp. 605 - 620.

Munn , F.J. , 1983. Pitwall Stability program at Cardinal River Coals Ltd. C.I.M. First District 5 Meeting. , Cardinal River Coals Ltd. , 13 p.

Rogan , M. , 1978. Geology and Underground Potential of the Cardinal River Mine Area , Luscar , Alberta , Luscar Ltd.

Saito , M. , 1969. Forecasting Time of Slope Failure by Tertiary Creep. Proceedings ,*In* 7th International Conference on Soil Mechanics and Foundation Engineering , Mexico City , Mexico , 2 , pp. 677 - 683.

Saito , M. , 1980. Semi Logarithmic Representation for Forecasting Slope Failure. Proceedings , International Symposium on Landslides , New Dehli , 1980 , 1 , 321 - 324.

Saito , M. , 1980. Evidential Study on Forecasting Occurrence of Slope Failure. Report No. RP-4116 , Technical Note 38 , Oyo Corporation , Tokyo , 17 pp.

Sandstorm , R. , and Kondyr , A. , 1980. Model for Tertiary Creep in Mo and CrMo Steels. Proceedings , 3rd International Conference on Mechanical Behavior of Materials , Cambridge , 2 , pp. 275 - 284.

Schumm , S.A. , and Chorley , R.J. , 1964. The Fall of Threatening Rock. American Journal of Science , 262 , pp. 1041 - 1054.

Servi , I.S. , and Grant , N.J. , 1951. Creep and Stress Rupture Behavior of Aluminum as a Function of Purity. Transactions , American Institute of Mining and Metallurgical Engineers , 191 , pp. 909 - 916.

Varnes , D.J. , 1982. Time-Deformation Relations in Creep to Failure of Earth Materials. , Proceedings , 7th South East Asian Geotechnical Conference , 2 , pp. 107 - 130.

Wyllie , D.C. , and Munn , F.J. , 1979. The Use of Movement Monitoring to Minimize Production Losses Due to Pit Slope Failures. Proceedings , 1st International Symposium on Stability in Coal Mining , Vancouver , B.C. , Miller Freeman Publications ,Inc. , San Francisco , pp. 75 - 94.

Yu , Y.S. , and Hedley , D.G.F. , 1973. A Trial of Monitoring Slope Wall Movement at Hilton Mines Using a High Precision Theodolite. Canadian Department of Energy

, Mines and Resources , Mines Branch , Mining Research center , Internal Report 73/18.

Zavodni , Z.M. , and Broadbent , C.D. , 1980. Slope Failure Kinematics. Bulletin Canadian Institute of Mining , 73 , No.816 , pp. 69 - 74.

APPENDIX - COMPUTER PROGRAM DOCUMENTATION

INTRODUCTION

Four programs have been developed for fits of power , exponential and Saito relations. There are two programs for the power law. Zavodni and Broadbent's fit can be tested by assuming 2 or more successive exponential fits.

One hundred displacement entries can be given in either one or two columns. When one column is used the other may be left blank. In this case , cumulative displacements can be given. When both columns are used , cumulative horizontal and vertical displacements may be inserted in the input data file. Then each program calculates the resultants of the displacement vectors.

All displacement entries are in feet. They are converted to millimetres by the programs. Time variables are given in minutes.

All parameters for accelerating creep relations can be obtained from slopes and intercepts of the fitted lines by consulting Table 5.1.

All programs listings , sample outputs and corresponding input data files are presented at the end of this Appendix.

The programs have been written in Fortran IV language for the Amdahl computer and are executable with MTS commands. Approximate storage and CPU time requirements for each program is 10 disc pages and 2 seconds , respectively.

PROGRAM POW

This program fits power law , using log velocity and log time , to the resultants of the displacement vectors or cumulative displacements and produces a plot.

The flow diagram of this program is shown in Figure 5.6. Displacements are smoothed to increase positively with time. If two successive data entries show decrease of displacement with time , they will be smoothed into a new pair of data by the following relations;

```
AE(I-1)=(AE(I)*W(I)+AE(I-1)*W(I-1))/(W(I)+W(I-1))
AT(I-1)=(AT(I)*W(I)+AT(I-1)*W(I-1))/(W(I)+W(I-1))
```

where , variables AE(I) , AT(I) and W(I) represent displacement , time and weighting factor , respectively. This smoothening will continue until all successive displacements increase positively with time.

Velocity is calculated by dividing the successive increase in displacements by that of times. Then natural logarithms of velocity and time and power law fit parameters are calculated. The transformed data and fit parameters will be written in output **UNIT 6**. Then the program prompts to plot a graph. The CIVE subroutine GRAPH was used. For detailed information , consult the CIVE:GRAPH.DOC. , the documentation file stored under the computer id CIVE.

INPUT

The input data file is attached to **UNIT 5.**

The first card has two variables NF and XT. NF , with the format I3 , is the number of data sets being processed , and , XT , with the format G20.0 , is a time constant which will be added to the time variables. NF and XT are set usually as 1 and 0.0.

The second card allows 32 characters to describe the data set.

Variable NR , the number of data , is given in the third card with the format I5.

The fourth card , describes the plot. The first 48 characters are used for plot title. The next 32 characters define the X and Y axes labels.

The fifth to the last cards , are employed for measurement records. Each card has 4 variables with the format 4G20.0. Variables N , AT1(I) , AE(I) and AV(I) represent data counter , time , cumulative horizontal displacement and vertical displacements respectively. On the other hand , variable AE(I) may be used for any type of cumulative displacements. In this case , no entries may be made for variable AV(I).

PROGRAM SAITO

This program fits the generalized Saito relation , using log time to failure and log velocity , to the resultants of the displacement vectors or cumulative displacements and produces a plot.

The flow diagram of this program is shown in Figures 5.4 and 5.5. A range of possible values of t and an upper limit Durbin Watson statistic are given. The program will stop computation and draws a plot , when the upper limit of either t or the Durbin Watson statistic is reached. Velocity is calculated in a similar way to that of program POW. To fit the Saito law , natural logarithms of velocity and time to failure are calculated. Fit parameters , transformed data and a plot are produced.

INPUT

The input data file is attached to **UNIT 5**.

The first and third cards are different from those of input data file for program POW. The other cards are identical to those of program POW.

The first card has four variables. Variable NF , with the format I3 , is the number of data sets being processed. Variables TF1 , TF2 and DTF , with the format 3G20.0 , are lower and upper limits and time increment for the time of failure , respectively.

The third card has two variables , NR and DW1 , with the format 2G20.0. The first , is the number of data , and the second is the upper limit for Durbin Watson statistic.

PROGRAM POW2

This program fits a power law , using velocity to acceleration ratio and time , to the resultants of the displacement vectors or cumulative displacements and produces a plot.

The flow diagram of this program is shown in Figure 5.7. Velocity and acceleration are computed as follows;

Velocity ;

DE(J) = (AE(J)-AE(J-1))/(AT(J)-AT(J-1))

Acceleration ;

D2E(J) = (DE(J)-DE(J-1))/(T1(J)-T1(J-1))

T1(J) = (AT(J)+AT(J-1))/2.0

where AT(J) and AE(J) are time and displacement variables. Then the velocity to acceleration ratio and power law fit parameters are calculated. The program will proceed to computation in a way similar to that of program POW.

INPUT

The input data file is attached to **UNIT 5.**

Variable NF , with the format I3 , is the number of data sets being processed and is given in the first card. All other cards are similar to those of program POW.

PROGRAM EXPO

This program fits an exponential law using log velocity and time to the resultants of the displacement vector or cumulative displacements and produces a plot.

The flow diagrams of this program is shown in Figure 5.8. The natural logarithm of velocity and time is used to fit exponential law. All other computational processes are similar to those of program POW.

INPUT

The input data file is attached to **UNIT 5.**

All cards of the input data file are exactly similar to those of program POW.

EXECUTION OF PROGRAMS

The execution of all programs described before follow an identical procedure. The compilation and execution of each program is done by the two following MTS commands;

```
R *FORTGTEST SCARDS=PROGRAM SPRINT=-LIST PAR=ID ,SOURCE T=2S
DEBUG -LOAD#+CIVE:GRAPH+*IG+*PLOTLIB 5=(DATA  FILE)
        6=(-OUTPUT) T=4S
```

A temporary plot description file named -PDF is assigned to unit 9 by CIVE:GRAPH. A plot description file may be generated from which hard copy may be produced on the Calcomp or Varian Electrostatic plotter (CIVE.GRAPH.DOC). The following is an example run:

example run:

```
#r *fortgltest scards=menu  sprint=-list par=id,source t=4s
#13:32:36
 MAIN       NO ERRORS
#13:32:39  T=0.294  RC=0
#debug -load#+civil:graph+*sig+*plotlib 5=dvl 6=-61 t=2s
#Ready
#run

   GRAPH   PRELIMINARY VERSION   DEC. 1, 1982

   PLOT FILE NAME IS -PDF

   SUMMARY FILE NAME IS -SUMMARY



41
40
39
38
37
36
35
34
33
32
31
30          +!!+--+---+--+--+--+--+---+--+--+--+
29             +-                              +     OPTION
28             +-                   +-         +
27            !+-                              +  1. PLOT
26          +!++-                   ++-       -+  2. BLOW-UP
25             +-                   !+         +
24             +-                  -XX        /+  3. REDRAW
23        .X!!!+                 ...++         !  4. SUBPICTURES
22        X-+!++-               ..            -+
21        ++   +-           -XX.    ++         +  5. MTS-SDS
20        XX   +-+-         .. +  ++           +  6. CONTINUE
19        ++!!X++- !   .... +-   +            -+
18        XX/! +-  +...                        +
17        XX   +- ..                           +
16             +X.       +                     +
15          +!++-                             -+
14             +-                              +
13             X-    +                         +
12             +-                              +
11          +!+++-++-++-++--++-++-++-++-++-++-++-
10             XX-++ +! +! +++++X!++ +! +! ++-+X-
09                       +!+    .+X
08          +X-X+X++-+ -X.+++ XX--X!+++X+--+++--+!++-X                6
07
06
05
04
03
02
01
00
Y            1         2         3         4         5         6
 X=0123456789012345678901234567890123456789012345678901234567890123456789

   SELECT MENU OPTION
?plot

   SELECT MENU OPTION
?continue
#User program return.
#Ready
#mts
#
```

```
CCCCCCCCCCCCCCCCCCCCCCCCCCCCCCCCCCCCCCCCCCCCCCCCCCCC
CCCCCCCCCCCCCCCCCCCCCCCCCCCCCCCCCCCCCCCCCCCCCCCCCCCC
CCCCC                                          CCCCC
CCCCC            PROGRAM  SAITO                CCCCC
CCCCC                                          CCCCC
CCCCC     THIS CREEP PROGRAM CALCULATES        CCCCC
CCCCC     RESULTANTS OF DISPLACEMENT VECTORS   CCCCC
CCCCC     OR THEIR COMPONENTS  AND FITS        CCCCC
CCCCC     SAITO LAW TO THEM AND FINDS THE      CCCCC
CCCCC     TIME OF SLIDE,i.e. TF .              CCCCC
CCCCC                                          CCCCC
CCCCC                                          CCCCC
CCCCCCCCCCCCCCCCCCCCCCCCCCCCCCCCCCCCCCCCCCCCCCCCCCCC
CCCCCCCCCCCCCCCCCCCCCCCCCCCCCCCCCCCCCCCCCCCCCCCCCCCC


      DIMENSION E(100),T(100),EE(100),A(10),DE(100),W1(100),
     1W(100),B(100),EA(100),AE(100),AT(100),D2E(100),T1(100),
     1DENT(48),AT1(100),X(100),Y(100),ALPHA(24),AV(100),
     1N(100),AE1(100),AT2(100)
      REAL*4 OPTNS(25)/25*'NO '/
      OPTNS(1)=1.0
      OPTNS(6)=2.0
      OPTNS(7)=2.0
      OPTNS(10)=5.0
      OPTNS(13)=5.0
      OPTNS(22)=3.0
      LL=0
```

University of Alberta

```
C
C
C       READ DATA
C
C
        READ(5,119) NF,TF1,TF2,DTF
   119  FORMAT(I3,3G20.0)
     8  READ(5,123) (DENT(J), J=1,8)
   123  FORMAT(8A4)
        WRITE(6,134)DENT
   134  FORMAT(1H1,9X,12A4)
        READ(5,112) NR,DW1
        READ(5,502) (ALPHA(M),M=1,24)
   202  READ(5,151)(N(I),AT1(I),AE1(I),AV(I),I=1,NR)
        DO 20 I=1,NR
C
C       CALCULATE RESULTANTS OF DISPLACEMENT VECTORS
C       OR THEIR COMPONENTS.
C
C
    20  AE1(I)=SQRT(AE1(I)*AE1(I)+AV(I)*AV(I))*304.8
        WRITE(6,206)
C
C
C       WRITE RESULTANTS OF DISPLACEMENT VECTORS
C       OR THEIR COMPONENTS AND TIME.
C
C
   518  WRITE(6,205)(N(I),AT1(I),AE1(I),I=1,NR)
    21  CONTINUE
        WW=0.
        BB=0.
        CONB1=0.
        CONBO=0.
        TE=0.
        DW=0.
        EER=0.
        EEM=0.
        EES=0.
        SUMT=0.
        SUMET=0.
        SUMT2=0.
        SUME=0.
        SUME2=0.
        SXX=0.0
        DWW=0.
        SXY=0.0
        WWA=0.
        AF=0.
   502  FORMAT(24A4)
   112  FORMAT(2G20.0)
   206  FORMAT(1H1,'        DATA ')
        WRITE(6,207)
   207  FORMAT(15X,'T                E')
        I=0.0
        M=0.0
    12  I=I+1
        M=M+1
   151  FORMAT(4G20.0)
     C  AT(I)=AT(I)*60.
```

University of Alberta

```
            W(I)=1.0
      C
      C  CALCULATE TIME PRIOR TO FAILURE
      C
      C
      516   AT(I)=TF1-AT1(M)
            AE(I)=AE1(M)
      205   FORMAT(I5,2X,E15.8,2X,E13.6)
      C
      C
      C  SMOOTH DISPLACEMENT TO INCREASE POSITIVELY
      C
      C
      11    IF(I .EQ.1) GO  TO 12
      14    IF(AE(I)-AE(I-1)) 13, 13, 4
      13    AE(I-1)=(AE(I)*W(I)+AE(I-1)*W(I-1))/(W(I)+W(I-1))
            AT(I-1)=(AT(I)*W(I)+AT(I-1)*W(I-1))/(W(I)+W(I-1))
            W(I-1)=W(I)+W(I-1)
            I=I-1
            IF(I-2)12,14,14
          4 CONTINUE
            IF(M.LT.NR) GO TO 12
            WRITE(6,300)
      300   FORMAT(5X,'INCREASING DISPLACEMENT WITH TIME')
            WRITE(6,301)
      301   FORMAT(3X,'NO',5X,'AT',15X,'AE',12X,'W')
            WRITE(6,305)(L,AT(L),AE(L),W(L),L=1,I)
      305   FORMAT(I5,2X,E15.8,2X,E13.6,F7.2)
      C
      C
      C  CALCILATE VELICITY.
      C  CONVERT TO LOG VELOCITY AND
      C  LOG TIME TO FAILURE.
      C
      C
      503   DO 1 J=2,I
            E(J)=(AE(J)-AE(J-1))/ABS(AT(J)-AT(J-1))
            Y(J-1)=E(J)
            T(J)=ALOG((AT(J)+AT(J-1))/2.0)
            X(J-1)=EXP(T(J))
          6 W(J)=(W(J)+W(J-1))/2.
          3 E(J)=ALOG(E(J))
        204 WW=WW+W(J)
            EE(J)=0.
            SUMT=SUMT+T(J)*W(J)
            SUME=SUME+E(J)*W(J)
            SUMET=SUMET+E(J)*T(J)*W(J)
            SUME2=SUME2+E(J)*E(J)*W(J)
          1 SUMT2=SUMT2+T(J)*T(J)*W(J)
            ND=J-1
      C
      C
      C  FIT SAITO LAW
      C
      C
      505   SUME2=SUME2-SUME*SUME/WW
            SUMT2=SUMT2-SUMT*SUMT/WW
            SUMET=SUMET-SUME*SUMT/WW
            FME=SUME/WW
            FMT=SUMT/WW
```

```
 506   DO 7 J=2,I
 508   SXY=SXY+(T(J)-FMT)*(E(J)-FME)*W(J)
     7 SXX=SXX+W(J)*(T(J)-FMT)**2
 17    CONTINUE
C
C
C  CALCULATE FIT PARAMETERS
C
C
       B1=SXY/SXX
       B0=FME-FMT*B1
C
C
C  WRITE TRANSFORMED DATA
C
C
       WRITE(6,208)
   208 FORMAT(//,9X,'TRANSFORMED DATA')
       WRITE(6,209)
   209 FORMAT(5X,'NO',14X,'LT',12X,'LE',12X,'LEE',10X,'(LE-LEE)',
      *6X,'W')
 509   DO 2 J=2,I
       K=J-1
       EE(J)=B0+B1*T(J)
       EES=EES+(EE(J)-E(J))*W(J)
       EA(J)=E(J)-EE(J)
       WRITE(6,106)K,T(J),E(J),EE(J),EA(J),W(J)
       EER=EER+W(J)*(EE(J)-E(J))**2
       EEM=EEM+W(J)*(EE(J)-FME)**2
 512   IF(J.LE.2)GO TO 2
       DW=DW+(EA(J)-EA(J-1))**2
       DWW=DWW+EA(J)*EA(J)
   2   CONTINUE
       SSDYX=EER
       EER=EER/(WW-2.)
       FF=EEM/EER
       CONB1=SQRT(EER/SUMT2)
       CONB0=CONB1*SQRT((SUMT2*WW+SUMT*SUMT)/(WW*WW))
       DW=DW/DWW
C
C
C  WRITE FIT PARAMETERS
C
C
       WRITE(6,210)
   210 FORMAT(//,9X,'FIT PARAMETERS')
       WRITE(6,105)B0
   105 FORMAT(11X,' INTERCEPT   ',E15.6)
       WRITE(6,115)B1
       WRITE(6,158)CONB0
       WRITE(6,157)CONB1
       WRITE (6,159)DW
   106 FORMAT(5X,I3,5X,4(1X,E13.6),F7.2)
   157 FORMAT(11X,' CONFIDENCE LIMIT ON B2     T. ',F12.7)
   115 FORMAT(11X,' SLOPE                         ',F12.7)
   158 FORMAT(11X,' CONFIDENCE LIMIT ON B1     T. ',F12.7)
   159 FORMAT(11X,' DURBIN WATSON STATISTIC       ',F7.3)
       WRITE(6,156)FF
   156 FORMAT(11X,' TEST OF SLOPE SIGNIFICANCE    ',F9.3)
       WRITE (6,211)
```

University of Alberta

```
  211 FORMAT(//,9X,'DATA FOR COMPARISON TESTS')
      WW=WW-2.
      WRITE(6,122)WW
  122 FORMAT(11X,' WEIGHTING ',F6.1)
      WRITE(6,124)K
  124 FORMAT(11X,' TRANSFORMED DATA NUMBER   ',I3)
      WRITE(6,104)FME,FMT
      WRITE(6,214)SUME2,SUMT2
  104 FORMAT(11X,' MEAN STRAIN  ',F11.3,
     *'    MEAN TIME ',F11.3)
      WRITE(6,213)SUMET,SSDYX
  214 FORMAT(11X,' SSDY ',5X,F20.3,' SSDX    ',F20.3)
  213 FORMAT(11X,' SPDXY',5X,F20.3,' SSDYX    ',F20.3)
      WRITE(6,212)
  212 FORMAT(/,9X,'CHECK')
      WRITE(6,107)EES
  107 FORMAT(11X,'SUM OF RESIDUALS',14X,F12.6)
      WRITE(6,215)TF1
  215 FORMAT(11X,'TIME OF FAILURE=',F13.6)
      LL=LL+1
C
C
C  UPPER LIMIT OF DURBIN WATSON STATISTICS SATISFIED ?
C
C
      IF(DW1.LT.DW)GO TO 22
C
C
C  UPPER LIMIT OF THE TIME OF FAILURE ?
C
C
      IF(TF1-TF2)23,22,22
C
C
C  ADD TIME INCREMENT TO THE PREVIOUS
C  TIME OF FAILURE
C
C
   23 TF1=TF1+DTF
      GO TO 21
C
C
C  CALL GRAPH
C
C
   22 CALL GRAPH (X,Y,ND,ALPHA,1,OPTNS)
      OPTNS(21)=4.0
      X(1)=EXP(T(2))
      X(2)=EXP(T(I))
      Y(1)=EXP(EE(2))
      Y(2)=EXP(EE(I))
      ND=2
      CALL GRAPH (X,Y,ND,ALPHA,-2,OPTNS)
      IF(LL.LT.NF)GO TO 8
      CALL GRAPH (X,Y,ND,ALPHA,0,OPTNS)
      STOP
      END
```

University of Alberta

input data file for program SAITO ;

```
1.358390.358980.10.
268 PRISM DISPLACEMENTS
   27.1.46.
SAITO FIT TO DISPLACEMENT VECTORS RESULTANTS    LOG(t -t)       LOG(VELOCITY)
 1. 90660.0.058.0.000.
 2.100740.0.096.-0.021.
 3.113700.0.184.-0.067.
 4.139545.0.258.-0.087.
 5.171210.0.271.-0.055.
 6.230235.0.311.-0.042.
 7.240450.0.429.-0.146.
 8.250380.0.448.-0.211.
 9.261930.0.603.-0.207.
10.270570.0.638.-0.271.
11.305280.0.753.-0.318.
12.312450.0.812.-0.313.
13.320430.0.893.-0.352.
14.331200.0.983.-0.468.
15.340680.1.682.-0.856.
16.344281.1.862.-0.809.
17.344985.1.993.-0.995.
18.346845.2.169.-1.093.
19.348330.2.305.-1.109.
20.349815.2.421.-1.162.
21.351390.2.479.-1.240.
22.352815.2.678.-1.345.
23.354330.2.869.-1.475.
24.355770.3.138.-1.621.
25.356910.3.463.-1.817.
26.357390.3.576.-1.857.
27.358380.4.544.-2.339.
```

output example for program SAITO ;

University of Alberta

```
  1          268 PRISM DISPLACEMENTS          @@@@@@@@@@@@@@@@
  1          @@@@@@@@@@@@@@@@@@@@@@@@@@@@@@@@@@@@@@@@@@@@@
  1          @@@@@@@@@@@@@@@@@@@@@@@@@@@@@@@@@@@@@@@@@@@@@
  1          @@@@@@@@@@@@@@@@@@@@@@@@@@@@@@@@@@@@@@@@@@@@@
  1        DATA
          1   0.90660000E+05   0.176784E+02
          2   0.10074000E+06   0.299527E+02
          3   0.11370000E+06   0.596855E+02
          4   0.13954500E+06   0.829889E+02
          5   0.17121000E+06   0.842847E+02
          6   0.23023500E+06   0.956532E+02
          7   0.24045000E+06   0.138124E+03
          8   0.25038000E+06   0.150937E+03
          9   0.26193000E+06   0.194322E+03
         10   0.27057000E+06   0.211278E+03
         11   0.30528000E+06   0.249142E+03
         12   0.31245000E+06   0.265248E+03
         13   0.32043000E+06   0.292568E+03
         14   0.33120000E+06   0.331842E+03
         15   0.34068000E+06   0.575245E+03
         16   0.34428100E+06   0.618791E+03
         17   0.34498500E+06   0.678963E+03
         18   0.34684500E+06   0.740307E+03
         19   0.34833000E+06   0.779651E+03
         20   0.34981500E+06   0.818515E+03
         21   0.35139000E+06   0.844853E+03
         22   0.35281500E+06   0.913419E+03
         23   0.35433000E+06   0.983271E+03
         24   0.35577000E+06   0.107654E+04
         25   0.35691000E+06   0.119199E+04
         26   0.35739000E+06   0.122817E+04
         27   0.35838000E+06   0.155773E+04
                    T                E
        INCREASING DISPLACEMENT WITH TIME
         NO     AT                  AE             W
          1   0.26773000E+06   0.176784E+02   1.00
          2   0.25765000E+06   0.299527E+02   1.00
          3   0.24469000E+06   0.596855E+02   1.00
          4   0.21884500E+06   0.829889E+02   1.00
          5   0.18718000E+06   0.842847E+02   1.00
          6   0.12815500E+06   0.956532E+02   1.00
          7   0.11794000E+06   0.138124E+03   1.00
          8   0.10801000E+06   0.150937E+03   1.00
          9   0.96460000E+05   0.194322E+03   1.00
         10   0.87820000E+05   0.211278E+03   1.00
         11   0.53110000E+05   0.249142E+03   1.00
         12   0.45940000E+05   0.265248E+03   1.00
         13   0.37960000E+05   0.292568E+03   1.00
         14   0.27190000E+05   0.331842E+03   1.00
         15   0.17710000E+05   0.575245E+03   1.00
         16   0.14109000E+05   0.618791E+03   1.00
         17   0.13405000E+05   0.678963E+03   1.00
         18   0.11545000E+05   0.740307E+03   1.00
         19   0.10060000E+05   0.779651E+03   1.00
         20   0.85750000E+04   0.818515E+03   1.00
         21   0.70000000E+04   0.844853E+03   1.00
         22   0.55750000E+04   0.913419E+03   1.00
         23   0.40600000E+04   0.983271E+03   1.00
         24   0.26200000E+04   0.107654E+04   1.00
         25   0.14800000E+04   0.119199E+04   1.00
         26   0.10000000E+04   0.122817E+04   1.00
         27   0.10000000E+02   0.155773E+04   1.00
```

output example for program SAITO con't ;

University of Alberta

```

     TRANSFORMED DATA
NO         LT              LE              LEE             (LE-LEE)       W
 1     0.124787E+02 -0.671080E+01 -0.741879E+01  0.707990E+00   1.00
 2     0.124339E+02 -0.607737E+01 -0.737042E+01  0.129305E+01   1.00
 3     0.123535E+02 -0.701127E+01 -0.728370E+01  0.272426E+00   1.00
 4     0.122210E+02 -0.101039E+02 -0.714081E+01 -0.296306E+01   1.00
 5     0.119682E+02 -0.855487E+01 -0.686815E+01 -0.168672E+01   1.00
 6     0.117203E+02 -0.548279E+01 -0.660073E+01  0.111793E+01   1.00
 7     0.116349E+02 -0.665283E+01 -0.650860E+01 -0.144223E+00   1.00
 8     0.115350E+02 -0.558433E+01 -0.640085E+01  0.816520E+00   1.00
 9     0.114311E+02 -0.623354E+01 -0.628871E+01  0.551662E-01   1.00
10     0.111629E+02 -0.682080E+01 -0.599942E+01 -0.821381E+00   1.00
11     0.108102E+02 -0.609844E+01 -0.561904E+01 -0.479399E+00   1.00
12     0.106442E+02 -0.567706E+01 -0.543998E+01 -0.237082E+00   1.00
13     0.103913E+02 -0.561398E+01 -0.516715E+01 -0.446828E+00   1.00
14     0.100190E+02 -0.366222E+01 -0.476561E+01  0.110339E+01   1.00
15     0.967467E+01 -0.441516E+01 -0.439415E+01 -0.210171E-01   1.00
16     0.952930E+01 -0.245956E+01 -0.423734E+01  0.177778E+01   1.00
17     0.943148E+01 -0.341184E+01 -0.413183E+01  0.719983E+00   1.00
18     0.928753E+01 -0.363083E+01 -0.397655E+01  0.345725E+00   1.00
19     0.913965E+01 -0.364308E+01 -0.381704E+01  0.173953E+00   1.00
20     0.896028E+01 -0.409101E+01 -0.362355E+01 -0.467461E+00   1.00
21     0.874632E+01 -0.303413E+01 -0.339276E+01  0.358631E+00   1.00
22     0.848001E+01 -0.307680E+01 -0.310550E+01  0.287066E-01   1.00
23     0.811373E+01 -0.273693E+01 -0.271041E+01 -0.265198E-01   1.00
24     0.762560E+01 -0.228991E+01 -0.218388E+01 -0.106039E+00   1.00
25     0.712287E+01 -0.258543E+01 -0.164160E+01 -0.943831E+00   1.00
26     0.622456E+01 -0.109994E+01 -0.672624E+00 -0.427319E+00   1.00


     FIT PARAMETERS
        INTERCEPT       0.604160E+01
        SLOPE                               -1.0786667
        CONFIDENCE LIMIT ON B1     T.        1.1547041
        CONFIDENCE LIMIT ON B2     T.        0.1124731
        DURBIN WATSON STATISTIC             1.560
        TEST OF SLOPE SIGNIFICANCE            91.965


     DATA FOR COMPARISON TESTS
        WEIGHTING   24.0
        TRANSFORMED DATA NUMBER    26
        MEAN STRAIN          -4.875   MEAN TIME        10.121
        SSDY                     113.320 SSDX                       77.247
        SPOXY                    -83.315 SSDYX                      23.453

     CHECK
       SUM OF RESIDUALS                      -0.000367
       TIME OF FAILURE=358390.000000
```

```
CCCCCCCCCCCCCCCCCCCCCCCCCCCCCCCCCCCCCCCCCCCCCCCCCCCCCCC
CCCCCCCCCCCCCCCCCCCCCCCCCCCCCCCCCCCCCCCCCCCCCCCCCCCCCCC
CCCCC                                             CCCCC
CCCCC             PROGRAM  POW                    CCCCC
CCCCC                                             CCCCC
CCCCC     THIS CREEP PROGRAM CALCULATES           CCCCC
CCCCC     RESULTANTS OF DISPLACEMENT VECTORS      CCCCC
CCCCC     OR THEIR COMPONENTS  AND FITS           CCCCC
CCCCC     POWER LAW TO THEM.                      CCCCC
CCCCC                                             CCCCC
CCCCCCCCCCCCCCCCCCCCCCCCCCCCCCCCCCCCCCCCCCCCCCCCCCCCCCC
CCCCCCCCCCCCCCCCCCCCCCCCCCCCCCCCCCCCCCCCCCCCCCCCCCCCCCC


      DIMENSION E(100),T(100),EE(100),A(10),DE(100),W1(100),
     1W(100),B(100),EA(100),AE(100),AT(100),D2E(100),T1(100),
     1DENT(48),AT1(100),X(100),Y(100),ALPHA(24),AV(100)
      REAL*4 OPTNS(25)/25*'NO '/
      OPTNS(1)=1.0
      OPTNS(6)=2.0
      OPTNS(7)=2.0
      OPTNS(10)=5.00
      OPTNS(13)=5.0
      OPTNS(22)=3.0
      LL=0
C
C  READ DATA
C
      READ(5,119) NF,XT
  119 FORMAT(I3,G20.0)
    8 READ(5,123) (DENT(J), J=1,8)
  123 FORMAT(8A4)
      WRITE(6,134)DENT
  134 FORMAT(1H1,9X,12A4)
      WW=0.
      BB=0.
      CONB1=0.
      CONB0=0.
      TE=0.
      DW=0.
      EER=0.
      EEM=0.
      EES=0.
      SUMT=0.
      SUMET=0.
      SUMT2=0.
      SUME=0.
      SUME2=0.
      SXX=0.0
      DWW=0.
      SXY=0.0
      WWA=0.
      AF=0.
      I=0
      READ(5,112)NR
      READ(5,502) (ALPHA(M),M=1,24)
  502 FORMAT(24A4)
  112 FORMAT(I5)
      WRITE(6,206)
  206 FORMAT(1H1,'      DATA ')
```

University of Alberta

```
        WRITE(6,207)
 207    FORMAT(15X,'T                 E                W',6X,'(t+X)')
 12     I=I+1
 202    READ(5,151) N,AT1(I),AE(I),AV(I)
 151    FORMAT(4G20.0)
C       AT(I)=AT(I)*60.
C
C  CALCULATE RESULTANTS OF DISPLACEMENT VECTORS
C  OR THEIR COMPONENTS AND TIME.
C
        AE(I)=SQRT(AE(I)*AE(I)+AV(I)*AV(I))*304.8
        W(I)=1.0
 517    AT(I)=AT1(I)+XT
C
C  WRITE RESULTANTS OF DISPLACEMENT VECTORS
C  OR THEIR COMPONENTS AND TIME.
C
 518    WRITE(6,205)N,AT1(I),AE(I),W(I),AT(I)
 205    FORMAT(I5,2X,E15.8,2X,E13.6,F7.2,2X,E15.8)
C
C  SMOOTH DISPLACEMENT TO INCREASE POSITIVELY
C
 11     IF(I .EQ.1) GO  TO 12
 14     IF(AE(I)-AE(I-1)) 13, 13, 4
 13     AE(I-1)=(AE(I)*W(I)+AE(I-1)*W(I-1))/(W(I)+W(I-1))
        AT(I-1)=(AT(I)*W(I)+AT(I-1)*W(I-1))/(W(I)+W(I-1))
        W(I-1)=W(I)+W(I-1)
        I=I-1
        IF(I-2)12,14,14
      4 CONTINUE
        IF(N.LT.NR) GO TO 12
        WRITE(6,300)
 300    FORMAT(5X,'INCREASING DISPLACEMENT WITH TIME')
        WRITE(6,301)
 301    FORMAT(3X,'NO',5X,'AT',15X,'AE',12X,'W')
        WRITE(6,305)(L,AT(L),AE(L),W(L),L=1,I)
 305    FORMAT(I5,2X,E15.8,2X,E13.6,F7.2)
C
C  CALCULATE VELOCITY.
C  CONVERT TO LOG VELOCITY AND LOG TIME.
C
 503    DO 1 J=2,I
        E(J)=(AE(J)-AE(J-1))/(AT(J)-AT(J-1))
        Y(J-1)=E(J)
        T(J)=ALOG((AT(J)+AT(J-1))/2.0)
        X(J-1)=EXP(T(J))
      6 W(J)=(W(J)+W(J-1))/2.
      3 E(J)=ALOG(E(J))
    204 WW=WW+W(J)
        EE(J)=0.
        SUMT=SUMT+T(J)*W(J)
        SUME=SUME+E(J)*W(J)
        SUMET=SUMET+E(J)*T(J)*W(J)
        SUME2=SUME2+E(J)*E(J)*W(J)
      1 SUMT2=SUMT2+T(J)*T(J)*W(J)
        ND=J-1
C
C  CALL GRAPH
C
        CALL GRAPH (X,Y,ND,ALPHA,1,OPTNS)
```

University of Alberta

University of Alberta

```
C
C  FIT POWER LAW
C
505    SUME2=SUME2-SUME*SUME/WW
       SUMT2=SUMT2-SUMT*SUMT/WW
       SUMET=SUMET-SUME*SUMT/WW
       FME=SUME/WW
       FMT=SUMT/WW
506    DO 7 J=2,I
508    SXY=SXY+(T(J)-FMT)*(E(J)-FME)*W(J)
     7 SXX=SXX+W(J)*(T(J)-FMT)**2
17     CONTINUE
C
C  CALCULATE FIT PARAMETERS.
C
       B1=SXY/SXX
       B0=FME-FMT*B1
C
C  WRITE TRANSFORMED DATA
C
       WRITE(6,208)
   208 FORMAT(//,9X,'TRANSFORMED DATA')
       WRITE(6,209)
   209 FORMAT(5X,'NO',14X,'LT',12X,'LE',12X,'LEE',10X,'(LE-LEE)',
      *6X,'W')
509    DO 2 J=2,I
       K=J-1
       EE(J)=B0+B1*T(J)
       Y(K)=EXP(EE(J))
       EES=EES+(EE(J)-E(J))*W(J)
       EA(J)=E(J)-EE(J)
       WRITE(6,106)K,T(J),E(J),EE(J),EA(J),W(J)
       EER=EER+W(J)*(EE(J)-E(J))**2
       EEM=EEM+W(J)*(EE(J)-FME)**2
512    IF(J.LE.2)GO TO 2
       DW=DW+(EA(J)-EA(J-1))**2
       DWW=DWW+EA(J)*EA(J)
  2    CONTINUE
       OPTNS(21)=4.0
       SSDYX=EER
       EER=EER/(WW-2.)
       FF=EEM/EER
       CONB1=SORT(EER/SUMT2)
       CONB0=CONB1*SORT((SUMT2*WW+SUMT*SUMT)/(WW*WW))
       DW=DW/DWW
       WRITE(6,210)
C
C  WRITE FIT PARAMETERS
C
   210 FORMAT(//,9X,'FIT PARAMETERS')
       WRITE(6,105)B0
   105 FORMAT(11X,' INTERCEPT    ',E15.6)
       WRITE(6,115)B1
       WRITE(6,158)CONB0
       WRITE(6,157)CONB1
       WRITE (6,159)DW
   106 FORMAT(5X,I3,5X,4(1X,E13.6),F7.2)
   157 FORMAT(11X,' CONFIDENCE LIMIT ON B2     T. ',F12.7)
   115 FORMAT(11X,' SLOPE                         ',F12.7)
   158 FORMAT(11X,' CONFIDENCE LIMIT ON B1     T. ',F12.7)
  159 FORMAT(11X,' DURBIN WATSON STATISTIC        ',F7.3)
      WRITE(6,156)FF
  156 FORMAT(11X,' TEST OF SLOPE SIGNIFICANCE     ',F9.3)
      WRITE (6,211)
  211 FORMAT(//,9X,'DATA FOR COMPARISON TESTS')
      WW=WW-2.
      WRITE(6,122)WW
  122 FORMAT(11X,' WEIGHTING ',F6.1)
      WRITE(6,124)K
  124 FORMAT(11X,' TRANSFORMED DATA NUMBER    ',I3)
      WRITE(6,104)FME,FMT
      WRITE(6,214)SUME2,SUMT2
  104 FORMAT(11X,' MEAN STRAIN  ',F11.3,
     *'    MEAN TIME ',F11.3)
      WRITE(6,213)SUMET,SSDYX
  214 FORMAT(11X,' SSDY ',5X,F20.3,' SSDX      ',F20.3)
  213 FORMAT(11X,' SPDXY',5X,F20.3,' SSDYX     ',F20.3)
      WRITE(6,212)
  212 FORMAT(/,9X,'CHECK')
      WRITE(6,107)EES
  107 FORMAT(11X,'SUM OF RESIDUALS',14X,F12.6)
      WRITE(6,215)XT
  215 FORMAT(11X,'     X=',F10.2)
      LL=LL+1
C
C  CALL GRAPH
C
      CALL GRAPH (X,Y,NO,ALPHA,-2,OPTNS)
      IF(LL.LT.NF)GO TO 8
      CALL GRAPH (X,Y,NO,ALPHA,0,OPTNS)
      STOP
      END
```

rsity of Alberta

input data file for program POW ;

```
1.0.0.
268 PRISM DISPLACEMENTS
   27.
POWER LAW FIT TO DISPLACEMENT VECTORS RESULTANTSLOG(time)        LOG(VELOCITY)
  1. 90660.0.058.0.000.
  2.100740.0.096.-0.021.
  3.113700.0.184.-0.067.
  4.139545.0.258.-0.087.
  5.171210.0.271.-0.055.
  6.230235.0.311.-0.042.
  7.240450.0.429.-0.146.
  8.250380.0.448.-0.211.
  9.261930.0.603.-0.207.
 10.270570.0.638.-0.271.
 11.305280.0.753.-0.318.
 12.312450.0.812.-0.313.
 13.320430.0.893.-0.352.
 14.331200.0.983.-0.468.
 15.340680.1.682.-0.856.
 16.344281.1.862.-0.809.
 17.344985.1.993.-0.995.
 18.346845.2.169.-1.093.
 19.348330.2.305.-1.109.
20.349815.2.421.-1.162.
21.351390.2.479.-1.240.
22.352815.2.678.-1.345.
23.354330.2.869.-1.475.
24.355770.3.138.-1.621.
25.356910.3.463.-1.817.
26.357390.3.576.-1.857.
27.358380.4.544.-2.339.
```

output example for program POW ;

```
1         268 PRISM DISPLACEMENTS          aaaaaaaaaaaaaaaa
1         aaaaaaaaaaaaaaaaaaaaaaaaaaaaaaaaaaaaaaaaaaaaaaaaa
1         aaaaaaaaaaaaaaaaaaaaaaaaaaaaaaaaaaaaaaaaaaaaaaaaa
1         aaaaaaaaaaaaaaaaaaaaaaaaaaaaaaaaaaaaaaaaaaaaaaaaa
1      DATA
                  T                  E            W       (t+X)
        1   0.90660000E+05    0.176784E+02    1.00    0.90660000E+05
        2   0.10074000E+06    0.299527E+02    1.00    0.10074000E+06
        3   0.11370000E+06    0.596855E+02    1.00    0.11370000E+06
        4   0 13954500E+06    0.829889E+02    1.00    0.13954500E+06
        5   0.17121000E+06    0.842847E+02    1.00    0.17121000E+06
        6   0.23023500E+06    0.956532E+02    1.00    0.23023500E+06
        7   0.24045000E+06    0.138124E+03    1.00    0.24045000E+06
        8   0.25038000E+06    0.150937E+03    1.00    0.25038000E+06
        9   0.26193000E+06    0.194322E+03    1.00    0.26193000E+06
       10   0.27057000E+06    0.211278E+03    1.00    0.27057000E+06
       11   0.30528000E+06    0.249142E+03    1.00    0.30528000E+06
       12   0.31245000E+06    0.265248E+03    1.00    0.31245000E+06
       13   0.32043000E+06    0.292568E+03    1.00    0.32043000E+06
       14   0.33120000E+06    0.331842E+03    1.00    0.33120000E+06
       15   0.34068000E+06    0.575245E+03    1.00    0.34068000E+06
       16   0.34428100E+06    0.618791E+03    1.00    0.34428100E+06
       17   0.34498500E+06    0.678963E+03    1.00    0.34498500E+06
       18   0.34684500E+06    0.740307E+03    1.00    0.34684500E+06
       19   0.34833000E+06    0.779651E+03    1.00    0.34833000E+06
       20   0.34981500E+06    0.818515E+03    1.00    0.34981500E+06
       21   0.35139000E+06    0.844853E+03    1.00    0.35139000E+06
       22   0.35281500E+06    0.913419E+03    1.00    0.35281500E+06
       23   0.35433000E+06    0.983271E+03    1.00    0.35433000E+06
       24   0.35577000E+06    0.107654E+04    1.00    0.35577000E+06
       25   0.35691000E+06    0.119199E+04    1.00    0.35691000E+06
       26   0.35739000E+06    0.122817E+04    1.00    0.35739000E+06
       27   0.35838000E+06    0.155773E+04    1.00    0.35838000E+06
     INCREASING DISPLACEMENT WITH TIME
      NO      AT                  AE            W
        1   0.90660000E+05    0.176784E+02    1.00
        2   0.10074000E+06    0.299527E+02    1.00
        3   0.11370000E+06    0.596855E+02    1.00
        4   0.13954500E+06    0.829889E+02    1.00
        5   0.17121000E+06    0.842847E+02    1.00
        6   0.23023500E+06    0.956532E+02    1.00
        7   0.24045000E+06    0.138124E+03    1.00
        8   0.25038000E+06    0.150937E+03    1.00
        9   0.26193000E+06    0.194322E+03    1.00
       10   0.27057000E+06    0.211278E+03    1.00
       11   0.30528000E+06    0.249142E+03    1.00
       12   0.31245000E+06    0.265248E+03    1.00
       13   0.32043000E+06    0.292568E+03    1.00
       14   0.33120000E+06    0.331842E+03    1.00
       15   0.34068000E+06    0.575245E+03    1.00
       16   0.34428100E+06    0.618791E+03    1.00
       17   0.34498500E+06    0.678963E+03    1.00
       18   0.34684500E+06    0.740307E+03    1.00
       19   0.34833000E+06    0.779651E+03    1.00
       20   0.34981500E+06    0.818515E+03    1.00
       21   0.35139000E+06    0.844853E+03    1.00
       22   0.35281500E+06    0.913419E+03    1.00
       23   0.35433000E+06    0.983271E+03    1.00
       24   0.35577000E+06    0.107654E+04    1.00
       25   0.35691000E+06    0.119199E+04    1.00
       26   0.35739000E+06    0.122817E+04    1.00
       27   0.35838000E+06    0.155773E+04    1.00
```

University of Alberta

output example for program POW con't ;

```
               TRANSFORMED DATA
        NO                LT           LE             LEE          (LE-LEE)       W
         1       0.114590E+02 -0.671080E+01 -0.875526E+01  0.204446E+01   1.00
         2       0.115826E+02 -0.607737E+01 -0.833078E+01  0.225341E+01   1.00
         3       0.117490E+02 -0.701127E+01 -0.770961E+01  0.698338E+00   1.00
         4       0.119536E+02 -0.101039E+02 -0.694534E+01 -0.315853E+01   1.00
         5       0.122097E+02 -0.855487E+01 -0.598904E+01 -0.256582E+01   1.00
         6       0.123688E+02 -0.548279E+01 -0.539481E+01 -0.879889E-01   1.00
         7       0.124107E+02 -0.665283E+01 -0.523830E+01 -0.141453E+01   1.00
         8       0.124535E+02 -0.558433E+01 -0.507832E+01 -0.506003E+00   1.00
         9       0.124922E+02 -0.623354E+01 -0.493398E+01 -0.129957E+01   1.00
        10       0.125705E+02 -0.682080E+01 -0.464169E+01 -0.217911E+01   1.00
        11       0.126407E+02 -0.609844E+01 -0.437952E+01 -0.171892E+01   1.00
        12       0.126649E+02 -0.567706E+01 -0.428903E+01 -0.138803E+01   1.00
        13       0.126941E+02 -0.561398E+01 -0.417999E+01 -0.143398E+01   1.00
        14       0.127247E+02 -0.366222E+01 -0.406570E+01  0.403485E+00   1.00
        15       0.127440E+02 -0.441516E+01 -0.399368E+01 -0.421480E+00   1.00
        16       0.127502E+02 -0.245956E+01 -0.397029E+01  0.151073E+01   1.00
        17       0.127539E+02 -0.341184E+01 -0.395642E+01  0.544579E+00   1.00
        18       0.127588E+02 -0.363083E+01 -0.393842E+01  0.307589E+00   1.00
        19       0.127630E+02 -0.364308E+01 -0.392249E+01  0.279403E+00   1.00
        20       0.127674E+02 -0.409101E+01 -0.390616E+01 -0.184853E+00   1.00
        21       0.127717E+02 -0.303413E+01 -0.389021E+01  0.856082E+00   1.00
        22       0.127758E+02 -0.307680E+01 -0.387465E+01  0.797851E+00   1.00
        23       0.127800E+02 -0.273693E+01 -0.385909E+01  0.112216E+01   1.00
        24       0.127836E+02 -0.228991E+01 -0.384554E+01  0.155562E+01   1.00
        25       0.127859E+02 -0.258543E+01 -0.383705E+01  0.125162E+01   1.00
        26       0.127880E+02 -0.109994E+01 -0.382938E+01  0.272943E+01   1.00


               FIT PARAMETERS
                  INTERCEPT      -0.515870E+02
                  SLOPE                              3.7345781
                  CONFIDENCE LIMIT ON B1     T.      9.9375172
                  CONFIDENCE LIMIT ON B2     T.      0.7941183
                  DURBIN WATSON STATISTIC          0.742
                  TEST OF SLOPE SIGNIFICANCE          21.991


               DATA FOR COMPARISON TESTS
                  WEIGHTING   24.0
                  TRANSFORMED DATA NUMBER     26
                  MEAN STRAIN         -4.875   MEAN TIME       12.508
                  SSDY                      113.320 SSDX                           3.907
                  SPDXY                      14.505 SSDYX                         59.136

               CHECK
                 SUM OF RESIDUALS                     0.004055
                     X=      0.0
```

University of Alberta

```
CCCCCCCCCCCCCCCCCCCCCCCCCCCCCCCCCCCCCCCCCCCCCCCCCCCCCC
CCCCCCCCCCCCCCCCCCCCCCCCCCCCCCCCCCCCCCCCCCCCCCCCCCCCCC
CCCCC                                            CCCCC
CCCCC          PROGRAM  POW2                     CCCCC
CCCCC                                            CCCCC
CCCCC     THIS CREEP PROGRAM CALCULATES          CCCCC
CCCCC     RESULTANTS OF DISPLACEMENT VECTORS     CCCCC
CCCCC     OR THEIR COMPONENTS  AND FITS POWER    CCCCC
CCCCC     LAW, VELOCITY/ACCELERATION VERSUS      CCCCC
CCCCC     TIME, TO THEM.                         CCCCC
CCCCC                                            CCCCC
CCCCCCCCCCCCCCCCCCCCCCCCCCCCCCCCCCCCCCCCCCCCCCCCCCCCCC
CCCCCCCCCCCCCCCCCCCCCCCCCCCCCCCCCCCCCCCCCCCCCCCCCCCCCC


      DIMENSION E(100),T(100),EE(100),A(10),DE(100),W1(100),
     1W(100),B(100),EA(100),AE(100),AT(100),D2E(100),T1(100),
     1DENT(48),AT1(100),X(100),Y(100),ALPHA(24),AV(100)
      REAL*4 OPTNS(25)/25*'NO '/
      OPTNS(1)=1.0
      LL=0
      OPTNS(10)=5.0
      OPTNS(13)=5.0
      OPTNS(22)=3.0
C
C
C  READ DATA
C
C
      READ(5,119) NF
119   FORMAT(I3)
  8   READ(5,123) (DENT(J), J=1,8)
123   FORMAT(8A4)
      WRITE(6,134)DENT
134   FORMAT(1H1,9X,12A4)
      WW=0.
      BB=0.
      CONB1=0.
      CONB0=0.
      TE=0.
      DW=0.
      EER=0.
      EEM=0.
      EES=0.
      SUMT=0.
      SUMET=0.
      SUMT2=0.
      SUME=0.
      SUME2=0.
      SXX=0.0
      DWW=0.
      SXY=0.0
      WWA=0.
      AF=0.
      I=0
      READ(5,112)NR
      READ(5,502) (ALPHA(M),M=1,24)
502   FORMAT(24A4)
112   FORMAT(I5)
      WRITE(6,206)
206   FORMAT(1H1,'      DATA ')
      WRITE(6,207)
207   FORMAT(15X,'T              E             W')
```

University of Alberta

```
12     I=I+1
202    READ(5,151) N,AT1(I),AE(I),AV(I)
151    FORMAT(4G20.0)
C      AT(I)=AT(I)*60.
C
C
C  CALCULATE RESULTANTS OF DISPLACEMENT VECTORS
C  OR THEIR COMPONENTS.
C
C
C
C
C  CALCULATE RESULTANTS OF DISPLACEMENT VECTORS
C  OR THEIR COMPONENTS.
C
       AE(I)=SQRT(AE(I)*AE(I)+AV(I)*AV(I))*304.8
       W(I)=1.0
517    AT(I)=AT1(I)
C
C  WRITE RESULTANTS OF DISPLACEMENT VECTORS
C  OR THEIR COMPONENTS AND TIME.
C
518    WRITE(6,205)N,AT(I),AE(I),W(I)
205    FORMAT(I5,2X,E15.8,2X,E13.6,F7.2)
C
C  SMOOTH DISPLACEMENT TO INCREASE POSITIVELY.
C
11     IF(I .EQ.1) GO  TO 12
14     IF(AE(I)-AE(I-1)) 13, 13, 4
13     AE(I-1)=(AE(I)*W(I)+AE(I-1)*W(I-1))/(W(I)+W(I-1))
       AT(I-1)=(AT(I)*W(I)+AT(I-1)*W(I-1))/(W(I)+W(I-1))
       W(I-1)=W(I)+W(I-1)
       I=I-1
       IF(I-2)12,14,14
     4 CONTINUE
       IF(N.LT.NR) GO TO 12
       WRITE(6,300)
300    FORMAT(5X,'INCREASING DISPLACEMENT WITH TIME')
       WRITE(6,301)
301    FORMAT(3X,'NO',5X,'AT',15X,'AE',12X,'W')
       WRITE(6,305)(L,AT(L),AE(L),W(L),L=1,I)
305    FORMAT(I5,2X,E15.8,2X,E13.6,F7.2)
C
C  CALCULATE VELOCITY TO ACCELERATION RATIO.
C
504    DO 15 J=2,I
       DE(J)=(AE(J)-AE(J-1))/(AT(J)-AT(J-1))
       T1(J)=(AT(J)+AT(J-1))/2.0
       W1(J)=(W(J)+W(J-1))/2.0
15     CONTINUE
       DO 16 J=3,I
       D2E(J)=(DE(J)-DE(J-1))/(T1(J)-T1(J-1))
       T(J)=(T1(J)+T1(J-1))/2.0
       W(J)=(W1(J)+W1(J-1))/2.0
       E(J)=((DE(J)+DE(J-1))/2)/D2E(J)
       X(J-2)=T(J)
       Y(J-2)=E(J)
       WW=WW+W(J)
       EE(J)=0.
       SUMT=SUMT+T(J)*W(J)
```

University of Alberta

```
      SUME=SUME+E(J)*W(J)
      SUMET=SUMET+E(J)*T(J)*W(J)
      SUME2=SUME2+E(J)*E(J)*W(J)
 16   SUMT2=SUMT2+T(J)*T(J)*W(J)
      ND=J-2
C
C  CALL GRAPH
C
      CALL GRAPH (X,Y,ND,ALPHA,1,OPTNS)
C
C  FIT POWER LAW
C  BY VELOCITY/ACCELERATION VERSUS TIME
C
 505  SUME2=SUME2-SUME*SUME/WW
      SUMT2=SUMT2-SUMT*SUMT/WW
      SUMET=SUMET-SUME*SUMT/WW
      FME=SUME/WW
      FMT=SUMT/WW
 507  DO 17 J=3,I
 508  SXY=SXY+(T(J)-FMT)*(E(J)-FME)*W(J)
     7 SXX=SXX+W(J)*(T(J)-FMT)**2
 17   CONTINUE
C
C  CALCULATE FIT PARAMETERS
C
      B1=SXY/SXX
      BO=FME-FMT*B1
C
C  WRITE TRANSFORMED DATA
C
      WRITE(6,208)
  208 FORMAT(//,9X,'TRANSFORMED DATA')
      WRITE(6,209)
  209 FORMAT(5X,'NO',14X,'LT',12X,'LE',12X,'LEE',10X,'(LE-LEE)',
     *6X,'W')
 510  DO 18 J=3,I
      K=J-2
 511  EE(J)=BO+B1*T(J)
      Y(K)=EE(J)
      EES=EES+(EE(J)-E(J))*W(J)
      EA(J)=E(J)-EE(J)
      WRITE(6,106)K,T(J),E(J),EE(J),EA(J),W(J)
      EER=EER+W(J)*(EE(J)-E(J))**2
      EEM=EEM+W(J)*(EE(J)-FME)**2
      IF(J.LE.3)GO TO 18
      DW=DW+(EA(J)-EA(J-1))**2
      DWW=DWW+EA(J)*EA(J)
 18   CONTINUE
      OPTNS(21)=4.0
      SSDYX=EER
      EER=EER/(WW-2.)
      FF=EEM/EER
      CONB1=SORT(EER/SUMT2)
      CONBO=CONB1*SORT((SUMT2*WW+SUMT*SUMT)/(WW*WW))
      DW=DW/DWW
      WRITE(6,210)
C
C  WRITE FIT PARAMETERS
C
  210 FORMAT(//,9X,'FIT PARAMETERS')
```

University of Alberta

```
      WRITE(6,105)B0
  105 FORMAT(11X,' INTERCEPT    ',E15.6)
      WRITE(6,115)B1
      WRITE(6,158)CONB0
      WRITE(6,157)CONB1
      WRITE (6,159)DW
  106 FORMAT(5X,I3,5X,4(1X,E13.6),F7.2)
  157 FORMAT(11X,' CONFIDENCE LIMIT ON B2     T. ',F12.7)
  115 FORMAT(11X,' SLOPE                           ',F12.7)
  158 FORMAT(11X,' CONFIDENCE LIMIT ON B1     T. ',F12.4)
  159 FORMAT(11X,' DURBIN WATSON STATISTIC        ',F7.3)
      WRITE(6,156)FF
  156 FORMAT(11X,' TEST OF SLOPE SIGNIFICANCE     ',F9.3)
      WRITE (6,211)
  211 FORMAT(//,9X,'DATA FOR COMPARISON TESTS')
      WW=WW-2.
      WRITE(6,122)WW
  122 FORMAT(11X,' WEIGHTING ',F6.1)
      WRITE(6,124)K
  124 FORMAT(11X,' TRANSFORMED DATA NUMBER    ',I3)
      WRITE(6,104)FME,FMT
      WRITE(6,214)SUME2,SUMT2
  104 FORMAT(11X,' MEAN STRAIN  ',F11.3,
     *'    MEAN TIME ',F11.3)
      WRITE(6,213)SUMET,SSDYX
  214 FORMAT(11X,' SSDY ',5X,F20.3,' SSDX      ',F20.3)
  213 FORMAT(11X,' SPDXY',5X,F20.3,' SSDYX     ',F20.3)
      WRITE(6,212)
  212 FORMAT(/,9X,'CHECK')
      WRITE(6,107)EES
  107 FORMAT(11X,'SUM OF RESIDUALS',14X,F12.6)
      LL=LL+1
C
C  CALL GRAPH
C
      CALL GRAPH (X,Y,ND,ALPHA,-2.OPTNS)
      IF(LL.LT.NF)GO TO 8
      CALL GRAPH (X,Y,ND,ALPHA,0,OPTNS)
      STOP
      END
```

University of Alberta

input data file for program POW2 ;

```
 1.
268 PRISM DISPLACEMENTS
   27.
POWER LAW FIT TO DISPLACEMENT VECTORS RESULTANTSTIME                 LOG(VELOCITY)
 1. 90660,0.058,0.000,
 2.100740,0.096,-0.021,
 3.113700,0.184,-0.067,
 4.139545,0.258,-0.087,
 5.171210,0.271,-0.055,
 6.230235,0.311,-0.042,
 7.240450,0.429,-0.146,
 8.250380,0.448,-0.211,
 9.261930,0.603,-0.207,
10.270570,0.638,-0.271,
11.305280,0.753,-0.318,
12.312450,0.812,-0.313,
13.320430,0.893,-0.352,
14.331200,0.983,-0.468,
15.340680,1.682,-0.856,
16.344281,1.862,-0.809,
17.344985,1.993,-0.995,
18.346845,2.169,-1.093,
19.348330,2.305,-1.109,
20.349815,2.421,-1.162,
21.351390,2.479,-1.240,
22.352815,2.678,-1.345,
23.354330,2.869,-1.475,
24.355770,3.138,-1.621,
25.356910,3.463,-1.817,
26.357390,3.576,-1.857,
27.358380,4.544,-2.339,
```

output example for program POW2 ;

```
 1            26B PRISM DISPLACEMENTS          aaaaaaaaaaaaaaaa
 1            aaaaaaaaaaaaaaaaaaaaaaaaaaaaaaaaaaaaaaaaaaaaaaaaaa
 1            aaaaaaaaaaaaaaaaaaaaaaaaaaaaaaaaaaaaaaaaaaaaaaaaaa
 1            aaaaaaaaaaaaaaaaaaaaaaaaaaaaaaaaaaaaaaaaaaaaaaaaaa
 1        DATA
                     T                  E            W
         1   0.90660000E+05    0.176784E+02    1.00
         2   0.10074000E+06    0.299527E+02    1.00
         3   0.11370000E+06    0.596855E+02    1.00
         4   0.13954500E+06    0.829889E+02    1.00
         5   0.17121000E+06    0.842847E+02    1.00
         6   0.23023500E+06    0.956532E+02    1.00
         7   0.24045000E+06    0.138124E+03    1.00
         8   0.25038000E+06    0.150937E+03    1.00
         9   0.26193000E+06    0.194322E+03    1.00
        10   0.27057000E+06    0.211278E+03    1.00
        11   0.30528000E+06    0.249142E+03    1.00
        12   0.31245000E+06    0.265248E+03    1.00
        13   0.32043000E+06    0.292568E+03    1.00
        14   0.33120000E+06    0.331842E+03    1.00
        15   0.34068000E+06    0.575245E+03    1.00
        16   0.34428100E+06    0.618791E+03    1.00
        17   0.34498500E+06    0.678963E+03    1.00
        18   0.34684500E+06    0.740307E+03    1.00
        19   0.34833000E+06    0.779651E+03    1.00
        20   0.34981500E+06    0.818515E+03    1.00
        21   0.35139000E+06    0.844853E+03    1.00
        22   0.35281500E+06    0.913419E+03    1.00
        23   0.35433000E+06    0.983271E+03    1.00
        24   0.35577000E+06    0.107654E+04    1.00
        25   0.35691000E+06    0.119199E+04    1.00
        26   0.35739000E+06    0.122817E+04    1.00
        27   0.35838000E+06    0.155773E+04    1.00
          INCREASING DISPLACEMENT WITH TIME
        NO       AT                 AE           W
         1   0.90660000E+05    0.176784E+02    1.00
         2   0.10074000E+06    0.299527E+02    1.00
         3   0.11370000E+06    0.596855E+02    1.00
         4   0.13954500E+06    0.829889E+02    1.00
         5   0.17121000E+06    0.842847E+02    1.00
         6   0.23023500E+06    0.956532E+02    1.00
         7   0.24045000E+06    0.138124E+03    1.00
         8   0.25038000E+06    0.150937E+03    1.00
         9   0.26193000E+06    0.194322E+03    1.00
        10   0.27057000E+06    0.211278E+03    1.00
        11   0.30528000E+06    0.249142E+03    1.00
        12   0.31245000E+06    0.265248E+03    1.00
        13   0.32043000E+06    0.292568E+03    1.00
        14   0.33120000E+06    0.331842E+03    1.00
        15   0.34068000E+06    0.575245E+03    1.00
        16   0.34428100E+06    0.618791E+03    1.00
        17   0.34498500E+06    0.678963E+03    1.00
        18   0.34684500E+06    0.740307E+03    1.00
        19   0.34833000E+06    0.779651E+03    1.00
        20   0.34981500E+06    0.818515E+03    1.00
        21   0.35139000E+06    0.844853E+03    1.00
        22   0.35281500E+06    0.913419E+03    1.00
        23   0.35433000E+06    0.983271E+03    1.00
        24   0.35577000E+06    0.107654E+04    1.00
        25   0.35691000E+06    0.119199E+04    1.00
        26   0.35739000E+06    0.122817E+04    1.00
        27   0.35838000E+06    0.155773E+04    1.00
```

University of Alberta

output example for program POW2 con't ;

```
            TRANSFORMED DATA
      NO            LT              LE             LEE          (LE-LEE)       W
       1     0.101460E+06   0.187908E+05   0.779958E+04  -0.109912E+05    1.00
       2     0.116921E+06  -0.222642E+05   0.721480E+04  -0.294790E+05    1.00
       3     0.141000E+06  -0.157446E+05   0.630409E+04  -0.220486E+05    1.00
       4     0.178050E+06   0.349055E+05   0.490277E+04   0.300028E+05    1.00
       5     0.218033E+06   0.189917E+05   0.339055E+04   0.156011E+05    1.00
       6     0.240379E+06  -0.956914E+04   0.254536E+04  -0.121145E+05    1.00
       7     0.250785E+06   0.109901E+05   0.215177E+04   0.883834E+04    1.00
       8     0.261203E+06  -0.160920E+05   0.175776E+04  -0.178498E+05    1.00
       9     0.277088E+06  -0.379635E+05   0.115695E+04  -0.391205E+05    1.00
      10     0.298395E+06   0.302379E+05   0.351055E+03   0.298869E+05    1.00
      11     0.312653E+06   0.182421E+05  -0.188195E+03   0.184303E+05    1.00
      12     0.321128E+06   0.148657E+06  -0.508738E+03   0.149165E+06    1.00
      13     0.330878E+06   0.673853E+04  -0.877508E+03   0.761604E+04    1.00
      14     0.339210E+06  -0.909313E+04  -0.119267E+04  -0.790046E+04    1.00
      15     0.343557E+06   0.143097E+04  -0.135706E+04   0.278803E+04    1.00
      16     0.345274E+06  -0.144647E+04  -0.142202E+04  -0.244558E+02    1.00
      17     0.346751E+06  -0.766803E+04  -0.147789E+04  -0.619014E+04    1.00
      18     0.348330E+06  -0.121168E+06  -0.153760E+04  -0.119630E+06    1.00
      19     0.349838E+06  -0.347264E+04  -0.159462E+04  -0.187803E+04    1.00
      20     0.351353E+06   0.154899E+04  -0.165192E+04   0.320090E+04    1.00
      21     0.352838E+06  -0.344583E+05  -0.170808E+04  -0.327502E+05    1.00
      22     0.354311E+06   0.438898E+04  -0.176382E+04   0.615281E+04    1.00
      23     0.355695E+06   0.293373E+04  -0.181616E+04   0.474989E+04    1.00
      24     0.356745E+06  -0.276089E+04  -0.185588E+04  -0.905017E+03    1.00
      25     0.357518E+06   0.582594E+03  -0.188509E+04   0.246768E+04    1.00


           FIT PARAMETERS
              INTERCEPT        0.116370E+05
              SLOPE                              -0.0378223
              CONFIDENCE LIMIT ON B1     T.      33075.1055
              CONFIDENCE LIMIT ON B2     T.       0.1100183
              DURBIN WATSON STATISTIC            1.809
              TEST OF SLOPE SIGNIFICANCE            0.118


           DATA FOR COMPARISON TESTS
              WEIGHTING    23.0
              TRANSFORMED DATA NUMBER     25
              MEAN STRAIN          669.511    MEAN TIME   289975.250
              SSDY              44033245184.000 SSDX             157360848896.000
              SPDXY             -5951754240.000 SSDYX             43808124928.000

           CHECK
             SUM OF RESIDUALS                     -0.287598
```

University of Alberta

University of Alberta

```
CCCCCCCCCCCCCCCCCCCCCCCCCCCCCCCCCCCCCCCCCCCCCCCC
CCCCCCCCCCCCCCCCCCCCCCCCCCCCCCCCCCCCCCCCCCCCCCCC
CCCCC                                      CCCCC
CCCCC            PROGRAM  EXPO             CCCCC
CCCCC                                      CCCCC
CCCCC     THIS CREEP PROGRAM CALCULATES    CCCCC
CCCCC     RESULTANTS OF DISPLACEMENT VECTORS  CCCCC
CCCCC     OR THEIR COMPONENTS  AND FITS    CCCCC
CCCCC     EXPONENTIAL LAW TO THEM.         CCCCC
CCCCC                                      CCCCC
CCCCCCCCCCCCCCCCCCCCCCCCCCCCCCCCCCCCCCCCCCCCCCCC
CCCCCCCCCCCCCCCCCCCCCCCCCCCCCCCCCCCCCCCCCCCCCCCC


      DIMENSION E(100),T(100),EE(100),A(10),DE(100),W1(100),
     1W(100),B(100),EA(100),AE(100),AT(100),D2E(100),T1(100),
     1DENT(48),AT1(100),X(100),Y(100),ALPHA(24),AV(100)
      REAL*4 OPTNS(25)/25*'NO '/
      OPTNS(1)=1.0
      OPTNS(7)=2.0
      OPTNS(10)=5.0
      OPTNS(13)=5.0
      OPTNS(22)=3.0
      LL=0
C
C  READ DATA
C
      READ(5,119) NF,XT
  119 FORMAT(I3,G20.0)
    8 READ(5,123) (DENT(J), J=1,8)
  123 FORMAT(8A4)
      WRITE(6,134)DENT
  134 FORMAT(1H1,9X,12A4)
      WW=0.
      BB=0.
      CONB1=0.
      CONB0=0.
      TE=0.
      DW=0.
      EER=0.
      EEM=0.
      EES=0.
      SUMT=0.
      SUMET=0.
      SUMT2=0.
      SUME=0.
      SUME2=0.
      SXX=0.0
      DWW=0.
      SXY=0.0
      WWA=0.
      AF=0.
```

```
          I=0
          READ(5,112)NR
          READ(5,502) (ALPHA(M),M=1,24)
    502   FORMAT(24A4)
    112   FORMAT(I5)
          WRITE(6,206)
    206   FORMAT(1H1,'       DATA ')
          WRITE(6,207)
    207   FORMAT(15X,'T                E              W',6X,'(t+X)')
    12    I=I+1
    202   READ(5,151) N,AT1(I),AE(I),AV(I)
    151   FORMAT(4G20.0)
    C     AT(I)=AT(I)*60.
    C
    C  CALCULATE RESULTANT  OF DISPLACEMENT VECTORS
    C  OR THEIR COMPONENTS.
    C
          AE(I)=SQRT(AE(I)*AE(I)+AV(I)*AV(I))*304.8
          W(I)=1.0
    517   AT(I)=AT1(I)+XT
    C
    C  WRITE RESULTANT OF DISPLACEMENT VECTORS
    C  OR THEIR COMPONENTS AND TIME.
    C
    518   WRITE(6,205)N,AT1(I),AE(I),W(I),AT(I)
    205   FORMAT(I5,2X,E15.8,2X,E13.6,F7.2,2X,E15.8)
    C
    C  SMOOTH DISPLACEMENT TO INCREASE POSITIVELY.
    C
    11    IF(I .EQ.1) GO  TO 12
    14    IF(AE(I)-AE(I-1)) 13, 13, 4
    13    AE(I-1)=(AE(I)*W(I)+AE(I-1)*W(I-1))/(W(I)+W(I-1))
          AT(I-1)=(AT(I)*W(I)+AT(I-1)*W(I-1))/(W(I)+W(I-1))
          W(I-1)=W(I)+W(I-1)
          I=I-1
          IF(I-2)12,14,14
        4 CONTINUE
          IF(N.LT.NR) GO TO 12
          WRITE(6,300)
    300   FORMAT(5X,'INCREASING DISPLACEMENT WITH TIME')
          WRITE(6,301)
    301   FORMAT(3X,'NO',5X,'AT',15X,'AE',12X,'W')
          WRITE(6,305)(L,AT(L),AE(L),W(L),L=1,I)
    305   FORMAT(I5,2X,E15.8,2X,E13.6,F7.2)
    C
    C  CALCULATE VELOCITY.
    C  CONVERT TO LOG VELOCITY.
    C
    503   DO 1 J=2,I
          E(J)=(AE(J)-AE(J-1))/(AT(J)-AT(J-1))
          Y(J-1)=E(J)
          T(J)=(AT(J)+AT(J-1))/2.0
          X(J-1)=T(J)
        6 W(J)=(W(J)+W(J-1))/2.
        3 E(J)=ALOG(E(J))
      204 WW=WW+W(J)
          EE(J)=0.
          SUMT=SUMT+T(J)*W(J)
          SUME=SUME+E(J)*W(J)
          SUMET=SUMET+E(J)*T(J)*W(J)
```

University of Alberta

University of Alberta

```
      SUME2=SUME2+E(J)*E(J)*W(J)
    1 SUMT2=SUMT2+T(J)*T(J)*W(J)
      ND=J-1
C
C  CALL GRAPH
C
      CALL GRAPH (X,Y,ND,ALPHA,1,OPTNS)
C
C  FIT EXPONENTIAL LAW
C
505   SUME2=SUME2-SUME*SUME/WW
      SUMT2=SUMT2-SUMT*SUMT/WW
      SUMET=SUMET-SUME*SUMT/WW
      FME=SUME/WW
      FMT=SUMT/WW
506   DO 7 J=2,I
508   SXY=SXY+(T(J)-FMT)*(E(J)-FME)*W(J)
    7 SXX=SXX+W(J)*(T(J)-FMT)**2
17    CONTINUE
C
C  CALCULATE FIT PARAMETERS
C
      B1=SXY/SXX
      B0=FME-FMT*B1
      WRITE(6,208)
C
C  WRITE TRANSFORMED DATA
C
  208 FORMAT(//,9X,'TRANSFORMED DATA')
      WRITE(6,209)
  209 FORMAT(5X,'NO',14X,'LT',12X,'LE',12X,'LEE',10X,'(LE-LEE)',
     *6X,'W')
509   DO 2 J=2,I
      K=J-1
      EE(J)=B0+B1*T(J)
      Y(K)=EXP(EE(J))
      EES=EES+(EE(J)-E(J))*W(J)
      EA(J)=E(J)-EE(J)
      WRITE(6,105)K,T(J),E(J),EE(J),EA(J),W(J)
      EER=EER+W(J)*(EE(J)-E(J))**2
      EEM=EEM+W(J)*(EE(J)-FME)**2
512   IF(J.LE.2)GO TO 2
      DW=DW+(EA(J)-EA(J-1))**2
      DWW=DWW+EA(J)*EA(J)
  2   CONTINUE
      OPTNS(21)=4.0
      SSDYX=EER
      EER=EER/(WW-2.)
      FF=EEM/EER
      CONB1=SQRT(EER/SUMT2)
      CONB0=CONB1*SQRT((SUMT2*WW+SUMT*SUMT)/(WW*WW))
      DW=DW/DWW
      WRITE(6,210)
C
C  WRITE FIT PARAMETRERS
C
  210 FORMAT(//,9X,'FIT PARAMETERS')
      WRITE(6,105)B0
  105 FORMAT(11X,' INTERCEPT    ',E15.6)
      WRITE(6,115)B1
      WRITE(6,158)CONB0
      WRITE(6,157)CONB1
      WRITE (6,159)DW
  106 FORMAT(5X,I3,5X,4(1X,E13.6),F7.2)
  157 FORMAT(11X,' CONFIDENCE LIMIT ON B2    T.  ',F12.7)
  115 FORMAT(11X,' SLOPE                           ',F12.7)
  158 FORMAT(11X,' CONFIDENCE LIMIT ON B1    T.  ',F12.7)
  159 FORMAT(11X,' DURBIN WATSON STATISTIC       ',F7.3)
      WRITE(6,156)FF
  156 FORMAT(11X,' TEST OF SLOPE SIGNIFICANCE      ',F9.3)
      WRITE (6,211)
  211 FORMAT(//,9X,'DATA FOR COMPARISON TESTS')
      WW=WW-2.
      WRITE(6,122)WW
  122 FORMAT(11X,' WEIGHTING ',F6.1)
      WRITE(6,124)K
  124 FORMAT(11X,' TRANSFORMED DATA NUMBER    ',I3)
      WRITE(6,104)FME,FMT
      WRITE(6,214)SUME2,SUMT2
  104 FORMAT(11X,' MEAN STRAIN  ',F11.3,
     *'    MEAN TIME ',F11.3)
      WRITE(6,213)SUMET,SSDYX
  214 FORMAT(11X,' SSDY ',5X,F20.3,' SSDX      ',F20.3)
  213 FORMAT(11X,' SPDXY',5X,F20.3,' SSDYX     ',F20.3)
      WRITE(6,212)
  212 FORMAT(/,9X,'CHECK')
      WRITE(6,107)EES
  107 FORMAT(11X,'SUM OF RESIDUALS',14X,F12.6)
      WRITE(6,215)XT
  215 FORMAT(11X,'     X=',F10.2)
      LL=LL+1
C
C CALL GRAPH
C
      CALL GRAPH (X,Y,ND,ALPHA,-2,OPTNS)
      IF(LL.LT.NF)GO TO 8
      CALL GRAPH (X,Y,ND,ALPHA,0,OPTNS)
      STOP
      END
End of file
```

University of Alberta

input data file for program EXPO ;

```
1.0.0.
268 PRISM DISPLACEMENTS
   27.
EXPONENTIAL LAW FIT TO CUMULATIVE DISPLACEMENTS TIME               LOG(VELOCITY)
 1, 90660.0.058.0.000.
 2.100740.0.096.-0.021.
 3.113700.0.184.-0.067.
 4.139545.0.258.-0.087.
 5.1[illegible]210.0.271.-0.055.
 6.230235.0.311.-0.042.
 7.240450.0.429.-0.146.
 8.250380.0.448.-0.211.
 9.261930.0.603.-0.207.
10.270570.0.638.-0.271.
11.305280.0.753.-0.318.
12.312450.0.812.-0.313.
13.320430.0.893.-0.352.
14.331200.0.983.-0.468.
15.340680.1.682.-0.856.
16.344281.1.862.-0.809.
17.344985.1.993.-0.995.
18.346845.2.169.-1.093.
19.348330.2.305.-1.109.
20.349815.2.421.-1.162.
21.351390.2.479.-1.240.
22.352815.2.678.-1.345.
23.354330.2.869.-1.475.
24.355770.3.138.-1.621.
25.356910.3.463.-1.817.
26.357390.3.576.-1.857.
27.358380.4.544.-2.339.
```

output example for program EXPO ;

```
 1    1          26B PRISM DISPLACEMENTS          aaaaaaaaaaaaaaaa
 2    1          aaaaaaaaaaaaaaaaaaaaaaaaaaaaaaaaaaaaaaaaaaaaaaaa
 3    1          aaaaaaaaaaaaaaaaaaaaaaaaaaaaaaaaaaaaaaaaaaaaaaaa
 4    1          aaaaaaaaaaaaaaaaaaaaaaaaaaaaaaaaaaaaaaaaaaaaaaaa
 5    1       DATA
 6                    T                  E            W       (t+X)
 7           1  0.90660000E+05   0.176784E+02   1.00   0.90660000E+05
 8           2  0.10074000E+06   0.299527E+02   1.00   0.10074000E+06
 9           3  0.11370000E+06   0.596855E+02   1.00   0.11370000E+06
10           4  0.13954500E+06   0.829889E+02   1.00   0.13954500E+06
11           5  0.17121000E+06   0.842847E+02   1.00   0.17121000E+06
12           6  0.23023500E+C6   0.956532E+02   1.00   0.23023500E+06
13           7  0.24045000E+06   0.138124E+03   1.00   0.24045000E+06
14           8  0.25038000E+06   0.150937E+03   1.00   0.25038000E+06
15           9  0.26193000E+06   0.194322E+03   1.00   0.26193000E+06
16          10  0.27057000E+06   0.211278E+03   1.00   0.27057000E+06
17          11  0.30528000E+06   0.249142E+03   1.00   0.30528000E+06
18          12  0.31245000E+06   0.265248E+03   1.00   0.31245000E+06
19          13  0.32043C00E+06   0.292568E+03   1.00   0.32043000E+06
20          14  0.33120000E+06   0.331842E+03   1.00   0.33120000E+06
21          15  0.34068000E+06   0.575245E+03   1.00   0.34068000E+06
22          16  0.34428100E+06   0.618791E+03   1.00   0.34428100E+06
23          17  0.34498500E+06   0.678963E+03   1.00   0.34498500E+06
24          18  0.34684500E+06   0.740307E+03   1.00   0.34684500E+06
25          19  0.34833000E+06   0.779651E+03   1.00   0.34833000E+06
26          20  0.34981500E+06   0.818515E+03   1.00   0.34981500E+06
27          21  0.35139000E+06   0.844853E+03   1.00   0.35139000E+06
28          22  0.35281500E+06   0.913419E+03   1.00   0.35281500E+06
29          23  0.35433000E+06   0.983271E+03   1.00   0.35433000E+06
30          24  0.35577000E+06   0.107654E+04   1.00   0.35577000E+06
31          25  0.35691000E+06   0.119199E+04   1.00   0.35691000E+06
32          26  0.35739000E+06   0.122817E+04   1.00   0.35739000E+06
33          27  0.35838C00E+06   0.155773E+04   1.00   0.35838000E+06
34            INCREASING DISPLACEMENT WITH TIME
35          NO      AT                AE            W
36           1  0.90660000E+05   0.176784E+02   1.00
37           2  0.10074000E+06   0.299527E+02   1.00
38           3  0.11370000E+06   0.596855E+02   1.00
39           4  0.13954500E+06   0.829889E+02   1.00
40           5  0.17121000E+06   0.842847E+02   1.00
41           6  0.23023500E+06   0.956532E+02   1.00
42           7  0.24045000E+06   0.138124E+03   1.00
43           8  0.25038000E+06   0.150937E+03   1.00
44           9  0.26193C00E+06   0.194322E+03   1.00
45          10  0.27057000E+C6   0.211278E+03   1.00
46          11  0.30528000E+C6   0.249142E+03   1.00
47          12  0.31245C00E+06   0.265248E+03   1.00
48          13  0.32043000E+06   0.292568E+03   1.00
49          14  0.33120000E+06   0.331842E+03   1.00
50          15  0.34068000E+06   0.575245E+03   1.00
51          16  0.34428100E+06   0.618791E+03   1.00
52          17  0.34498500E+06   0.678963E+03   1.00
53          18  0.34684500E+06   0.740307E+03   1.00
54          19  0.34833000E+06   0.779651E+03   1.00
55          20  0.34981500E+06   0.818515E+03   1.00
56          21  0.35139000E+06   0.844853E+03   1.00
57          22  0.35281500E+06   0.913419E+03   1.00
58          23  0.35433000E+06   0.983271E+03   1.00
59          24  0.35577000E+06   0.107654E+04   1.00
60          25  0.35691000E+06   0.119199E+04   1.00
```

University of Alberta

output example for program EXPO con't ;

```
          26   0.35739000E+06    0.122817E+04    1.00
          27   0.35838000E+06    0.155773E+04    1.00


             TRANSFORMED DATA
          NO               LT                LE                LEE             (LE-LEE)       W
           1         0 957000E+05 -0.671080E+01 -0.860172E+01  0.189092E+01    1.00
           2         0 107220E+06 -0.607737E+01 -0.837795E+01  0.230058E+01    1.00
           3         0.126623E+06 -0.701127E+01 -0.800108E+01  0.989807E+00    1.00
           4         0.155378E+06 -0 101039E+02 -0.744255E+01 -0.266132E+01    1.00
           5         0.200723E+06 -0.855487E+01 -0.656177E+01 -0.199310E+01    1.00
           6         0.235343E+06 -0.548279E+01 -0.588931E+01  0.406518E+00    1.00
           7         0.245415E+06 -0.665283E+01 -0.569367E+01 -0.959160E+00    1.00
           8         0.256155E+06 -0.558433E+01 -0.548505E+01 -0.992804E-01    1.00
           9         0.266250E+06 -0.623354E+01 -0.528897E+01 -0.944573E+00    1.00
          10         0.287925E+06 -0.682080E+01 -0.486795E+01 -0.195284E+01    1.00
          11         0.308865E+06 -0.609844E+01 -0.446122E+01 -0.163722E+01    1.00
          12         0.316440E+06 -0.567706E+01 -0.431408E+01 -0.136298E+01    1.00
          13         0.325815E+06 -0.561398E+01 -0.413198E+01 -0.148199E+01    1.00
          14         0.335940E+06 -0.366222E+01 -0.393532E+01  0.273096E+00    1.00
          15         0.342481E+06 -0.441516E+01 -0.380827E+01 -0.606890E+00    1.00
          16         0.344633E+06 -0.245956E+01 -0.376646E+01  0.130690E+01    1.00
          17         0.345915E+06 -0.341184E+01 -0.374156E+01  0.329720E+00    1.00
          18         0.347588E+06 -0.363083E+01 -0.370908E+01  0.782490E-01    1.00
          19         0.349073E+06 -0.364308E+01 -0.368023E+01  0.371485E-01    1.00
          20         0.350603E+06 -0.409101E+01 -0.365051E+01 -0.440498E+00    1.00
          21         0.352103E+06 -0.303413E+01 -0.362138E+01  0.587246E+00    1.00
          22         0.353573E+06 -0.307680E+01 -0.359282E+01  0.516025E+00    1.00
          23         0.355050E+06 -0.273693E+01 -0.356412E+01  0.827198E+00    1.00
          24         0.356340E+06 -0.228991E+01 -0.353907E+01  0.124915E+01    1.00
          25         0.357150E+06 -0.258543E+01 -0.352333E+01  0.937904E+00    1.00
          26         0.357885E+06 -0.109994E+01 -0.350906E+01  0.240912E+01    1.00


             FIT PARAMETERS
                INTERCEPT        -0.104606E+02
                SLOPE                                 0.0000194
                CONFIDENCE LIMIT ON B1      T.        0.9710286
                CONFIDENCE LIMIT ON B2      T.        0.0000032
                DURBIN WATSON STATISTIC             0.915
                TEST OF SLOPE SIGNIFICANCE            35.854


             DATA FOR COMPARISON TESTS
                WEIGHTING   24.0
                TRANSFORMED DATA NUMBER      26
                MEAN STRAIN          -4.875   MEAN TIME  287545.250
                SSDY                      113.320 SSDX            179915718656.000
                SPDXY                 3494816.000 SSDYX                     45.439

             CHECK
               SUM OF RESIDUALS                       0.000285
                   X=       0.0
```

University of Alberta